อิทธิพลของการลดความหนืดของพอลิคาร์บอเนตโดยสารผลึกเหลวมวลโมเลกุลต่ำ

นางสาว นพวรรณ โม้ทอง

EFFECTS OF MELT VISCOSITY REDUCTION OF POLYCARBONATE

BY LOW MOLAR MASS LIQUID CRYSTAL

Miss Noppawan Motong

A Dissertation Submitted in Partial Fulfillment of the Requirements

for the Degree of Doctor of Engineering Program in Chemical Engineering

Department of Chemical Engineering

Faculty of Engineering

Chulalongkorn University

Academic year 2007

Thesis Title	EFFECTS OF MELT VISCOSITY REDUCTION OF POLYCARBONATE BY LOW MOLAR MASS LIQUID CRYSTAL
By	Miss Noppawan Motong
Field of Study	Chemical Engineering
Thesis Advisor	Associate Professor M.L. Supakanok Thongyai, Ph. D.
Thesis Co-advisor	Nigel Clarke, Ph. D.

Accepted by the Faculty of Engineering, Chulalongkorn University in Partial Fulfillment of the Requirements for the Doctoral Degree

.... Dean of the Faculty of Engineering

(Professor Direk Lavansiri, Ph.D.)

THESIS COMMITTEE

.... Chairman

(Professor Piyasan Prasertdam, Dr. Ing.)

.... Thesis Advisor

(Associate Professor M.L. Supakanok Thongyai, Ph. D.)

.... Thesis Co-advisor

(Nigel Clarke, Ph. D.)

.... Member

(Associate Professor Siriporn Damrongsakkul, Ph. D.)

.... Member

(Associate Professor Seeroong Prichanont, Ph. D.)

.... Member

(Saran Poshyachinda, Ph. D.)

นพวรรณ ไม้ทอง : อิทธิพลของการลดความหนืดของพอลิคาร์บอเนตโดยสารผลึกเหลวมวล
โมเลกุลต่ำ (EFFECTS OF MELT VISCOSITY REDUCTION OF POLYCARBONATE BY
LOW MOLAR MASS LIQUID CRYSTAL) อ. ที่ปรึกษา : รศ.ดร.มล. ศุภกนก ทองใหญ่, อ.ที่
ปรึกษาร่วม : Nigel Clarke, Ph.D.,117หน้า.

งานวิจัยนี้ศึกษาอิทธิพลของการลดความหนืดของพอลิคาร์บอเนตโดยสารผลึกเหลวมวลโมเลกุลต่ำ
แบบจำลองพื้นฐานทางวิสโคอิลาสติกของMaxwellถูกนำมาใช้อธิบายปรากฏการณ์ลดลงของความหนืดและประมาณ
ค่าสมบัติทางรีโอโลยีของพอลิเมอร์ผสม ในขั้นแรกทำการศึกษาพฤติกรรมการเปลี่ยนเฟสของพอลิคาร์บอเนตผสมสาร
ผลึกเหลวมวลโมเลกุลต่ำโดยใช้เครื่องวัดการกระเจิงแสงพบว่าที่ความเข้มข้นของสารผลึกเหลวมวลโมเลกุลต่ำมี
ปริมาณต่ำกว่า6%โดยน้ำหนักสารผสมสามารถผสมเข้ากันได้

พอลิเมอร์ผสมระหว่างพอลิคาร์บอเนตที่มีมวลโมเลกุลต่างกันและสารผลึกเหลวมวลโมเลกุลต่ำสองชนิดถูก
เตรียมขึ้นเพื่อศึกษาสมบัติทางรีโอโลยี พบว่าความหนืดของพอลิเมอร์ผสมลดลงเมื่อเพิ่มปริมาณสารผลึกเหลวมวลโม
กุลต่ำ จากการวัดค่าความหนืดของพอลิเมอร์ผสมที่แรงเฉือนต่ำพบว่าค่าความหนืดของพอลิเมอร์ผสมไม่แตกต่างจาก
พอลิคาร์บอเนตบริสุทธิ์ในขณะที่เมื่อแรงเฉือนเพิ่มขึ้นพอลิเมอร์ผสมแสดงสมบัติคล้ายกับสารผลึกเหลวและพอลิเมอร์
ผลึกเหลว โดยสมบัติทางรีโอโลยีของพอลิเมอร์ผสมจะเกิดการเปลี่ยนแปลงอย่างชัดเจนแม้ปริมาณสารผลึกเหลวมวล
โมเลกุลต่ำเพียง 1% โดยการลดลงของความหนืดได้รับการพิสูจน์จากการทดลองให้แรงเฉือนแบบออสซิลาโทรีว่า
ไม่ได้เป็นผลมาจากการหล่อลื่นบริเวณผิวสัมผัส

งานวิจัยนี้ยังได้ศึกษาผลของการเติมสารผลึกเหลวมวลโมเลกุลต่ำที่มีต่อสมบัติการแพร่ ค่าสัมประสิทธิ์การ
แพร่ของฟิล์มสองชั้นถูกตรวจวัดโดยเทคนิคการวิเคราะห์การเกิดปฏิกิริยานิวเคลียร์ พบว่าพอลิเมอร์ผสมที่มีความ
เข้มข้นของสารผลึกเหลวมวลโมเลกุลต่ำ1%โดยน้ำหนักมีค่าสัมประสิทธิ์การแพร่เพิ่มสูงขึ้น แต่เมื่อสารผลึกเหลวมวล
โมเลกุลต่ำมีปริมาณสูงขึ้นพบว่าสัมประสิทธิ์การแพร่มีค่าลดต่ำลง เมื่อศึกษาอุณหภูมิเปลี่ยนสถานะคล้ายแก้วโดยใช้
เครื่องวิเคราะห์สมบัติเชิงกลทางพลวัตพบว่าค่าอุณหภูมิเปลี่ยนสถานะคล้ายแก้วของพอลิเมอร์ผสมลดลงเมื่อปริมาณ
ของสารผลึกเหลวมวลโมเลกุลต่ำเพิ่มขึ้น นอกจากนั้นการตรวจพบค่าอุณหภูมิเปลี่ยนสถานะคล้ายแก้วเพียงค่าเดียวใน
ระบบพอลิเมอร์ผสมยืนยันว่าเป็นการผสมแบบเข้ากันได้

ภาควิชา.........วิศวกรรมเคมี......... ลายมือชื่อนิสิต...............................

สาขาวิชา.........วิศวกรรมเคมี......... ลายมือชื่ออาจารย์ที่ปรึกษา...............................

ปีการศึกษา ....2550......... ลายมือชื่ออาจารย์ที่ปรึกษาร่วม...............................
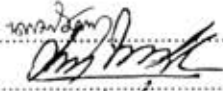
4671814921 : MAJOR CHEMICAL ENGINEERING

KEY WORD: LOW MOLAR MASS LIQUID CRYSTAL / POLYCARBONATE / VISCOSITY / DIFFUSION / POLYMER BLEND
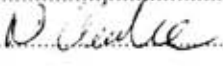
NOPPAWAN MOTONG : EFFECTS OF MELT VISCOSITY REDUCTION OF POLYCARBONATE BY LOW MOLAR MASS LIQUID CRYSTAL. THESIS ADVISOR : ASSOC. PROF. M.L. SUPAKANOK THONGYAI, Ph.D., THESIS COADVISOR : NIGEL CLARKE, Ph.D., 117 pp.

This work is devoted to the investigation of the effect of the reduction in melt viscosity of Polycarbonate by low molar mass liquid crystal chemical. The simple viscoelastic model, Maxwell model, was also chosen to explain the mechanism of the reduction and investigate the rheological parameters of the system. The phase behaviour of low molar mass liquid crystal (LLC) and polycarbonate blends is firstly reported. The results of small angle light scattering (SALS) indicate that the LLC is miscible in the mixture for weight fractions of LLC less than 6%.

For the study of the rheological properties, mixtures of two different liquid crystals with different molecular weight of polycarbonate were prepared inside the miscible regime of the blends. Both the complex and steady shear viscosities of the blends were found to be significantly decreased upon addition of small amounts of liquid crystal. At low shear rate, the steady state shear viscosity was similar to the pure polycarbonate, whilst, at higher shear rates, three further regimes of behaviour, as has been described for liquid crystals and liquid crystal polymers, were found despite the low concentration of LLC; hence, the rheological properties of the blends can be significantly modified by small concentrations of LLC (as low as 1%). The decrease in melt viscosity of polycarbonate that we observe upon addition of LLC is not due to lubrication effects at the interfaces, as shown by reproducible oscillatory shear flow sweeps.

To further study the effect of LLC content on the interdiffusion property, the diffusion coefficient was obtained using Nuclear Reaction Analysis (NRA) of bilayer films. An addition of only 1wt% liquid crystal to the polycarbonate significantly increased the diffusion coefficient, but at higher concentration the converse was found. To examine the bulk mechanical property, Dynamic mechanical analysis was used for observe the glass transition temperature of the blend. The decrease in Tg with liquid crystal content was found, in all cases the presence of a single Tg indicates that blends are miscible.

Department......Chemical Engineering......Student's signature...........................

Field of study......Chemical Engineering...... Advisor's signature...........................

Academic year ....2007............ Co-advisor's signature...........................

Acknowledgements

Contents

List of Tables

List of Figures

PAGE

Contents

CHAPTER

สถาบันวิทยบริการ
จุฬาลงกรณ์มหาวิทยาลัย

List of Tables

List of Figures

Nomenclature

Abbreviations

AFM	Atomic force microscopy
DMA	Dynamic mechanical analysis
DSC	Differential Scanning Calorometry
ERD	Elastic recoil detection
FTIR	Fourier transform infrared spectroscopy
FRAPP	Fluorescence recovery after pattern photobleaching
GC	Gas chromatography
GPC	Gel permeable chromatography
HDPE	High density polyethylene
LC	Liquid crystal
LCST	Lower critical solution temperature
LCP	Liquid crystal polymers
LDPE	Low density polyethylene
LLC	Low molar mass liquid crystal
MWD	Molecular weight distribution
NRA	Nuclear reaction analysis
PA	Polyamide
PBT	Polybutylenesterephthalate
PC	Polycarbonate
PEO	Polyethyleneoxide
PET	Polyethyleneterephthalate
PMMA	Poly (methyl methacrylate)
POCA	P-pentyloxycinnamic acid
POM	Polyoxymethylene
PP	Polypropylene
PPS	Poly (phenylene sulfide)
PS	Polystyrene
PVC	Polyvinylchloride
PVDF	Poly (vinylidene fluoride)

RBS	Rutherford backscattering spectrometry
SALS	Small angle light scattering
SAN	Styrene-acrylonitrile
SEM	Scanning electron microscopy
SIMS	Secondary ion mass spectroscopy
TBBA	Terephtal-bis-4-n-butyaniline
THF	Tetrahydrofuran
TMA	Thermo Mechanical Analysis
UCST	Upper critical solution temperature
WLF	Williams-Landel-Ferry equation
XPS	X-ray photoelectron spectroscopy

Symbols

T_i	Clearing temperature or temperature of isotropisation
$\overline{M}_n$	Number average molar mass
$\overline{M}_w$	Weight average molar mass
ΔG_m	Gibbs free energy of mixing
ΔH_m	Enthalpy of mixing
$I(q,t)$	Scattered intensity
ΔS_m	Entropy of mixing
n	Refractive index
q	Scattering wave number
T	Temperature
θ	Scattering angle
ϕ_i	Volume fraction of component i
F	Rate of transfer of material per unit area
C	Concentration of the diffusing material
x	Distance measured in the direction of diffusion
D	Diffusion coefficient
A	An arbitrary constant

t	Time
M_g	Total amount of material present
h_0	Original depth of interface
T_g	Glass transition temperature
T_m	Melting temperature
I	Excitation energy of an electron
α	Angle with respect to the sample surface
N	Number of layers
Δx	Layer Thickness
δx	Depth resolution
w_{width}	Diffused width of the deuterated polymer
τ	Shear stress
$\dot{\gamma}$	Shear rate
η	Shear viscosity
η_0	Zero shear viscosity
γ	Strain
γ°	Amplitude of the applied strain
ω	Angular frequency
f	Frequency
δ	Phase angle
G	Modulus
$\gamma^\bullet$	Complex strain
$\tau^\bullet$	Complex stress
$G^\bullet$	Complex modulus
G'	Storage modulus
G''	Loss modulus
λ	Relaxation time
G_r	Stress relaxation modulus
ζ	Monometric friction coefficient
k_B	Boltzmann constant
M_0	Molecular weight of the monomer

M	Molecular weight of the chain
M_e	Entanglement molecular weight
G_N^0	Plateau modulus
$<R^2>$	Root mean square end-to- end distance
T_{ref}	Reference temperature
$D(\phi)$	Mutual diffusion coefficient
χ	Interaction parameter
N_A	Number of segments that comprise an A chain
D_T	Transport diffusion coefficient
χ_s	Interaction parameter at the spinodal point
$D_A^\bullet$	Tracer diffusion coefficient of polymer A
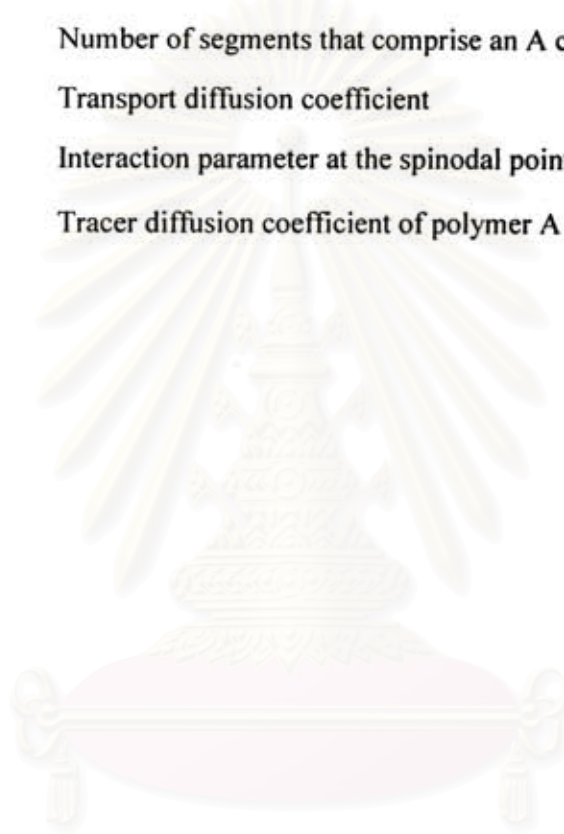
CHAPTER I

INTRODUCTION

Many thermoplastics are now accepted as *engineering material*s, a term that probably originated as a classification to distinguish the materials that could be substituted for metals in many applications. By such a criterion, thermoplastics have a disadvantage compared with metals because their properties change with time and have inferior strengths except in rather special circumstances. However, these disadvantages can be compensated by other advantages such as their high strength to density ratio, and their resistance to many of the liquids that corrode metals.

Polycarbonate is classified as an amorphous engineering thermoplastic because of its excellent balance of toughness, clarity, and high heat deflection temperature. Major market segments where polycarbonate has a broad range of applications are automotive, electronics, lighting and laser-read compact recording disks.

The engineering polymers, especially polycarbonate, have a high viscosity and require higher processing temperatures than other thermoplastics such as polystyrene, polyethylene to reduce the processing viscosity. However a high processing temperature may deteriorate the excellent properties by thermal degradation. There are several processing additives to enable processing at lower temperatures such as lubricant and plasticizers, but they may cause negative effects on other important properties, especially the clarity and mechanical properties of the final products.

A plasticizer is a substance which is added to a material to improve its processibility, flexibility and stretchability. A plasticizer can decrease melt viscosity, glass transition temperature and modulus of elasticity of the product without altering the fundamental chemical character of the plasticized material. In contrast, a lubricant is a substance that when added in small quantities, provides a considerable decrease in resistance to the movement of chains or segments of a

polymer or at least partly amorphous structure. There is, from the physical point of view, lubricant only cause partial plasticizing.

Liquid crystal polymers (LCP) are polymers whose molecules can be aligned. They have been considered for use as aids in reducing the melt viscosity of high performance polymers.[1-9] Oriented liquid crystal polymer can lubricate the polymer melt and reduce the melt viscosity leading to a reduction of the processing temperature. However, there was no significant reduction in viscosity at low LCP content (more than 10% by weight is usually required), and LCPs are generally detrimental to the clarity of the blends.

Low molar mass liquid crystal (LLC) in polymer matrices constitute interesting systems from many points of view. Many studies concerning phase behaviour, miscibility, morphology and properties have been done on such blends.[10-18] Blending an LLC with an engineering polymer can also reduce the melt viscosity but without detriment to the mechanical properties of the blend.

In the United States Patent [4,434,262], Buckley, A. et. al.[11] patented the improvement of melt processable blends comprising polymers selected from a group of polyolefins or polyesters with certain LLC. A small concentration of LLC in the polymer is enough to generate the viscosity reduction phenomenon. Watcharawichanant et al.[18] studied the effect on molecular motion in poly (styrene-co-acrylonitrile) and poly (methylmethacrylate) blends after the addition of liquid crystals. The authors found that low molar mass liquid crystal can increase the molecular mobility of the blends observed through early stage phase separation via spinodal decomposition, even when used in small amounts (less than 1% w/w).

Consequently, this present work presents a study and elucidation of the mechanism of the reduction in melt viscosity of polycarbonate and LLC blends. The phase behavior and the reduction of viscosity, due to orientational ordering under flow[19-21], by the addition of a low molar mass liquid crystal to polycarbonate was explored. 4, 4'-Bis-(4-propyl-cyclohexyl)-biphenyl (CBC33) and 4'-(4-Pentyl-cyclohexyl)-4-(4-propyl-cyclohexyl)-biphenyl (CBC53) were chosen as the low molar mass liquid crystal because they exibit a nematic phase in the same range as

the typical processing temperatures of polycarbonates.[22-23] The melt rheological properties of these mixtures, subjected to both steady and oscillatory shear flows are studied.

An important complementary characteristic to viscosity is the diffusion coefficient. Whilst the two are closely related, they differ in that viscosity reflects microscopic stresses due to an imposed strain rate, whereas the diffusion coefficient measures the rate at which molecules diffuse under quiescent conditions. In order to determine the diffusion coefficient of the PC and the blends, Nuclear Reaction Analysis (NRA) is used to follow the diffusion of deuterated polycarbonate in a polycarbonate matrix. This technique can be used for detection of the polymer diffusion over a large range of depth scales.[24]

1.1 Objective of the Study

1.1.1 Study the effects of the reduction in melt viscosity of Polycarbonate by low molar mass liquid crystal.

1.1.2 To understand the mechanism of the reduction in melt viscosity of polycarbonate by low molar mass liquid crystal.

1.2 Presentation of this thesis

This thesis comprises 6 chapters. The first chapter introduces general ideas of this work. Chapter 2 reviews the published literature concerned with the properties of liquid crystalline materials and polymer blends. Also included are studies of diffusion. All background theories relevant to this thesis are described in Chapter 3. The experimental techniques employed in this work are given in Chapter 4 in which a brief introduction of each instrument is included as well as the experimental procedures. This is followed by the results and discussion of the miscibility, rheological behaviour, interdiffusion property and thermal properties of the low molar mass liquid crystal and bisphenol A-polycarbinate blends in Chapter 5. Finally, in Chapter 6, the conclusions from the discussion and summary of the previous chapter including the recommendations for future work are presented.

CHAPTER II

LITERATURE

This chapter reviews the literature concerned with polymer blends containing liquid crystal. The topic is further subdivided in order to group studies that had similar objectives. Studies of the diffusion of polymers are also included.

2.1 Literature Review of Polymer Blends Containing Liquid crystals

The review surveys the published literature of polymer blends containing high and low molar mass liquid crystal. High molecular weight liquid crystalline polymers have been primarily used in polymer blends as processing aids and as an incipient reinforcing phase. Whilst most of the low molar mass liquid crystal studies have been concerned with the phase behaviour of the blends, several have described the applications.

2.1.1 Phase behaviour

The phase behaviour and miscibility of blends containing an LCP have been widely investigated[25-30] Zhuang, P.; Kyu, T.; White, J. L.[26] studied the phase behaviour of blends of Liquid crystalline copolyester with thermoplastic polymer such as polystyrene (PS), polycarbonate (PC) and poly(ethylene terephthalate) (PET).While PS and PC blends were found to be completely immiscible, the PET blends were partially miscible. Immiscibility of 40 PET/60 PHB liquid crystalline copolyesters with PC was also reported by Nobile, M. R.; Amendola, E.; Nicolasis, L.; Acierno, D.; Carfagna, C. [30]. Various investigators have studied and reported that the rate and degree of crystallinity of flexible-coil polymers was increased by the addition of an LCP[31-33]. Joseph, E. G.; Wilkes, G. L.; Baird, D. G.[32] studied the thermal behaviour and also found that the crystallization rates for the blends were higher than that of pure PET.

LLC/polymer blends have also been studied [14, 34-38] The blend of PC and p-pentyloxycinnamic acid (POCA) was investigated by Belfiore, L. A. [36]. Experimental results based on DSC and ^{13}C NMR were used to construct the phase diagram. The blends were partially miscible. George, E. R.; Porter, R. S.; Griffin, A. C. [34] constructed phase diagrams for blends of linear thermotropic liquid crystalline polyester with an LLC of similar structure. The LLC depressed the melting point of the polyester. Lipatov, Y.; Tsukruk, V. V.; Shilov, V. V.; Boyarski, G. Y. [38] used a cobalt gun to irradiate phase – separated mixture of cholesteric LLC microdomains dispersed in a polyurethane matrix. The result was attributed to the formation of an additional network of microdomains as the polyurethane crosslink density increased. Similar reports are selected to illustrate the phase behaviour in detail ,as below.

Lin, Y.C.; Lee, H. W. and Winter, H. H.[2] studied the miscibility and viscoelastic properties of blends of a segmented block copolyester that had average molecular weight 11,500 g/mol and poly (ethylene terephthalate) that had the average molecular weight 50,000 g/mol. They found that addition of a small quantity of LCP had an effect on rheology properties. The viscosity reduction effect is most pronounced for PET of higher molar masses. The melt viscosity decreases exponentially with the LCP content in the range of composition where the blends are miscible. However, there was no further significant reduction of viscosity when the LCP content exceeds 50 wt%. The addition of LCP also changes the distribution of the relaxation times of PET and broadens the zero shear viscosity regimes.

Brostow, W.; Mess, M.; Lopez, B. L. and Tomasz, S. [39] investigated the mechanical behaviors of blends on the basis of phase diagram. Connections between phase structures, the phase diagram and mechanical properties were studied for binary blends of Bisphenol-A-polycarbonate (PC) with PET/0.6PHB. The techniques used were Differential Scanning Calorometry (DSC), Thermo Mechanical Analysis (TMA) and Dynamic Mechanical Analysis (DMA). Results show that glass transition temperature drops by ~50°C after annealing, with evident consequences for mechanical properties.

Lee, S.; Mather, P. T. and Pearson, D. S. [40] investigated the phase behaviour and rheology of binary blends of polycarbonate and a liquid crystal polymer. Differential scanning colorimeter and optical microscopy have indicated that the liquid crystal polymer is soluble in the mixture for weight fractions of liquid crystal polymer less than 0.05 and shows partial miscibility with polycarbonate over the rest of the composition range.

Rodrigues, J. R. S.; Kaito, A.; Soldi, V.; Pires, A. T. N. [41] studied the microscopic behaviour of blends of poly (ethylene oxide)(PEO) with two different LLC in order to evaluate miscibility. The LLC were 4-cyano-4'-n-heptylbiphynyl (7CB) and p-cyanophenyl-p-pentyloxy-benzoate (pCP). Thermal analysis and morphology evaluation showed the influence of each component on the other and suggested that they are miscible at all ranges of concentration. The pCP dispersed in the PEO-rich-phase of the matrix, and shifted the transition temperature. Scanning microscopy analysis of the PEO/7CB system indicated that the blend components were uniformly mixed, which was believed to be due to chemical interactions between the constituent groups of PEO and 7CB. These results are agreement with the DSC analysis.

Thongyai, S. and Watcharawichanant, S. [18] studied the effect on molecular motion observed through early stage phase separation via spinodal decomposition, in melt mixed poly(styrene-co-acrylonitrile) and poly(methyl methacrylate) blends after adding low molar mass liquid crystal and lubricant. The major effect of the liquid crystal was to increase the molecular mobility of the blends. The lubricant can also improve the mobility of the blend but to lesser extent and the effect does not increase at higher concentration.

2.1.2 Viscoelastic Properties

One of the major advantages of blending LCPs with thermoplastic polymers is that the LCP acts as a processing aid[42-46]. Rheological characterization of LCP/polymer has been done mainly by capillary viscometer, though some researchers have used cone and plate or plate-plate rheometers. The viscosities of LCP/polymer blends were found to be much lower than that of the thermoplastic polymer alone by

Cogswell, F. N.; Griffin, B. P.; Rose, J. B. [42]. Acierno, D.; Amendola, E.; Carfagna, C.; Nicolais, L.; Nobile, R. [46] also reported that the blends of PET/PHB with PC showed a decrease in viscosity with the addition of the LCP.

Due to the wider range of the miscible region with thermoplastic polymers than LCP blend, few applications of LLC/polymers blend have been studied[10, 11, 47]. Huh, W.; Weiss, R. A.; Nicolais, L. [10] used the thermotropic liquid crystal, terephtal-bis-4-n-butyaniline (TBBA), as the plasticizer for polystyrene. TBBA are miscible in PS up to LLC concentrations of 11 percent and the melt viscosity decreased with increasing LLC content. Several reports of LCP and LLC blends with polymer are discussed below in detail.

Buckley, A.; Conciatori, A. B. and Calundann, G. W.[11] investigated the blend of low molecular weight liquid crystalline compound and polyolefin and polyester. The polymers were plasticized and the melt viscosities of blends were reduced by as much as 25 to 30 percent compared with the pure polymer.

Malik, T. M.; Carreau, P. J. and Chapleau, N.[48] investigated the mechanical and rheological properties of blends of a thermotropic liquid crystalline polyester with a polycarbonate. The blends are fibrillar in character and exhibit great hardness and toughness due to high degree of molecular orientation, which develops during the melt blending and processing steps. Increases of the Young modulus by 100 percent were observed for blends containing only 10 percent of LCP. Time-dependent behaviour of the blends was investigated by performing solid state relaxation measurements and the relaxation modulus was also found to increase by the addition of LCP. The effect is relatively small in the glassy zone of the viscoelastic response, but increased through the transition and viscous flow regions. The melt viscosity of the polycarbonate exhibits slight shear thinning whereas that of the unblended LCP increases rapidly with decreasing shear rate at low shear rate. This suggests the presence of yield stresses as confirmed by measurements made in the stress sweep mode. The melt viscosity of the blends was found to be similar to that of the unblended polycarbonate, but with more shear thinning and a lower viscosity.

Heino, M. T. and Seppala, J. V.[49] investigated blends of a polyester-type thermotropic liquid crystalline polymer (LCP) (Vectra A950) with poly(ethylene terephthalate) (PET), polypropylene (PP), and polyphenylene sulfide (PPS) respectively. They concluded that LCP was found to act as a significant reinforcement for all matrices studied. The tensile strength and elastic modulus of the blends increased with increasing LCP content, while the strain at break and the draw-ratio decreased. The improvements in strength and stiffness were most significant at higher LCP contents (20-30 wt %). However, at these compositions, the effects of draw ratio were greater. Moreover, they found that the mechanical properties of their blends were closely related to the blend morphologies.

Beery, D.; Kenig, S.; Siegmann, A. and Narkis, M.[50] investigated the shear and elongational viscosities of a thermotropic liquid crystalline polymer(LCP), polycarbonate and their 20%LCP/80%PC blend by capillary rheometry. The elongational viscosities of the LCP were found to be higher than those of the PC in the elongational-rate range studied, while shear viscosities of the LCP were higher in the lower shear rate region and lower in the higher shear rate region compared to those of the PC. This was attributed to the orientability of LCP in elongational and shear flows.

Brostow, W.; Sterzynski T. and Triouleyre, S.[51] studied rheological properties of binary blends of engineering polymers, Bisphenol-A-polycarbonate (PC), Poly(butylenes terephthalate) (PBT), isotactic polypropylene (PP) and Poly(vinylidene fluoride) (PVDF) with liquid crystalline copolymer (PET/0.6PHB), comprised of PET,poly(ethylene terephthalate), and PHB, p-hydroxybenzoic acid, with 0.6 representing the mole fraction of PHB in the copolymer. The blend concentration of 20wt% PET/0.6PHB was studied. In all binary systems for all shear rates, the addition of PET/0.6PHB to an engineering polymer resulted in lowering of the melt viscosity (**Figure 2-1 to Figure 2-4**).
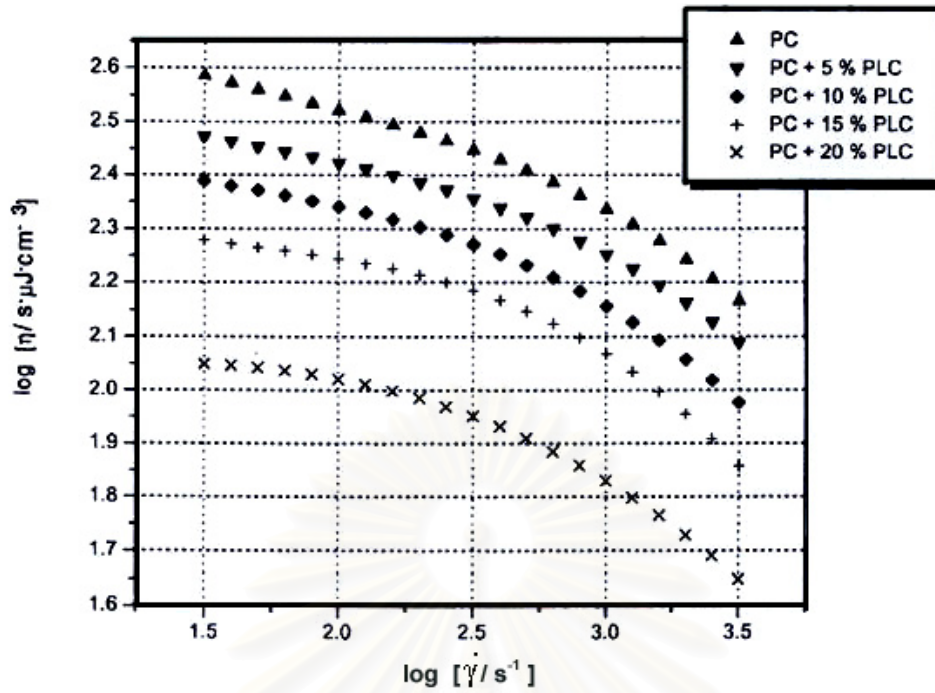
Figure 2-1 Logarithmic viscosity of blends of PC with 5, 10, 15 and 20 wt% PET/0.6PHB vs. logarithmic shear rate. [51]
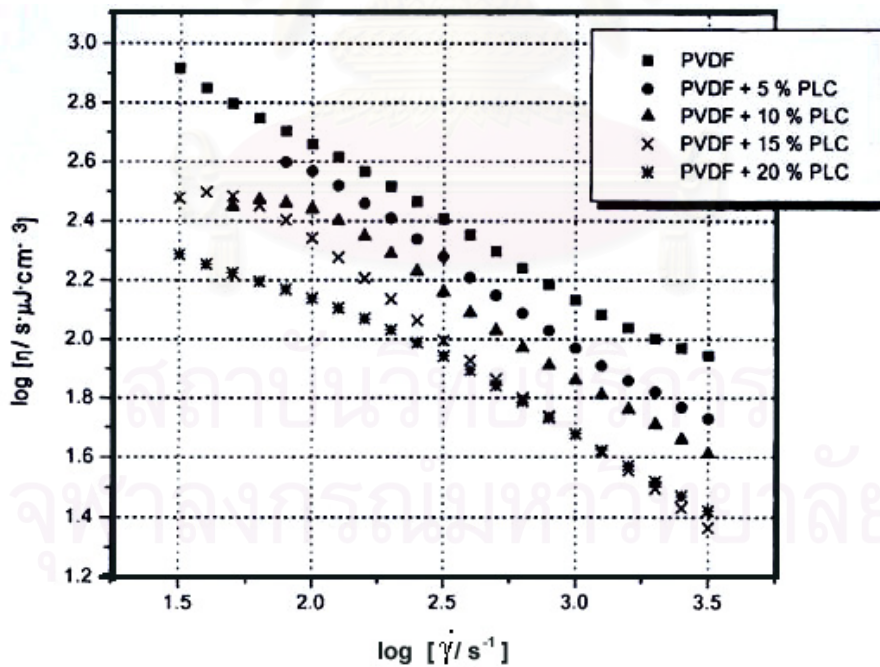
Figure 2-2 Logarithmic viscosities of blends of PVDF with 5, 10, 15 and 20 wt% PET/0.6PHB vs. logarithmic shear rate. [51]
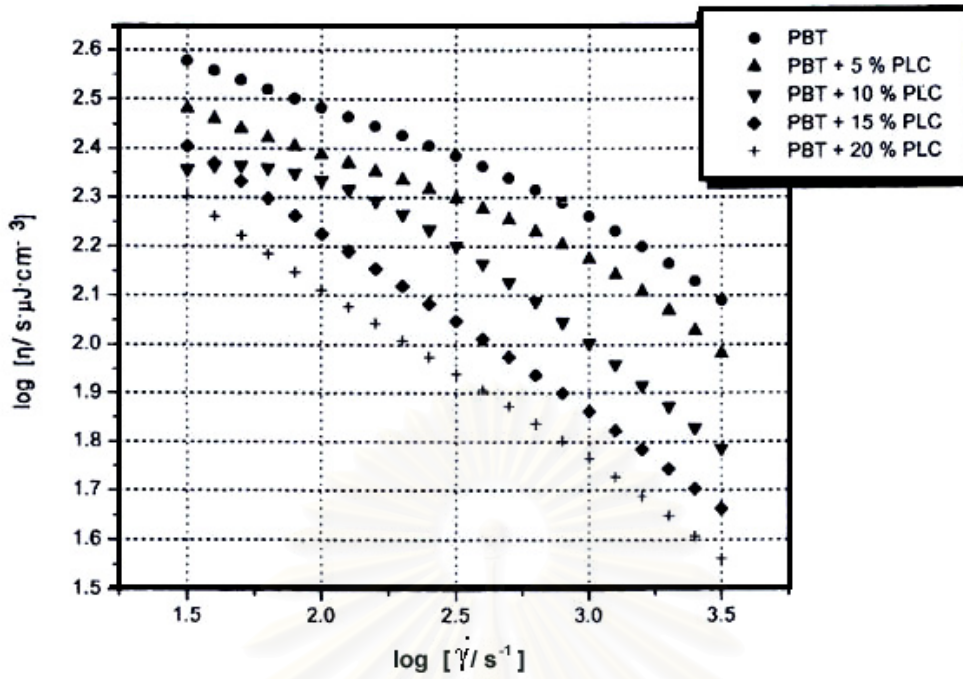
Figure 2-3 Logarithmic viscosities of blends of PBT with 5, 10, 15 and 20 wt% PET/0.6PHB vs. logarithmic shear rate. [51]
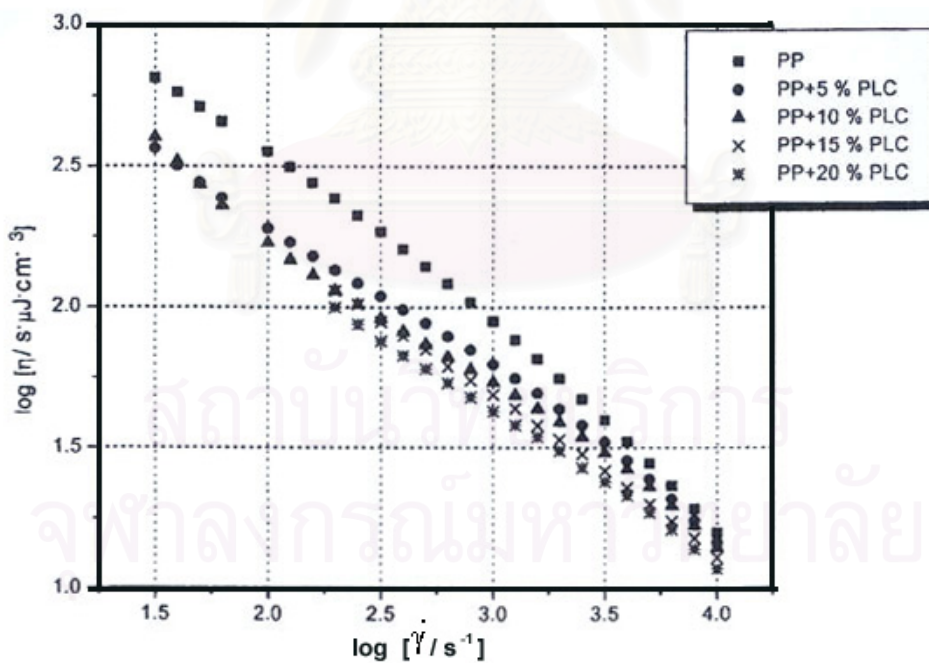
Figure 2-4 Logarithmic viscosities of blends of PP with 5, 10, 15 and 20 wt% PET/0.6PHB vs. logarithmic shear rate. [51]

Chik, G.L.; Li, R.K.Y. and Choy, C.L.[52] studied properties and morphologies of injection moulded liquid crystalline polymer / polycarbonate blends by mechanical, ultrasonic and thermal expansion techniques. The results were correlated with the morphologies by Scanning Electron Microscopy (SEM). They found that injection moulded LCP / PC blends exhibited a skin-core-skin-structure. In the skin layers, the LCP domains exhibited highly elongated fibrils, whilst in the middle of the core layer most of LCP domains exhibited spherical shapes and very few fibrils were observed.

Pezolet, M. et al[53] studied polymer orientation and relaxation by polarization modulation and FTIR spectroscopy. The dynamics of orientation during the deformation and relaxation process were presented for stretched films of polystyrene and poly (vinyl methyl ether) blends. Films of PS-PVME blends were stretched at a constant strain rate using a polymer stretcher. The dichroic difference spectra recorded during the relaxation period of blends were observed. The dichroic differences of the bands decrease with time as the chains relax to their isotropic state. The results showed that the PS chains are less orientated in the pure homopolymer than in the blend.

Xie, X. L.; Tjong, S. C. and Li, R. K. Y.[54] studied the ternary blend of poly(butylene terephthalate, PBT), polyamide 6,6 (PA6,6) and a liquid crystalline copolyester based on p-aminobenzoic acid (ABA) and poly(ethylene terephthalate), PET. The thermal, rheological and mechanical properties were investigated. The results showed that the melting temperatures of the PBT/PA6,6 phase tended to decrease with increased LCP content. The torque rheometer showed that the viscosity of the blends decreased dramatically at higher LCP concentration. Finally, the tensile tests showed that the stiffness and tensile strength of ternary in situ composites were generally improved with increasing LCP content.

Thongyai, S. and Powanusorn, S.[55] investigated the rheological and mechanical properties (tensile strength) of the blends of PP, PC, POM, HDPE, SAN, PMMA in order to compare with the pure polymers without liquid crystal(CBC33, CBC53, BCH5). The results showed that liquid crystals can reduce the melt viscosity of the base polymer without affecting the mechanical properties of the base polymer, so

the low molar mass liquid crystal may be successfully applied as an additive for polymers.

2.2 Literature Review of Diffusion studies

Diffusion is the process by which matter is transported from one part of a system to another as a result of molecular motions. The study of viscoelasticity and the molecular motion of polymers are, in fact, related to each other. The understanding of diffusion of the polymer molecules can be used to elucidate the molecular motion of polymers which useful to explain the viscoelastic behaviour of polymer blends.

Hutchings, L. R.; Richards, R. W.; Thompson, R. L.; Clough, A. S. and Langridge, S.[56] studied the effect of annealing over a range of the temperatures and times on the mixing, stability and interfacial width in thin bilayer films of PC on deuterated poly(methyl methacrylate). Films of PC were spin-coated from toluene:chloroform solutions. Nuclear reaction analysis showed that at 165 ^{o}C and below there was no effect on the interfacial width between the two polymer layers, whereas at higher temperature, the interfacial width increased. The measurements demonstrated that annealing did not induce significant levels of mixing of the polymers and there was no evidence of a thermally induced chemical reaction between the two polymers.

Helmroth, E.; Dekker, M.; Hankemier, Th.[57] studied the migration of additive within a polymer matrix as a function of space and time. By combining microtoming and GC analysis they were able to observe the migration of Irganox 1076 from LDPE to ethanol. The LDPE containing 0.4% Irganox, was prepared by compression molding and sliced using a microtome. The slices were extracted over night and the extracts analyzed by GC. They studied transport processes by checking the mass balance of Irganox in both the polymer and solvent and then comparing the experimental data with Fick's diffusion equation. The consistency of the mass balance was good and the concentration profile inside the polymer corresponded to the solution of Fick's diffusion equations.

Colley, F. R.; Collins, S. A. and Richards, R. W.[58] determined the tracer diffusions for diffusion of star polymers into linear and star polymer hydrogenous matrices use nuclear reaction analysis. Tracer diffusion coefficients for the diffusion of star polymers into star polymer matrices were compared with theoretical predictions by combining expressions for the self-diffusion coefficient with a proposed relation that incorporates both self-diffusion in a matrix of fixed obstacles by arm retraction and constraint release of the entanglements with the surrounding matrix. Such experiments are able to probe the validity of 'tube' theories of polymer dynamics in high molecular weight polymers[20].

Lopez, R.; Guedeau-Boudeville, M. A.; Gambin, Y.; Rodriguez-Beas, C.; Maldonado, A.; Urbach, W. [59] studied the interaction of low molecular weight poly (ethylene glycol) (PEG) with micelles of two different surfactants: tetradecyldimethyl aminoxide and pentaethylene glycol n-dodecyl monoether use dynamic light scattering and fluorescence recovery after pattern photobleaching (FRAPP). By using an amphiphilic fluorescent probe or a fluorescent-labeled PEG molecule, the FRAPP experiment allowed them to follow the diffusion of the surfactant-polymer complex either by looking at the micelle diffusion or at the polymer diffusion. Experiments performed with both fluorescent probes gave the same diffusion coefficient showing that the micelles and the polymer form a complex in dilute solution.

CHAPTER III

BACK GROUND THEORY

3.1 Poly(bisphenol A)carbonates,PC

Poly (bisphenal A) carbonates, PC is polyester of carbonic acid. Virtually all general purpose polycarbonates are based on bisphenol A as the repeating unit shown in **Figure 3-1**.
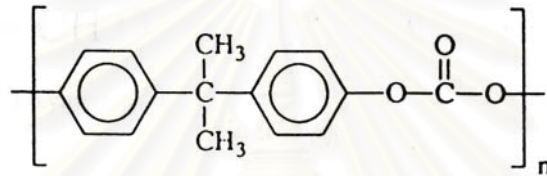
Figure 3-1 The structure of Poly (bisphenol A) carbonate[22].

3.1.1 General Properties

Although somewhat more expensive than the general purpose thermoplastics, Polycarbonates have established themselves in a number of applications. The desirable features of the polymer may be listed as follow[22]:

(1)   Rigidity up to 150°C.

(2)   Toughness up to 150°C.

(3)   Transparency.

(4)   Very good electrical insulation characteristics.

(5)   Virtually self-extinguishing.

(6)   Physiological inertness.

The principle disadvantages may be listed as:

(1)   More expensive than Polyethylene, Polystyrene and PVC.

(2)   Special care required in processing.

(3)   Pale yellow color (now commonly masked with dyes).

(4)   Limited resistance to chemicals and ultraviolet light.

Table 3-1 Typical properties of Poly (bisphenal A) carbonate[22].

Specific gravity (g/cm^3)	1.2
Refractive index (n$_D$^{25})	1.586
Tensile strength (psi)	8000-9500
Elongation (%)	100-130
Tensile modulus (10^5 psi)	3.5
Impact strength (ft-lb/in . of notch)	12-17.5
Heat-deflection temperature (^{O}F , 264 psi)	265-285
Dielectric constant (1000 cycles)	3.02
Dielectric loss (1000 cycles)	0.0021
Water absorption (one-eighth in bar, 24 hr., %)	0.15
Burning rate	Self-extinguishing
Effect of sunlight	Slight
Effect of strong acids bases	Attacked
Effect of organic solvents	soluble
Clarity	transparent

3.1.2 Applications of Poly(bisphenol A)carbonates

In spite of their rather complicated chemical structure, which consequently involves rather expensive production costs, the Polycarbonates have achieved an important place among the specialty plastic materials[60].

Success in the use of Polycarbonates arises from the advantages of toughness, rigidity, transparency, self-extinguishing characteristic, good electrical insulation characteristic and heat resistance. The main factors retarding growth are the cost, the special care needed in processing, limitations in chemical and ultraviolet light resistance, moderate electrical tracking resistance and notch sensitivity.

Some polymers are rigid, some are as transparent, some are even both more rigid and as transparent, but Polycarbonate is the only material that can provide such a combination of properties, at least at such a reasonable cost. The application of polycarbonates therefore largely arise where at least two and usually three or more of the advantageous properties are required and where there is no cheaper alternative.

The largest single field of application for moulded Polycarbonates is in electronics and electrical engineering[61]. Covers for time switches, batteries and relays, for example, utilize the good electrical insulation characteristics in conjunction with transparency, flame resistance and durability. Polycarbonates now dominate the compact disc market, where material of very high purity is required. The toughness and transparency of Polycarbonates has also led to a number of other industrial applications.

Figure 3-2 The applications of Poly(bisphenol A)carbonates.

3.2 Liquid crystal

3.2.1 Introduction to the liquid crystal

Liquid crystals were discovered more than a hundred years ago.[19,21] They are defined as liquid material, which also have the high degree of anisotropy. One of the important manifestations of LCs is their melting behavior. When heating normal crystalline solid, it changes from solid phase directly to isotropic liquids at its crystalline melting point (T_m). In liquid crystalline materials, several different mesophases may form after their T_m and the mesophases will become isotropic at the higher transition temperature called clearing temperature. The transition properties of liquid crystals come from the rigid parts of their molecules, which are called mesogens. Mesogens may consist of low molecular weight compounds. They may be arranged along the main polymer chain or on side branches of the graft molecules.

The liquid crystalline state can be discovered as small molecules or polymers and generally requires special chemical structures. The chemical structures are composed of the central core comprising aromatic or cycloaliphatic units joined by rigid links or either polar or flexible alkyl and alkoxy terminal groups.

3.2.2 Type of liquid crystals

Liquid crystals can be classified into main categories[19]:
1.   Thermotropic liquid crystals
2.   Lyotropic liquid crystal

These two types of liquid crystals are distinguished by the mechanisms that drive their self organization.

Thermotropic liquid crystals are occurred in most liquid crystals, and they are defined by the fact that the transitions to the liquid crystalline state are induced thermally. That is, one can arrive at the liquid crystalline state by raising the temperature of a solid and/or lowering the temperature of a liquid. In general

thermotropic mesophases occur because of anisotropic dispersion forces between the molecules and because of packing interactions. Thermotropic liquid crystals can be classified into two types:

1. Enantiotropic liquid crystals, which can be changed into the liquid crystal state from either lowering the temperature or raising the temperature.
2. Monotropic liquid crystal can be changed into the crystal state from lowering the temperature of a solid or raising the temperature of a liquid, but not both.

Lyotropic liquid crystal transitions occur with the influence of solvents, not by a change in temperature. Lyotropic mesophase occur as a result of solvent induced aggregation of the constituent mesogens into micellar structures. Lyotropic mesogens are composed of both lyophilic (solvent attracting) and lyophobic (solent repelling) parts. This causes them to form into micellar structures in the presence of a solvent, since the lyophobic ends will stay together as the lyophilic ends extend outward toward the solution. As the concentration of the solution is increased and the solution is cooled, the micelles increase in size and eventually coalesce. This separates the newly formed liquid crystalline state from the solvent.

The mesophase may exist in solution state (Lyotropic liquid crystal) or in a melting state (Thermotropic liquid crystal). The ability of the polymers to form Lyotropic or Thermotropic liquid crystalline mesophases depends on the chemical structure of the molecules.

The formation of a Lyotropic liquid crystalline mesophase can be present alone or in equilibrium with an isotropic liquid phase. At higher polymer concentrations the liquid crystalline mesophase can be present in equilibrium with crystalline solid.

The presence of mesogenic groups is important for the anisotropic formation of liquid crystals in solutions and melts, but the occurrence of liquid crystals also depends on many other factors such as temperature. Liquid crystals form only in a certain temperature range which lies between the melting point, Tm and the upper transition temperature at which a liquid crystalline phase changes into an isotropic liquid or clearing point, T_i. This temperature is also called the temperature of

isotropisation or the solution point. If the material being tested does not crystallize, liquid crystals are formed between the glass transition temperature, T_g, and the temperature of isotropisation, T_i.

In order to use liquid crystals, it is essential that the range of the mesophase extends over a wide temperature range. However, compounds containing a mesophase, particularly polymer, have a high melting point, and the melting point of crystals is often a limiting factor, since the range of liquid crystalline transition may be located in the range of thermal decomposition.

3.2.3 Structure of Liquid Crystals

Many kinds of mesophases can be classified by the different ways of the molecular arrangements. The anisotropic region ends at the clearing temperature because of the completely disordering of the molecules. There are many different types of liquid crystals.[19,21,62] However, the major liquid crystal mesophase topologies are shown in **Figure 3-3** to **Figure 3-6**.

3.2.3.1 Smectic structure

In the smectic structures, long molecules are arranged side by side in layers much like those in soap films. The term smectic (soap like) derives from the Greek word for grease or slime. The layers are not strictly rigid, but they are flexible. Two dimensional molecular sheets can slide pass each other (Figure3-3). Molecular motion is rather slow, so smectic mesophases are quite viscous.

Optically smectic layers behave like uniaxial, birefringent crystals. The intensity of light transmitted parallel to the molecular layer is greater than that transmitted perpendicularly. The temperature dependence of smectic interval tested by birefringence has slightly small effect to internal order.
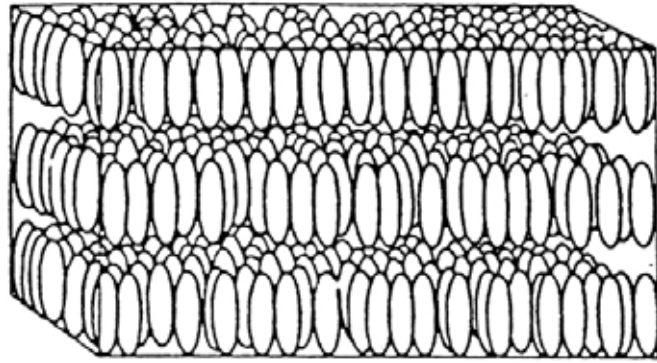
Figure 3-3 Smectic structure.[21]

3.2.3.2 Nematic structure

The molecular organization, classified as a nematic mesophase, involves in the irregular alignment in one dimension. Molecules remain parallel to each other in the nematic structure (**Figure 3-4**), but the position of their gravitational centers are disorganized. Molecules of nematic liquid crystals can be oriented in one dimension. Their mobilities can be reduced by the attraction to supporting surfaces. For examples, nematic molecules tend to lie parallel to the rough surface of a glass slide. A bright satin-like texture is observed when nematic liquid crystals are viewed between crossed polaroids. Characteristic dark threads appear at lines of optical discontinuity. These wavering filaments give the mesophase its name; take from the Greek word nematos, meaning fiber.
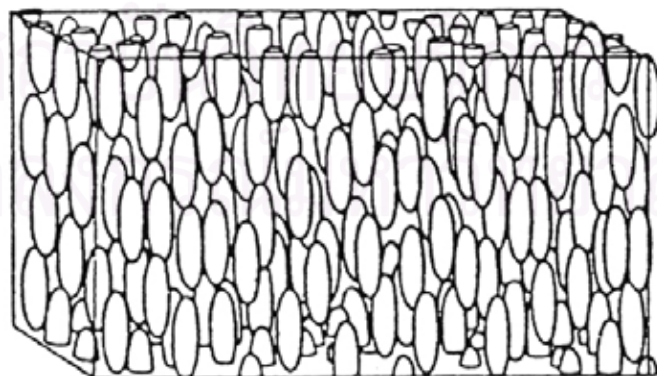
Figure 3-4 Nematic structure. [21]

3.2.3.3 Cholesteric or chiral nematic structure

The cholesteric structure is the third type of liquid crystal behaviors. It is so named because many compounds that form this mesophase are the derivatives of cholesterol. A cholesteric structure (**Figure 3-5**) is the shape of a nematic phase which is periodically wrapped around the axis. When chiral groups are present, the basic structure is helicoidal.
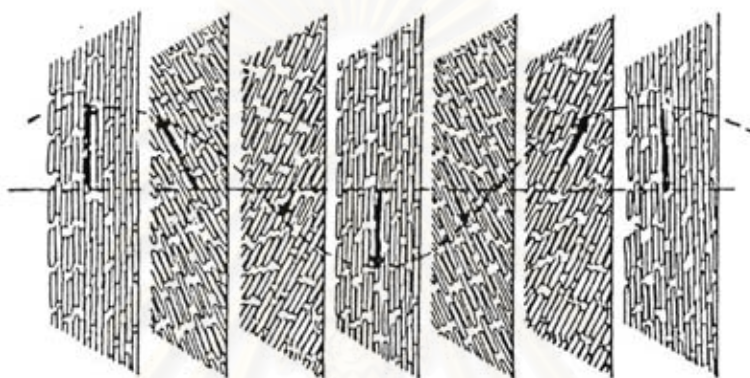
Figure 3-5 Cholesteric structure. [21]

3.2.3.4 Discotic structure

The discotic structure is the fourth type of liquid crystal behaviors. The discotic mesophase resemble stacks of dishes or coins (**Figure 3-6**).
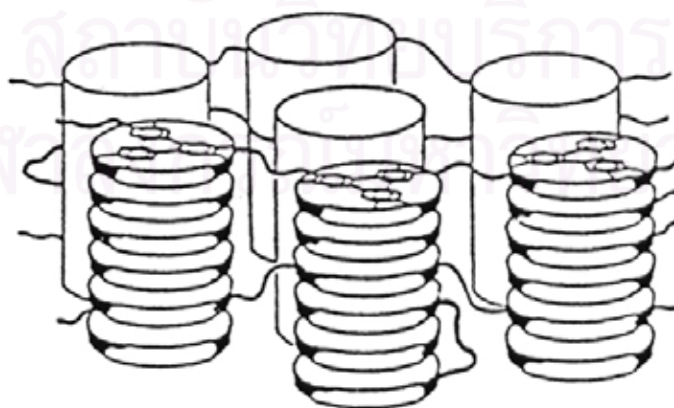
Figure 3-6 Discotic structure. [21]

3.2.4 Mesophasic Transition Temperature[19,62]

Liquid crystals can undergo various phase transitions as the temperature increases from the ordered to the least ordered states, can be shown as **Figure 3-7**.

The temperature, when liquid crystal changes from solid crystal to the first liquid crystalline phase, is called "crystalline melting temperature".

The temperature, when liquid crystal changes form smectic phase to nematic phase, is called "S→ N transition temperature".

The temperature, when the last (or only) liquid crystalline phase gives way to the isotropic melt or solution, is called "clearing temperature".
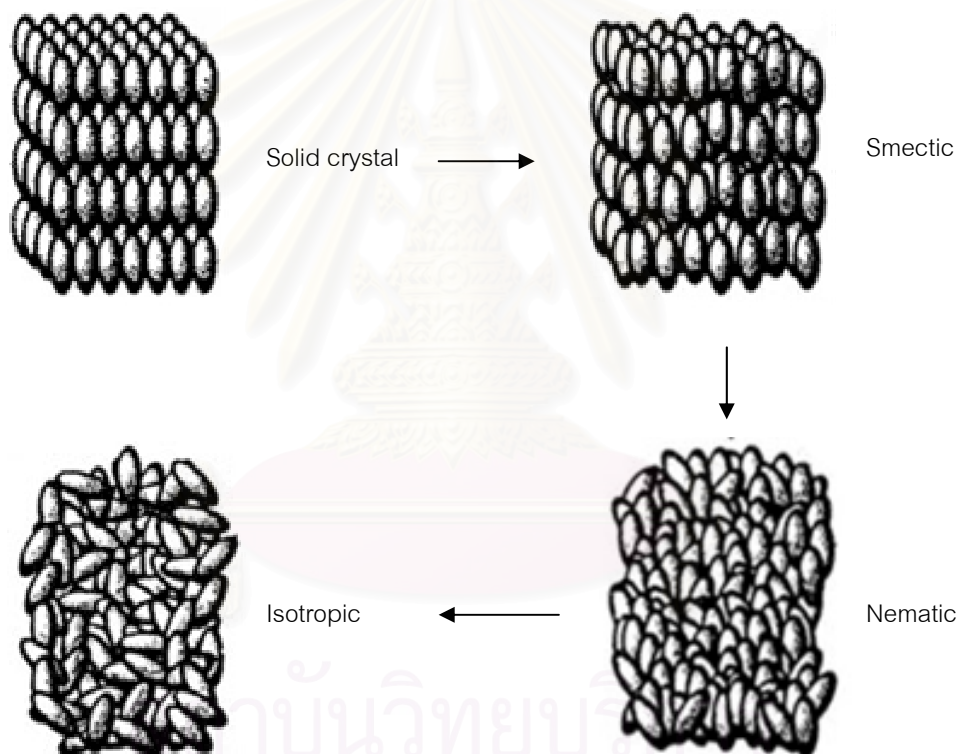
Figure 3-7 Phase transition of Liquid Crystal[19]

The flow properties of liquid crystal depend strongly on the positional order and the direction of flow. Small molecule nematics are generally rather low viscosity fluid, but reorient readily under a weak flow. Smectics have one-dimensional positional order, and thus are less fluid than nematics. The director of a flow-aligning nematic tends to orient at high shear rates toward a preferred alignment direction.

3.2.5 Flow properties of Liquid Crystal Polymer[20]

Liquid Crystal Polymers are commercially interesting because of their unusual bulk properties and their processability, resulting from their high molecular orientation. Their processability is enhanced by the low viscosity they have in the nematic melt state. A useful scheme for categorizing the viscosity versus shear rate behaviour of main chain LCPs is the "three- region" shear viscosity curve of Onogi and Asada (Figure 3-8). From Figure 3-8, region I and III are a low-shear-rate and a high-shear-rate shear thinning regions and region II is a Newtonian plateau.
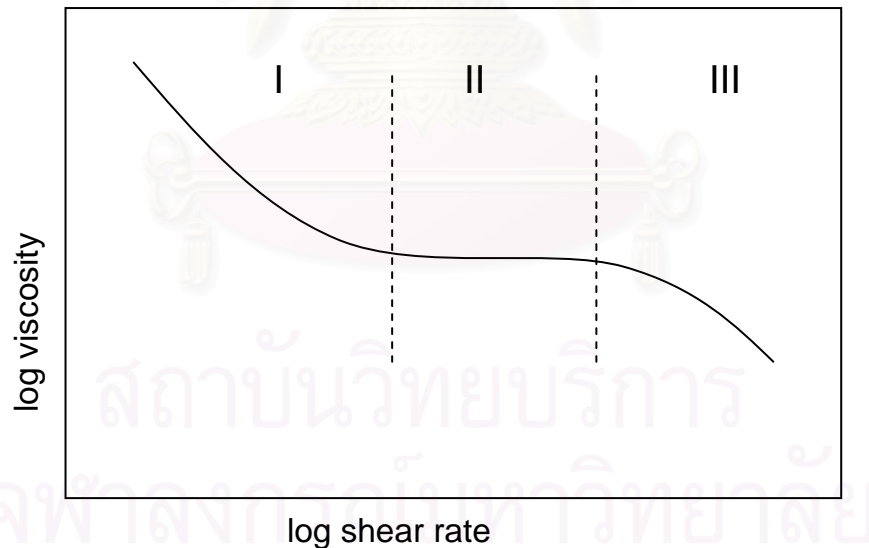
Figure 3-8 Onogi and Asada shear viscosity curve for Liquid Crystal Polymer. [20]

For both isotropic and anisotropic polymer, the Newtonian plateau (or region II) typically exists over range of shear rate for which the distribution of molecular orientations and conformations is not significantly distorted by the flow. The high shear rate shear thinning region (region III) occurs at shear rate where the molecular distribution function is disturbed by flow. Thus, compared to isotropic materials, the most distinguishing feature in the flow curve of LCPs is the appearance of a shear thinning region at low shear rate (region I). This feature must be attributed to the liquid-crystalline character.

3.3 Miscibility and Phase boundaries[63-68]

The basic and very useful thermodynamic equation that can describe the miscibility of two mixtures is the Gibbs free energy equation:

$$\Delta G_m = \Delta H_m - T \, \Delta S_m \qquad\qquad \text{Equation 3.1}$$

where ΔG_m is the Gibbs free energy of mixing

ΔH_m is the enthalpy of mixing

ΔS_m is the entropy of mixing

T is the temperature in Kelvin

The enthalpy and entropy of mixing are generally both positive so that the two mixtures will form a single phase only when the enthalpy term is less than the entropy term. The Gibbs free energy of mixing is usually controlled by the enthalpy term which has to be very small positive or even negative in order to be favorable to mixing. Equation 3.1 apparently can predict whether a blend is miscible, immiscible or partially miscible by taking into account the sign of ΔG_m as seen in Figure 3-9. With the positive sign of Gibbs free energy, the blend is immiscible whereas the negative sign indicate a miscible blend. Nevertheless, some can exhibit partially miscible, even with the negative sign of ΔG_m. Thus, the second criteria required for

complete miscibility is that the second derivative of the Gibbs free energy of mixing with respect to the compositions is always positive.
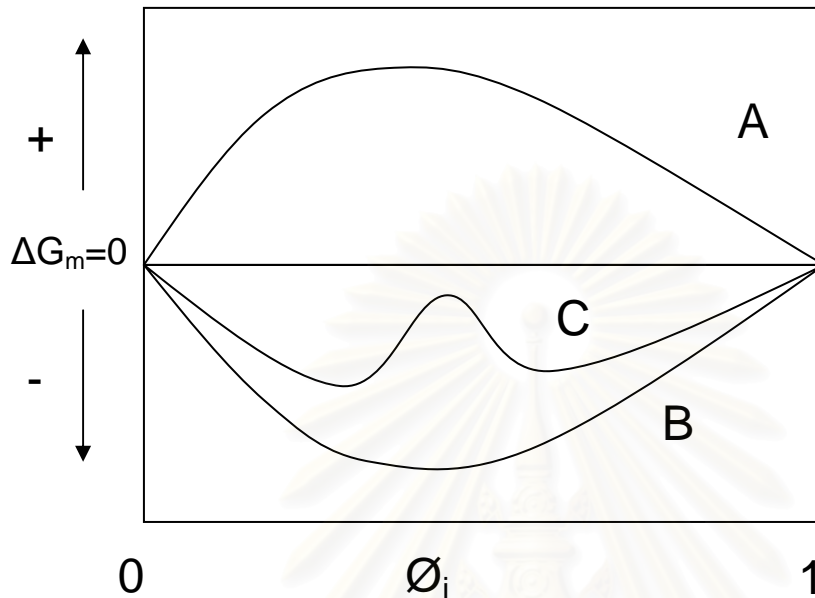
Figure 3-9 Plots of Gibbs free energy of mixing as a function of composition for a binary mixture exhibiting three types of mixing behaviour; immisciblity (A), complete miscibility (B) and partial miscibility (C). [67]

$$\frac{\partial^2 \Delta G_m}{\partial \phi_i^2} \rangle 0$$ Equation 3.2

Two examples of the phase diagrams of the mixtures related to curve C in Figure 3-9 are shown in Figure 3-10. In Figure 3-10(b), the phase separation occurs due to an increase in temperature, and this behaviour is known as the lower critical solution temperature (LCST). On the other hand, the behaviour shown in Figure 3-10(a) where the phase separates when decreasing the temperature is called the upper critical solution temperature (UCST).
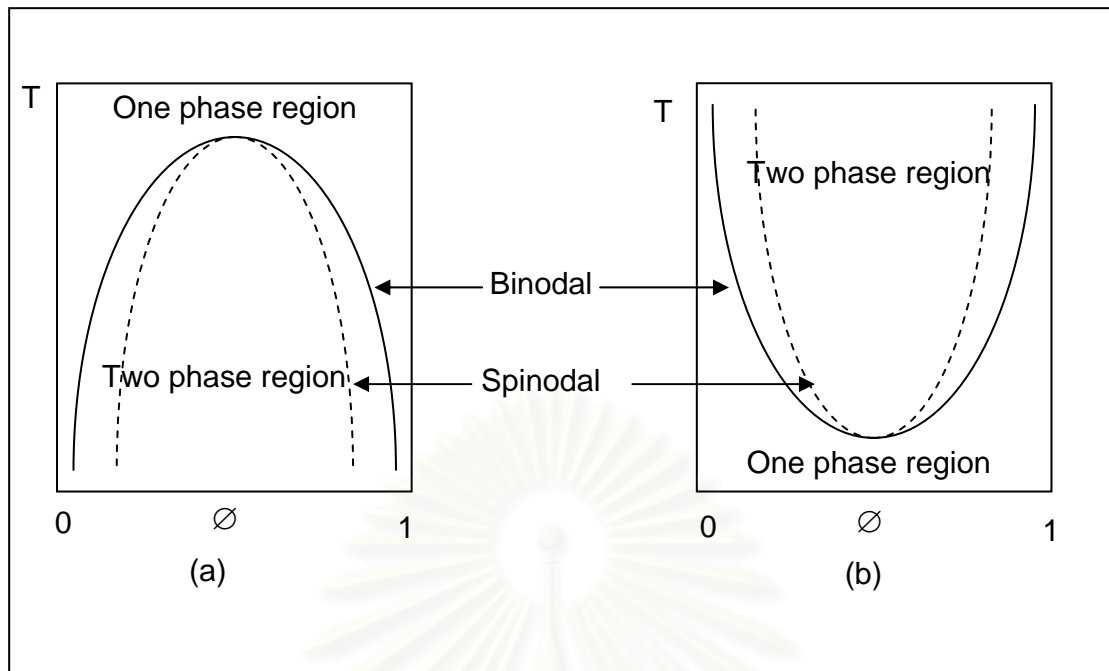
Figure 3-10 (a) The corresponding UCST-type phase diagram for binary mixture, (b) The corresponding LCST-type phase diagram for binary mixture.[66]

For polymers it appears that not only the UCST and LCST phase diagrams have been found, but other type of phase diagrams can also be observed. Figure 3-11 presents a schematic representation of various types of phase diagrams for polymer mixture. As can be seen from Figure 3-11(a), there is no instability regime indicating that the blend appears completely miscible. Figure 3-11 (b)-(c) clearly show that the UCST and the LCST exist separately, whereas in the Figures 3-11 (d)-(f,) the UCST merges with the LCST.
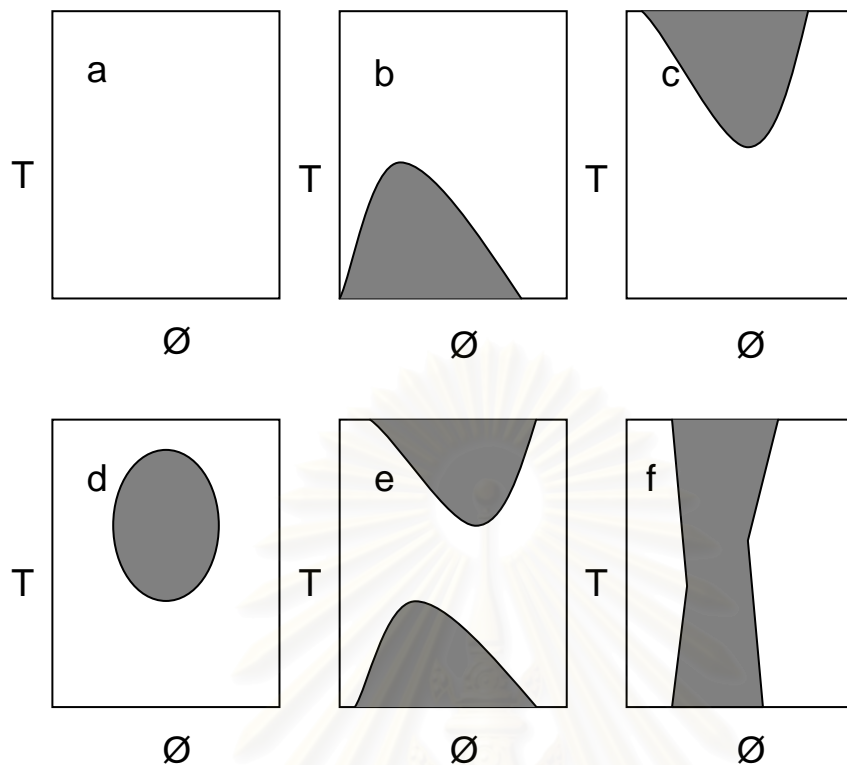
Figure 3-11 Presents a schematic representation of various types of phase diagrams for polymer mixtures. [67]

3.4 Diffusion

Diffusion is the transport of matter from an area of high concentration to another area of lower concentration as a result of molecular motions. There are several methods and models describing diffusion. One of the well known mathematical theories for mass transport phenomena of diffusion is based on Fick's laws. [69,70]

3.4.1 Fick's First law

When matter concentration gradient exists, it has the nature tendency to move in order to distribute itself more evenly within the matrix and decrease the gradient. Given enough time, the flow of matter will result in homogeneity, causing the net flow stop.

Fick recognized an analogy between the transport of matter and the transfer of heat by conduction. He put the diffusion on a quantitative basis by adopting Fourier's mathematical equation of heat conduction and postulated that the rate of transfer of diffusing substance through unit area is proportional to the concentration gradient measured normal to the section.

Thus, Fick's first law state:

$$F = -D\frac{\partial C}{\partial x}$$ Equation 3.3

where F is the rate of transfer per unit area, C is the concentration of the diffusing substance, x is the distance measured in the direction of diffusion so $\partial C/\partial x$ is the concentration gradient. D is the diffusion constant referred to as 'diffusion coefficient' or simply 'diffusivity' it is expressed in unit of length^2/time. The negative sign of the right side of equation indicate that the diffusion occurs in the opposite direction of increasing concentration. Fick's first law applies to steady state flux in a uniform concentration gradient.

3.4.2 Fick's Second Law

Fick's first law does not consider the fact that the concentration of matter decreases with an increases time and the gradient is not uniform. By assuming the diffusion coefficient is independent of concentration, Fick's second law shows that the change in concentration over time is equal to the rate at which the concentration gradient changes with distance in a given direction.

$$\frac{\partial C}{\partial t} = D\frac{\partial^2 C}{\partial x^2}$$ Equation 3.4

The solution of which is,

$$C = \frac{A}{t^{0.5}}e^{\frac{-x^2}{4Dt}}$$ Equation 3.5

where A is an arbitrary constant and t is time. This expression is symmetrical with respect to $x = 0$, it tends to zero as x approaches infinity, positively or negatively for $t > 0$. The total amount of substance present M_g, is given by,

$$M_g = \int_{-\infty}^{\infty} C dx \qquad\qquad \text{Equation 3.6}$$

If the concentration distribution is that of Equation 3.5 and defining ξ_C through,

$$\frac{x^2}{4Dt} = \xi_C^{\,2} \qquad\qquad \text{Equation 3.7}$$

so that,

$$dx = 2(Dt)^{0.5} d\xi_C \qquad\qquad \text{Equation 3.8}$$

then we find,

$$M_g = 2AD^{0.5} \int_{-\infty}^{\infty} e^{-\xi_C^{\,2}} d\xi_C = 2A(\pi D)^{0.5} \qquad\qquad \text{Equation 3.9}$$

Thus,

$$C = \frac{M_g}{2(\pi Dt)^{0.5}} e^{\frac{-x^2}{4Dt}} \qquad\qquad \text{Equation 3.10}$$

This describes the spreading by diffusion of an amount of substance M_g deposited at time $t = 0$ in the plane $x = 0$. This expression applies when the diffusing species moves in either direction, i.e. towards both positive and negative x. For the case when diffusion only occurs in the direction of positive x, the solution for negative x can be considered to be reflected in the plane $x = 0$ and superimposed on the original distribution in the region $x = 0$ so that,

$$C = \frac{M_g}{(\pi Dt)^{0.5}} e^{\frac{-x^2}{4Dt}} \qquad\qquad \text{Equation 3.11}$$

The above equations apply when the diffusing species is originally restricted to an infinitely thin plane. This is rarely adequate approximation to normal experimental conditions. If the diffusing substance in an element of width $d\xi_C$ is considered to be a line source of strength $C_0 \delta\xi_C$, then the concentration at point P, distance ξ_C from the element, at time t is given by,

$$C_P = \frac{C_0}{2(\pi Dt)^{0.5}} e^{\frac{-\xi_C^{\,2}}{4Dt}} \qquad\qquad \text{Equation 3.12}$$

C

C_0

ξ

δξ   x = 0   P   x
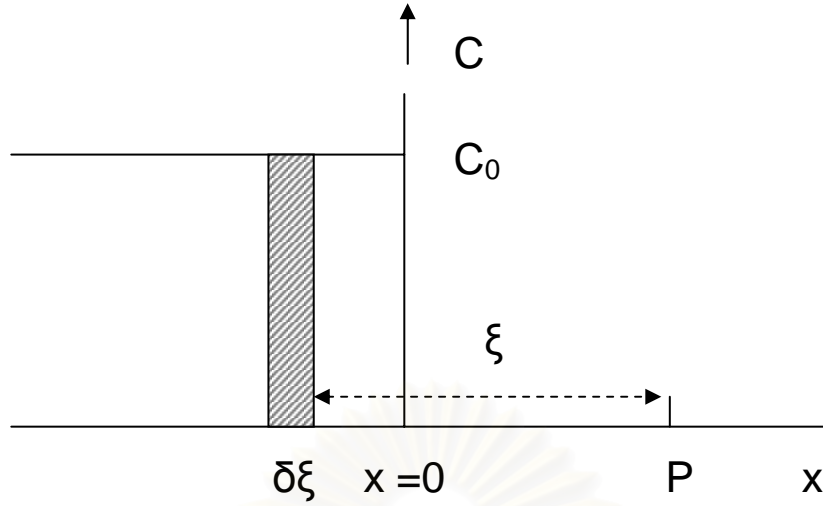
Figure 3-12 Extended initial distribution[69]

The complete solution, due to the initial distribution,

$$C = C_0, x < 0,\ C = C_0, x > 0,\ t = 0 \qquad\qquad \text{Equation 3.13}$$

is given by integrating over successive elements $d\xi_C$,

$$C(x,t) = \frac{C_0}{2(\pi D t)^{0.5}} \int_x^\infty e^{\frac{-\xi_C^2}{4Dt}}\, d\xi_C = \frac{C_0}{\pi^{0.5}} \int_{\frac{x}{2\sqrt{(Dt)}}}^\infty e^{-\eta^2}\, d\eta \qquad \text{Equation 3.14}$$

Where $\eta = \xi_C / 2\sqrt{(Dt)}$.

A standard mathematical function, of which extensive tables are available, the error function, $erf(z)$, is defined by

$$erf\ z = \frac{2}{\pi^{0.5}} \int_0^z e^{-\eta^2}\, d\eta \qquad\qquad \text{Equation 3.15}$$

which has the following properties,

$$erf(-z) = -erf\ z\ , erf(0) = 0,\ erf(\infty) = 1 \qquad\qquad \text{Equation 3.16}$$

Hence

$$\int_z^\infty e^{-\eta^2}\, d\eta = \int_0^\infty e^{-\eta^2}\, d\eta - \int_0^z e^{-\eta^2}\, d\eta = 1 - erf\ z = erfc\ z \qquad \text{Equation 3.17}$$

where $erfc(z)$ is the error-function complement. Hence,

$$C(x,t) = \frac{1}{2} C_0 erfc \frac{x}{2\sqrt{(Dt)}} \qquad\qquad \text{Equation 3.18}$$
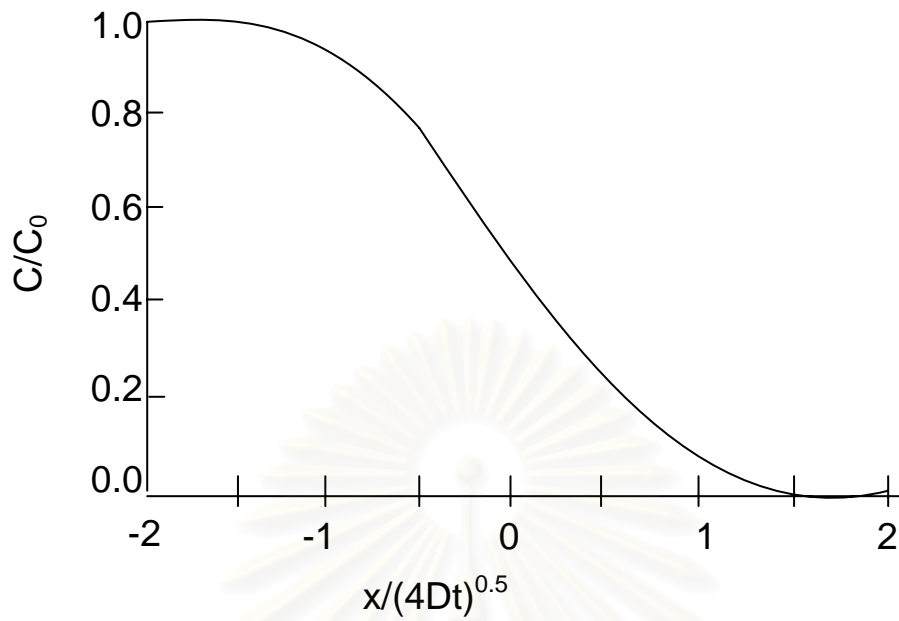
Figure 3-13 Concentration-distance curve for an extended source of infinite extent[69]

Looking at the form of the concentration distribution for this expression, $C = 0.5C_0$, at $x = 0$ for all $t > 0$. For a substance initially confined to the region $-h_0 < x < +h_0$, the summing over successive elements (integration) is from $x - h_0$ to $x + h_0$ instead of from x to ∞, leading to

$$C = \frac{1}{2}C_0\left\{erf\,\frac{h_0 - x}{2\sqrt{(Dt)}} + erf\,\frac{h_0 + x}{2\sqrt{(Dt)}}\right\}$$ Equation 3.19
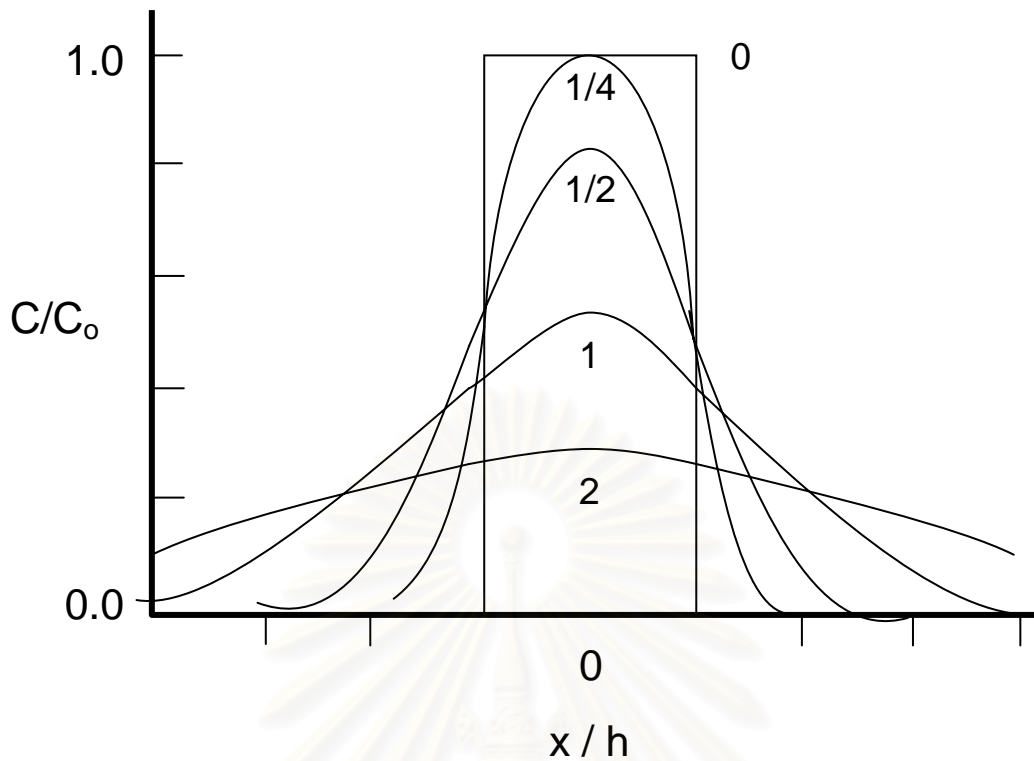
Figure 3-14 Concentration-distance curves for an extended source of limited extent. Numbers on curves are values of $(Dt/h^2)^{1/2}$ [69]

It is often more useful to consider volume fraction of a given substance φ_i rather than concentration

$$\varphi_A = \frac{1}{2}\left\{ erf\,\frac{h_0 - x}{2\sqrt{(Dt)}} + erf\,\frac{h_0 + x}{2\sqrt{(Dt)}} \right\}$$

Equation 3.20

This expression can therefore be used to calculate a diffusion coefficient for the interdiffusion of two polymer films, where $\varphi_i = 1$ within one film and $\varphi_i = 0$ in the other film at $t = 0$.

3.5 Rheology

3.5.1 Introduction

Rheology is the study of flow by definition, and polymer melt rheology is basically concerned with the description of the deformation of polymer melts under the influence of applied stresses. The flow behavior of polymer melts is of great practical importance in polymer manufacturing and polymer processing. Therefore the development of a quantitative description of flow phenomena on the basis of a number of material properties and process parameters is highly desirable.

For common liquids the viscosity is a material constant which is only dependent on temperature and pressure but not on rate of deformation and time. For polymeric liquids the situation is much more complicated: viscosities differ with deformation conditions. Furthermore the flow of polymeric melts is accompanied by elastics, due to part of the energy exerted on the system being in the form of stored recoverable energy. For this reason the viscosities are rate dependent: molten polymers are viscoelastic materials. Thermoplastic melts display the ability to recoil by virtue of their viscoelastic nature. However, they do not return completely to their original state when stretched because of their fading memory.

In the present thesis, the detail is restricted mainly to simple shear flow and small amplitude oscillatory shear flow.

3.5.2 Steady simple shear flow

Under idealized conditions the polymer melt subjected to simple shear is contained between two (infinitely extending) parallel walls, one of which is translated parallel to the other at a constant distance. The result of the shear stress (τ, the force exerted on the moving wall per unit of surface area) is a velocity gradient in the melt in a direction perpendicular to the wall. Under these ideal conditions the velocity profile is

linear, so that the gradient ($d\upsilon/dx = \dot{\gamma}$, also called shear rate) is constant. The shear viscosity is obtained as the ratio between shear stress and rate of shear.

Shear Viscosity[71,72] (η)

$$\eta = \frac{\text{shear stress}}{\text{shear rate}} = \frac{\text{shear component in the direction of shear deformation}}{\text{velocity gradient perpendicular to the direction of shear deformation}}$$

$$\eta = \frac{\tau}{\dfrac{d\upsilon}{dx}} = \frac{\tau}{\dot{\gamma}} \qquad\qquad \text{Equation 3.21}$$

For ordinary liquids is a constant; such a behavior is called Newtonian. At very low rates of deformation polymeric melts also show Newtonian behavior. In this case the shear viscosity will be characterized by the symbol η_0.

As a matter of fact

$$\eta_0 = \lim_{\dot{\gamma} \to 0} \eta(\dot{\gamma}) \qquad\qquad \text{Equation 3.22}$$

3.5.3 Small-amplitude oscillatory flow[71-73]

Small-amplitude oscillatory flow is often referred to as dynamic shear flow. It is one of unsteady shear flow types which occur when the stress involved are time dependent. In dynamic testing, the stress is measure as a function of strain that is some periodic function of time, usually sine wave.

For a strain that is a sinusoidal function of time, t, the strain function express as

$$\gamma = \gamma^\circ \sin(\omega t) \qquad\qquad \text{Equation 3.23}$$

In this expression, γ° is the amplitude of the applied strain and ω is the angular frequency of oscillation (unit of radians per second). The angular frequency is related to frequency, f, measured in cycles per second (Hz), as $\omega = 2\pi f$.

The stress resulting from the applied sinusoidal strain will also be sinusoidal function, which be written in the most general form as

$$\tau = \tau^\circ \sin(\omega t + \delta) \qquad\qquad \text{Equation 3.24}$$

where τ° is the amplitude of stress response and δ is the phase angle between the stress and the strain.

In the case of an ideal elastic solid, the stress is always in phase with strain ($\delta = 0$). This can be shown from substitution of Equation 3.23 into Hooke's law $(\tau = G\gamma)$,

$$\tau = G\gamma = G\gamma^{\circ}\sin(\omega t) = \tau^{\circ}\sin(\omega t) \qquad \text{Equation 3.25}$$

In contrast, the stress of an ideal viscous fluid is always 90° out of phase ($\delta = \pi/2$). This can be shown to result from Newton's law of viscosity, given as

$$\tau = \eta\left(\frac{d\gamma}{dt}\right) \qquad \text{Equation 3.26}$$

The derivative of γ, with respect of time is

$$\frac{d\gamma}{dt} = \omega\gamma^{\circ}\cos(\omega t) \qquad \text{Equation 3.27}$$

Substitution of this expression into Equation 3.26, and noting that the cosine function is 90° out of phase with the sine function gives,

$$\tau = \eta\omega\gamma^{\circ}\cos(\omega t) = \tau^{\circ}\sin\left(\omega t + \frac{\pi}{2}\right) \qquad \text{Equation 3.28}$$

where

$$\tau^{\circ} = \eta\omega\gamma^{\circ} \qquad \text{Equation 3.29}$$

At temperature below T_g, polymeric materials behave more as Hookean solid at small deformations, but higher temperature their behaviour is distinctly viscoelastic. Over these temperature, δ will have a temperature dependent between 0° (totally elastic) and 90° (totally viscous).

An alternative approach to discuss the dynamic response of a viscoelastic material to an applied cyclical strain is by use of complex number notation by which a complex strain, γ^{*}, can be represented as

$$\gamma^{*} = \gamma^{\circ}\exp(iwt) \qquad \text{Equation 3.30}$$

where $i = \sqrt{-1}$. The complex stress, τ^{*}, can be written as

$$\tau^{*} = \tau^{\circ}\exp[i(\omega t + \delta)] \qquad \text{Equation 3.31}$$

It follows from Hooke's law that a complex modulus, G^{*}, can be defined as the ratio of complex stress to complex stain as

$$G^* = \frac{\tau^*}{\gamma^*} = \left(\frac{\tau^o}{\gamma^o}\right)\exp(i\delta) \qquad \text{Equation 3.32}$$

This complex modulus can be resolved into two components-one that is in phase (G') and one that is out of phase (G'') with the applied strain. Substituted

$$\exp(i\delta) = \cos\delta + i\sin\delta \qquad \text{Equation 3.33}$$

into Equation 3.32 gives

$$G^* = \left(\frac{\tau^o}{\gamma^o}\right)\cos\delta + i\left(\frac{\tau^o}{\gamma^o}\right)\sin\delta \qquad \text{Equation 3.34}$$

Equation 3.34 may be written in the form given as

$$G^* = G' + iG'' \qquad \text{Equation 3.35}$$

where G' is called the storage modulus given as

$$G' = \left(\frac{\tau^o}{\gamma^o}\right)\cos\delta \qquad \text{Equation 3.36}$$

and G'' is the loss modulus:

$$G'' = \left(\frac{\tau^o}{\gamma^o}\right)\sin\delta \qquad \text{Equation 3.37}$$

The ratio of loss and storage moduli defines another useful parameter in dynamic-mechanical analysis called tan, where

$$\tan\delta = \frac{\sin\delta}{\cos\delta} = \frac{G''}{G'} \qquad \text{Equation 3.38}$$

3.6 Mechanical Models of Viscoelastic Behaviour

An insight into the nature of the viscoelastic properties of polymers can be obtained by analyzing the stress or strain response of mechanical models using an ideal spring as the Hookean element and a dashpot as the viscous element. A dashpot may be viewed as a shock absorber consisting of a piston in a cylinder filled with a Newtonian fluid of viscosity η.

Maxwell Element[74]; In the case of a series combination of a spring and dashpot, the total strain (or strain rate) is a summation of the individual strains (or strain rates) of

the spring and dashpot. From Hooke's law, the strain rate of an ideal elastic spring can be written as

$$\frac{d\gamma}{dt} = \left(\frac{1}{G}\right)\frac{d\tau}{dt}$$

Equation 3.39

while the strain rate for the dashpot is obtained by rearranging Newton's law of viscosity

$$\tau = \eta\left(\frac{d\gamma}{dt}\right)$$

Equation 3.40

as

$$\frac{d\gamma}{dt} = \frac{\tau}{\eta}$$

Equation 3.41

Therefore, the basic equation for strain rate in the Maxwell model is the summation of the strain rates for the spring and dashpot as

$$\frac{d\gamma}{dt} = \left(\frac{1}{G}\right)\frac{d\tau}{dt} + \frac{\tau}{\eta}$$

Equation 3.42

This differential equation can be solved for creep, stress relaxation, and dynamic response by applying the appropriate stress or strain function. In creep experiment, a constant stress, τ_0, is applied in stantaneously. Equation 3.42 then reduces to

$$\frac{d\gamma}{dt} = \frac{\tau_0}{\eta}$$

Equation 3.43

Rearrangement and integration of Equation 3.43 gives

$$\gamma(t) = \left(\frac{\tau_0}{\eta}\right)t + \gamma_0$$

Equation 3.44

where γ_0 represents the instanianeous (i.e., $t = 0$) strain response of the spring element. The creep compliance function, $J(t)$, is then obtained as

$$J(t) = \frac{\gamma(t)}{\tau_0} = \frac{t}{\eta} + \frac{\gamma_0}{\tau_0} = \frac{t}{\eta} + J$$

Equation 3.45

where $\left(J = \gamma_0 / \tau_0\right)$ is the instantaneous compliance (of the spring). An alternative from of Equation 3.45 may be obtained by defining a relaxation time, λ, as

$$\lambda = \frac{\eta}{G} = \eta J$$

Equation 3.46

Equation 3.45 can then be represented in normalized form as

$$\frac{J(t)}{J} = \frac{t}{\lambda} + 1$$

Equation 3.47

In a stress-relaxation experiment, the strain is constant and therefore, the strain rate is zero. Equation 3.42 then reduces to the first-order ordinary differential equation

$$\left(\frac{1}{G}\right)\frac{d\tau}{dt} + \frac{\tau}{\eta} = 0$$

Equation 3.48

Rearrangement of Equation 3.48 and introduction of λ gives

$$\frac{d\tau}{\tau} = -\left(\frac{1}{\lambda}\right)dt$$

Equation 3.49

Integration yield the stress response as

$$\tau = \tau_0 \exp\left(\frac{-t}{\lambda}\right)$$

Equation 3.50

where τ_0 is the instantaneous stress response of the spring. The stress relaxation modulus, $G_r(t)$ is then obtained as

$$G_r(t) = \frac{\tau}{\gamma_0} = \left(\frac{\tau_0}{\gamma_0}\right)\exp\left(\frac{-t}{\lambda}\right) = G\exp\left(\frac{-t}{\lambda}\right)$$

Equation 3.51

To obtain an expression for the dynamic mechanical response, the expression for complex stress, $\tau = \tau^0 \exp(i\omega t)$ is substituted into the Maxwell Equation 3.42 to give

$$\frac{d\gamma(t)}{dt} = \left(\frac{\tau^0}{G}\right)i\omega\exp(i\omega t) + \left(\frac{\tau^0}{\eta}\right)\exp(i\omega t)$$

Equation 3.52

Integration from time t_1 to t_2 gives

$$\gamma(t_2) - \gamma(t_1) = \left(\frac{\tau^0}{G}\right)\left[\exp(i\omega t_2) - \exp(i\omega t_1)\right]$$
$$+ \left(\frac{\tau^0}{\eta i\omega}\right)\left[\exp(i\omega t_2) - \exp(i\omega t_1)\right]$$

Equation 3.53

Since the corresponding stress increment can be written as

$$\tau(t_2) - \tau(t_1) = \tau^0\left[\exp(i\omega t_2) - \exp(i\omega t_1)\right]$$

Equation 3.54

Division of both sides of Equation 3.53 by this expression, and making use of λ, gives the complex compliance as

$$J^* = J - i\left(\frac{J}{\omega\lambda}\right)$$

Equation 3.55

Therefore, the storage compliance obtained from the Maxwell model is simply the compliance of the spring

$$J' = J \qquad \text{Equation 3.56}$$

which is dependent of time or frequency, while the loss compliance is

$$J'' = \frac{J}{\omega\lambda} \qquad \text{Equation 3.57}$$

The corresponding expression for complex modulus, G^*, is obtained by recalling that G^* is the reciprocal of J^* and utilizing the complex conjugate of J^* as

$$G^* = \frac{1}{J^*} = \frac{1}{J - i\dfrac{J}{\omega\lambda}} \times \frac{J + i\dfrac{J}{\omega\lambda}}{J + i\dfrac{J}{\omega\lambda}} \qquad \text{Equation 3.58}$$

Performing the multiplication, and using the inverse relation $G = 1/J$ gives

$$G^* = G' - iG'' = \frac{G(\omega\lambda)^2}{1 + (\omega\lambda)^2} + i\left[\frac{G\omega\lambda}{1 + (\omega\lambda)^2}\right] \qquad \text{Equation 3.59}$$

where

$$G' = \frac{G(\omega\lambda)^2}{1 + (\omega\lambda)^2} \qquad \text{Equation 3.60}$$

$$G'' = \frac{G\omega\lambda}{1 + (\omega\lambda)^2} \qquad \text{Equation 3.61}$$

It follows from Equation 3.60 and 3.61 that $\tan\delta$ for a Maxwell model is simply

$$\tan\delta = \frac{G''}{G'} = \frac{1}{\omega\lambda} \qquad \text{Equation 3.62}$$

3.7 Ion Beam Analysis

The use of ion beams for the modification, development and characterization of materials has had a major impact in areas of technological importance such as the microelectronics, polymer and biomedical technologies. This usage is bifurcated: beams with energies less than 1 MeV are usually used to modify materials, while beams with energies in excess of 1 Mev are typically used for materials analysis.

The high-energy (MeV) ion, unlike a neutron, loses energy in a well defined way that is a characteristic of its energy and of the elemental composition of the material it

traverses. In contrast to an electron, it undergoes very little lateral scattering as it travels through materials. For this reason, MeV ions are useful for determining the concentration versus depth distribution of elements in materials. The depth resolution of MeV ions in materials varies from a few tens to a few hundred angstroms, depending on type of ion used for the incident beam, the beam energy and the target composition. High-energy ions can probe depths in the near-surface regions ranging from 0.01 to over 10 μm. They offer distinct advantages over the use of techniques such as secondary ion mass spectroscopy (SIMS)[75] and X-ray photoelectron spectroscopy (XPS) [76] in the case of depth profiling materials. This is because the use of SIMS or XPS requires the sputtering of the target material surface, which is a highly destructive process and may alter the composition of the material being probed.

Generally, ion beam analysis experiments used for materials characterization fall into three main classes, depending on the nature of the interaction between the beam and the target nuclei. In typical experiments, the ions are produced by an ion source in an accelerator; these ions are then accelerated to MeV energies, and travel through an evacuated beam pipe toward a target. In Rutherford backscattering spectrometry (RBS) [77], a small percentage of the incident ions, upon approaching sufficiently close to target nuclei, are backscattered. A projectile that is backscattered from a nucleus in a target has a final energy that is dependent upon the nucleus from which it backscattered and the depth in the target at which the interaction occurred. The backscattered particles are detected by a silicon surface barrier detector. A detected particle creates a current pulse in the detector, the height of which is proportional to its energy. A plot of the number of pulse versus the height of each pulse is displayed on a multichannel analyzer. A nuclear reaction analysis (NRA) experiment involves the detection of products of a single nuclear reaction between an incident ion and a target nucleus, as opposed to simple to simple scattering as with RBS. The nuclear reaction of an incident ion with target nucleus results in the emission of characteristic subatomic particles whose energy is indicative of the depth in the material at which the reaction occurred. The third set of the experiments involves the kinematic recoile of target nuclei by the incident ions. The energy of these recoiled particles is characteristic of the depth at which they recoiled and their masses. This measurement technique is called elastic recoil detection (ERD) [78,79].

In general the use of one technique may be favoured over another. RBS is often used to profile elements of medium atomic mass. When the mass of the element that is being detected is lighter than the matrix in which it resides, the sensitivity of RBS is reduced because of the high background. ERD is a much better alternative in this case because it is well suited for the analysis of light mass element such as hydrogen. NRA is used when one chooses to profile a specific isotope and is, in general, not restricted to the detection of particles of any given mass range. The advantage of NRA technique over RBS/ERD is it has a better depth resolution than ERD or RBS.

3.8 Polymer/Polymer diffusion

3.8.1 Tracer Diffusion

The current understanding of the translational diffusion of a single chain comprised of N monomer segments in a highly entangled melt of chains, each comprised of P monomer segments, is based on the concept of reptation which was introduced by deGennes in 1971. In the melt, the diffusion of this N-mer chain is restricted to a tube-like region formed as a result of its intersections with the neighboring P-mer chains. Show in Figure 3-15(a) is a schematic of a labeled chain in a melt. Figure 3-15(b) shows a schematic of the labeled chain restricted to the "tube". The dynamical modes of this chain in its "tube" are assumed to be described by the Rouse model[80]. Therefore, the diffusion coefficient of the chain along an average trajectory defined by the tube is denoted by [81,82]

$$D_t = \frac{k_B T}{N\zeta}$$
<div align="right">Equation 3.63</div>

where ζ is the monometric friction coefficient, k_B is the Boltzmann constant, and T is the temperature; $N = M/M_0$. Here M_0 is the molecular weight of a monomer in the chain and M is the total molecular weight of the chain. The ends of the chain that emerge from the "tube" choose random directions in space in which move. As the chain diffuse, portions of a new tube are crated ahead, while portions of the old are abandoned. On long time scales defined by $\tau_d \approx \zeta N^3$, the chain loses complete memory of the old tube. The center of mass diffusion coefficient of a chain diffusing by reptation alone is given by [81-83]

$$D^* = D_{REP} = D_0 M^{-2}$$ Equation 3.64

where

$$D_0 = \frac{4}{5}\frac{M_0 M_e k_B T}{\zeta}$$ Equation 3.65

Here M_e is the molecular weight between entanglements. Both D^* and the zero shear rate viscosity, η_0, are related through τ_d, the longest relaxation time in the melt. Graessley has shown that one may easily express D^* in terms of η_0 [84]

$$D^* = \frac{G_N^0}{135}M_e^2 L\frac{M_c}{\eta_0(M_c)M^2}$$ Equation 3.66

In this equation $G_N^0 = \rho RT / M_e$ is the plateau modulus where ρ is the density of the polymer. M_c is the critical molecular weight for viscous flow and $L =< R^2 > / M$ where $< R^2 >$ is the root mean square end-to- end vector. Equation 3.66 allows one to calculate D^* based on knowledge of the viscoelastic parameters of the polymer. It establishes a definite link between diffusion and viscoelasticity.

(a)

(b)
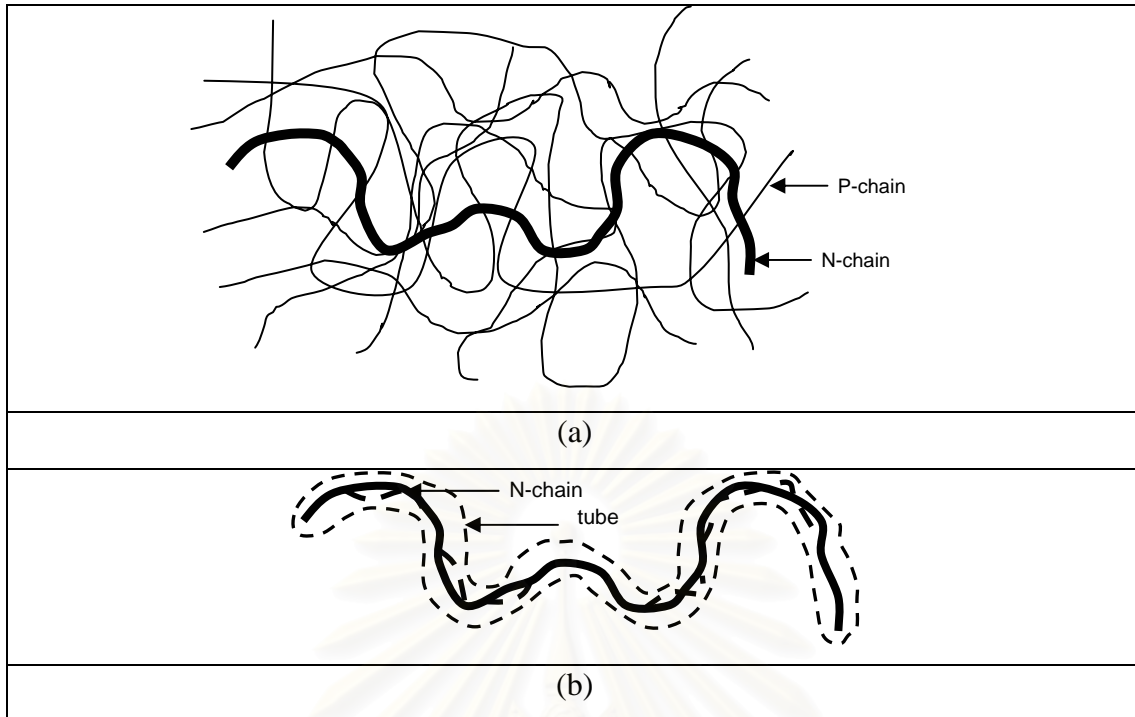
Figure 3-15 (a) Picture of a labeled chain comprised of N monomer segments in a melt of chains, each comprised of P-monomer segments. (b) The N-mer chain is confined to a tubelike region. [83]

The temperature dependence of the diffusion coefficient may be obtained by noting that Equation 3.66 suggests that D^*/T can be expressed in the terms of η_0 as follows

$$\log \frac{D^*}{T} = C(M) - \log \eta_0 \qquad \text{Equation 3.67}$$

$C(M)$ is a strong function of the molecular weight. This function vary slowly with temperature. It may change by a few percent over 100 degrees, whereas η_0 and D^* will vary by a few orders of magnitude in most polymers over this temperature range. It is well known that the temperature dependence of η_0 is accurately described by the Vogel-Fulcher equation, or equivalently by the WLF (Williams-Landel-Ferry) equation [85]

$$\log \eta_0 = A + \frac{B}{T - T_0} \qquad \text{Equation 3.68}$$

where T_0 and B are Vogel constants. The temperature dependence of D^*/T is easily shown to be [86,87]

$$\log\left(\frac{\dfrac{D^*}{T}}{\dfrac{D^*_{\text{ref}}}{T_{\text{ref}}}}\right) = \frac{B}{T_{\text{ref}} - T_0} - \frac{B}{T - T_0} \qquad \text{Equation 3.69}$$

In the above equation, T_{ref} is a reference temperature at which D^*_{ref} is determined.

When the P-mer chains are sufficiently short, the surroundings of the N-mer chain become altered on time scales comparable to τ_d. Consequently the tube may undergo a series of displacements. The foregoing description of the motion of the N-mer chain occurring in a fixed tube is inadequate. Theories[88-92] have shown that under the conditions, the D^* of the N-mer chain may be modified by the addition of a term, D_{CR}, which describes the effects of the environment on its motion; $D^* = D_{\text{ref}} + D_{\text{CR}}$. One of a number of theories which were designed to describe the effect of the environment on the N-mer chain is due to Graessley[89]. Graessley showed that the contribution of constaint release should be described by

$$D_{CR} = \alpha_{CR} D_0 M_e^2 M^{-1} P^{-3} \qquad \text{Equation 3.70}$$

where $\alpha_{CR} = (48/25)(12/\pi^2)^{z-1}$ depends on z, the number of suitably situated constraints per M_e. The tracer diffusion coefficient therefore becomes.

$$D^* = D_0 M^{-2}\left(1 + \alpha_{CR} D_0 M_e^2 M P^{-3}\right) \qquad \text{Equation 3.71}$$

3.8.2 Mutual Diffusion

The driving force for tracer diffusion is entropic in origin. The mutual diffusion coefficient, $D(\phi)$, in a mixture of two polymers A and B is highly composition dependent, and is influenced by enthalpic effects. For this reason it is possible, based on measurement of $D(\phi)$, to obtain information about the thermodynamics of a polymer mixture. In particular, information about the Flory-Huggins[83,93] interaction parameter, χ, which measures the strength of the interactions between the A and B segments maybe learned. If the A/B interactions strongly favor mixing, $\chi < 0$ then,

$D(\phi)$ is enhanced over the case where $\chi = 0$. On the other hand, if $\chi > 0$, but the mixture is still within the stable regime defined by $\chi < \chi_s$ where

$$\chi_s(\phi) = \left\{ [N_A \phi]^{-1} + [N_B(1-\phi)]^{-1} \right\} / 2 \qquad \text{Equation 3.72}$$

then $D(\phi)$ is observed to undergo the well-known "thermodynamic slowing down". In the above equation, N_A is the number of segments that comprise an A chain and N_B is the corresponding number in a B chain; ϕ is the volume fraction of A chain and $(1-\phi)$ is that of the B chains.

The free energy change per segment that arises from mixing A and B segments may be approximated by the mean field Flory-Huggins expression. [83,93]

$$\frac{\Delta F}{k_B T} = \frac{1}{N_A} \ln \phi + \frac{1}{N_B} \ln(1-\phi) + \phi(1-\phi)\chi \qquad \text{Equation 3.73}$$

The first two terms in this equation represent the combinatorial entropy of mixture. The third represents contributions from the enthalpic or noncombinatorial entropy of mixing. Since the combinatorial entropy of mixing varies as N^{-1}, the third term, which includes χ, is primarily responsible for the phase equilibrium behaviour of polymer mixtures. Within the mean field approximation, the compositional dependence of the mutual diffusion coefficient may be express as[94-96]

$$D(\phi) = 2\phi(1-\phi)D_T[\chi_s(\phi) - \chi] \qquad \text{Equation 3.74}$$

The first term, $\phi(1-\phi)D_T\chi_s$ in this expression describes the situation in which the driving force for interdiffusion is controlled by the combinatorial entropy of mixing. The second term is the correction to $\phi(1-\phi)D_T\chi_s$ in the presence of enthalpic and non-combinatorial entropy of mixing contributions to interdiffusion. The parameter D_T is the Onsager transport coefficient. The precise form of D_T for polymer/polymer diffusion was, until recently, uncertain. It was demonstrated that[97]

$$D_T = D_A^* N_A(1-\phi) + D_B^* N_B \phi \qquad \text{Equation 3.75}$$

In this equation, D_A^* is the tracer diffusion coefficient of species A into species B and D_B^* is defined accordingly.

3.9 The glass transition temperature of blends

At sufficiently low temperature all polymer are rigid solids (glassy). For an amorphous polymers, as temperature rises each polymer gains enough thermal energy to enable it's chains to move freely, enough for it to behave like a viscous liquid. The transition between glassy and rubbery behaviour is the glass transition temperature, T_g, which marks a major change in mechanical properties. A 100% crystalline polymer should become a viscous liquid over the melting point temperature ,T_m, this transition should be sharp. However, all polymers that crystallise exhibit both T_g and T_m corresponding to their behaviour of ordered and disordered portions known as semi-crystalline polymer.

When two polymers are fully miscible a single glass transition temperature is observed between the T_gs of the pure materials. The position of T_{gblend} can be predicted by the Fox equation, Equation 3.76

$$\frac{1}{T_{gblend}} = \frac{W_A}{T_{gA}} + \frac{W_B}{T_{gB}}$$

Equation 3.76

where W_A and W_B are the weight fraction of each polymer whose glass transition temperatures are T_{gA} and T_{gB} respectively. When the polymers do not form a miscible blend two glass transition temperature will be observed corresponding to those of two pure polymers. Intermediate cases exist where the polymers are partially miscible so that two T_gs are still observed but they are both between that of a fully phase separated blend. T_g is a kinetic effect, it is dependent on thermal prehistory and the physical method by which it is determined. T_g can be measure among other methods by differential scanning calorimetry (DSC) and dynamic mechanical analysis (DMA).

3.10 The Principles of Dynamic Mechanical Analysis[98-99]

Dynamic mechanical analysis (DMA) is becoming more commonly seen in the analytical laboratory. DMA can be simply described as applying an oscillating force to a sample and analyzing the material's response to that force (Figure 3-16).
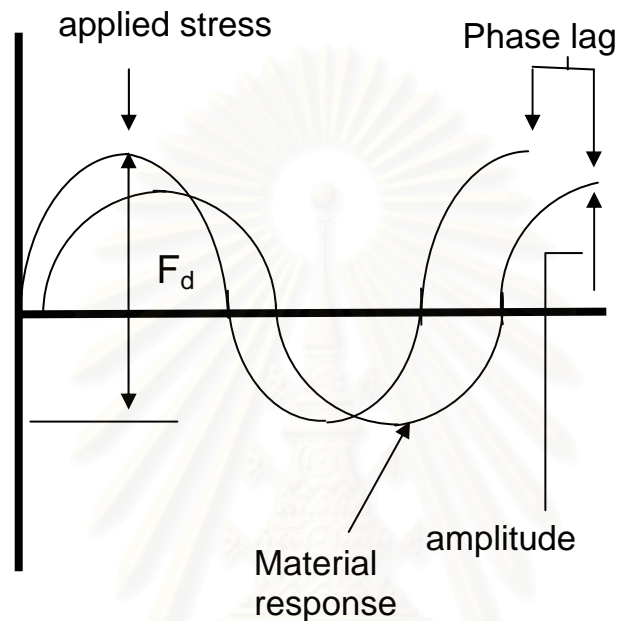
Figure 3-16 How a DMA works. [98]

The modulus measured in DMA is, not exactly the same as the Young's modulus of the classic stress-strain curve. Polymeric materials show both elasticity and flow, hence, 'viscoelasticity', where the stress and strain curves are out of phase by a value less than 90°. DMA applies a stress and measures the strain as well as the phase angle between them. The modulus can then be resolved into an in-phase storage component and an out of phase loss component. The damping factor or loss tangent (tan δ), is the amount of energy dissipated as heat during the loading/unloading cycle exerted on the sample by the DMA.
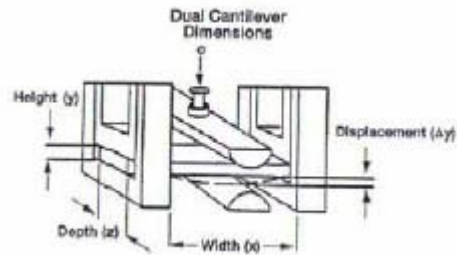
Figure 3-17 Dual cantilevers. [98]

Cantilever fixture clamp the ends of the specimen in place, introducing a shearing component to the distortion and increasing the stress required for a set displacement. Two types of cantilever fixture are normally used: dual cantilever and single cantilever. Both cantilever geometries require the specimen to be true as described above and to be loaded with the clamps perpendicular to the long axis of the sample. In addition, care must be taken to clamp the specimen evenly, with similar forces, and not to introduce a twisting or distortion in clamping. Moduli from dual cantilever fixtures tend to run 10-20% higher than the same material measured in three-point bending. This is due to shearing strain induced by clamping the specimen in place at the ends and center, which makes the sample more difficult to deform.

CHAPTER IV

EXPERIMENTAL METHOD

4.1 Materials

Three different molecular weights of Bisphenol A- polycarbonate were used in this study, PC27K (number-average molecular weight, $\bar{M}_n$ = 16,440 g/mol, polydispersity index, $\bar{M}_w/\bar{M}_n$ = 1.69) supplied by Bayer Polymer Co., Ltd. PC24K ($\bar{M}_n$ = 13,666 g/mol, $\bar{M}_w/\bar{M}_n$ = 1.81) and PC39K ($\bar{M}_n$ = 25,258 g/mol, $\bar{M}_w/\bar{M}_n$ = 1.57) were purchased from Aldrich Chemical Company, Inc. Molecular weights were determined via gel permeation chromatography based on polystyrene standard using chloroform as the solvent.

Deuterated polycarbonate, dPC, ($\bar{M}_n$ = 22,400 g/mol, $\bar{M}_w/\bar{M}_n$ = 1.83) was purchased from Polymer Source, Inc. Molecular weights were also determined via gel permeation chromatography using chloroform as the solvent.

The LLCs used in this study were obtained from Merck Co. Ltd. and are commercially known as CBC33 and CBC53. They were received in the form of a white powder. 4, 4'-Bis-(4-propyl-cyclohexyl)-biphenyl (CBC33) and 4'-(4-Pentyl-cyclohexyl)-4-(4-propyl-cyclohexyl)-biphenyl (CBC53) were chosen as the low molar mass liquid crystal because they exhibit a nematic phase in the same range as the typical processing temperatures of polycarbonates.[22,23]
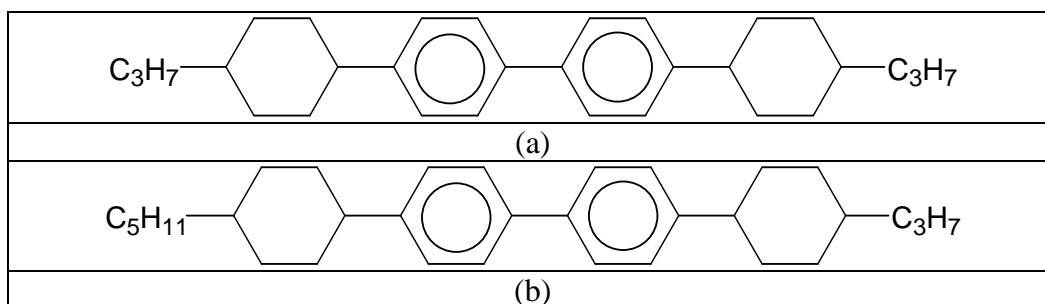
Figure 4-1 The chemical structures of low molar mass liquid crystal (a) CBC33
(b) CBC53

The molecular structures of the LLCs are shown in **Figure 4-1** and their molecular weight characteristics, transition temperature and other physical properties are shown in **Table 4-1**

Table 4-1 Properties of low molar mass liquid crystals.

Property	CBC33	CBC53
Melting Point (^{o}C)	158	64
Smectic-nematic temperature (^{o}C)	223	250
Clearing temperature (^{o}C)	327	317
Molecular weight (g/mol)	403	431

4.2 Small Angle Light Scattering (SALS)

4.2.1 Phase boundaries

For amorphous systems, homogeneous mixtures are usually transparent whereas heterogeneous mixtures are cloudy as a result of the refractive index difference between the two components. Variations of temperature, pressure and compositions of the mixture can change a miscible blend to immiscible (which results in a change from being transparent to cloudy). The first appearance of cloudiness denotes the cloud point (T_c). Using light scattering technique it is possible to investigate the phase separation phenomena. It should be noted that to make use of the scattering technique,

not only can a laser light source be used, but also x-ray and neutron are available as well. The latter two are particularly useful if the phase separation is occurring over length scales that are much less than the wavelength of visible light.

4.2.2 Equipment Details

The study of miscibility was performed using light scattering apparatus at the Department of Chemical Engineering, Chulalongkorn University, Thailand. A He/Ne laser of 5 mW (λ = 632.8 nm.) was used as an incident light source. Samples were placed on a LINKAM hot stage, which was mounted between the laser and CCD camera. The temperature of the LINKAM hot stage was controlled by a computer. The light scattering pattern is captured by the CCD camera and analysed using the Image-Pro Plus 3.0 program.

4.2.3 Sample preparation

Blends of various compositions were prepared by the solution casting method. Thin films of the blends were completely transparent for the weight fraction 10% and less. Consequently, we chose the liquid crystal contents of 1,2,4,6,8 and 10% by weight to study miscibility of the blends. The desired amounts of PC and LLC were dissolved in chloroform and stirred for 4 hours. The samples were dried in a vacuum oven at 40°C for 24 hours.

4.2.4 Cloud Point Determination for PC/LLC blends.

The study of PC/LLC blends phase boundaries was performed using small angle light scattering apparatus. The light scattering pattern was captured by a CCD camera, mounted on an arc between 7-42 degree (q = 0.000208- 0.001110 $\overset{\circ}{A}^{-1}$). The thin film samples were placed on a LINKAM hot stage, and heated at the heating rate of 3°C/min from 50 $^{\circ}$C to 350 $^{\circ}$C.

4.3 Rheological Measurement

From the processing point of view, one of the most fundamental questions is how to determine or predict the rheological properties of the polymer system in term of viscosities of mixing component, composition fraction and temperature. The purpose of this study is to investigate the rheological properties of the blends of low molar mass liquid crystals and polycarbonate, and to examine if a simple viscosity model is applicable to the system studied.

4.3.1 Parallel Plate[71]

The parallel plate geometry was suggested by Mooney[100]. The Mooney tester, which consists of a disk rotating inside a cylindrical cavity, is used extensively in the rubber industry (ASTM D 1646). Russell[101] first measured normal forces from the total thrust between two disks. Greensmith and Rivlin[102] measured the pressure distribution, and Kotaka et al.[103] used total thrust to study normal stresses in polymer melts. In many ways the flow is similar to the cone and plate. Most instruments are designed to permit the use of either geometry.

During the experiment, a few errors could be caused by secondary flow, edge failure, shear heating and non-homogeneous strain field. However, this method provided many advantages. For examples, sample preparation and loading is simpler for very viscous materials and soft solid. Shear rate (and shear strain) can be varied independently by rotation rate Ω (and θ) or by changing gap. Wall slip can be determined by checking measurement at two gaps. Moreover, edge failure can be delayed to high shear rate by decreasing gap during an experiment.
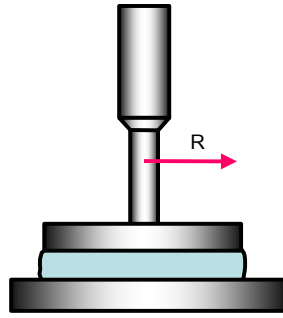
Figure 4-2 Schematic of a parallel plate rheometer.

The parallel plate geometry is sketched in **Figure 4-2** with assumption:

1. Steady, laminar, isothermal flow
2. $v\theta$ (r, z) only, vr = vz = 0
3. Negligible body forces
4. Cylindrical edge

The parallel disk rheometer is also very useful for obtaining viscosity and normal stress data at high shear rates. Shear rate can be increased by either increasing rotation rate or decreasing gap. Errors due to secondary flows, edge effects, and shear heating are all reduced by operating at small gaps.

4.3.2 Equipment Details

The rheological properties of pure polycarbonate and blends were firstly measured using a TA Instruments AR2000. Parallel plates with a diameter of 25 mm. were used to measure the shear viscosity as function of shear rate and the oscillatory shear flow properties as a function of angular frequency.

To confirm the viscosity behaviour is real and reproducible, a HAAKE Rheostress 600 was chose to measure the blend viscosity. The twenty mm. parallel plates were used to measure the oscillatory shear flow with increased and then decreased angular frequency on the same specimen.

4.3.3 Sample preparation

The samples for rheology measurements were prepared by solution casting in a common solvent. The amounts of LLCs used in the blends were 1, 2 and 5% by weight. Note that, these compositions are inside the miscible regime from the light scattering results. The PC and LLC were dissolved in chloroform at 14% w/v. and stirred for 4 hours. The solvent was then slowly evaporated at room temperature for 24 hours. In order to remove residual solvent, the samples were further dried in a vacuum oven at 40°C for 3 days. The blends were prepared as discs by compression moulding at 255°C. The samples were removed from the stainless mould prior to the rheological measurements.

4.3.4 Rheological Measurement

The disc-shape samples were used to measure the shear viscosity and the oscillatory shear flow properties. The shear viscosity, η, as a function of shear rate, $\dot{\gamma}$, at a fixed temperature of 255 $^{\circ}$C and the range of shear rates employed, from 1×10^{-2} to 1×10^{2} s^{-1}, were measured. The storage modulus, G', loss modulus, G", and dynamic complex viscosity, η^{*}, were measured as a function of angular frequency, ω, from 1×10^{-1} to 1×10^{2} rad/s at three different temperatures, 255 °C, 260 °C and 265 °C.

4.4 Nuclear Reaction Analysis (NRA)

4.4.1 Introduction to NRA

Nuclear Reaction Analysis (NRA) is one of ion beam techniques for depth profiling deuterium, first used to detect trace amounts of deuterium in materials such as silicon[104] and later for studying polymer. In an NRA experiment the products of a nuclear reaction between the incident ion and the target nucleus detected. An incident ^{3}He ion reacts with deuterium in the sample. These incident ions may undergo nuclear reactions with deuterium atoms, fusing to form a short-lived compound nucleus of ^{5}Li. This intermediate rapidly disintegrates to a proton and alpha particle (^{4}He).

$$^3He + {}^2H \longrightarrow {}^4He + {}^1H + Q$$
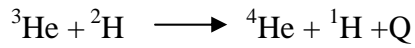
The protons and alpha particles are ejected from the sample and their energy and number collected using a particle detector.
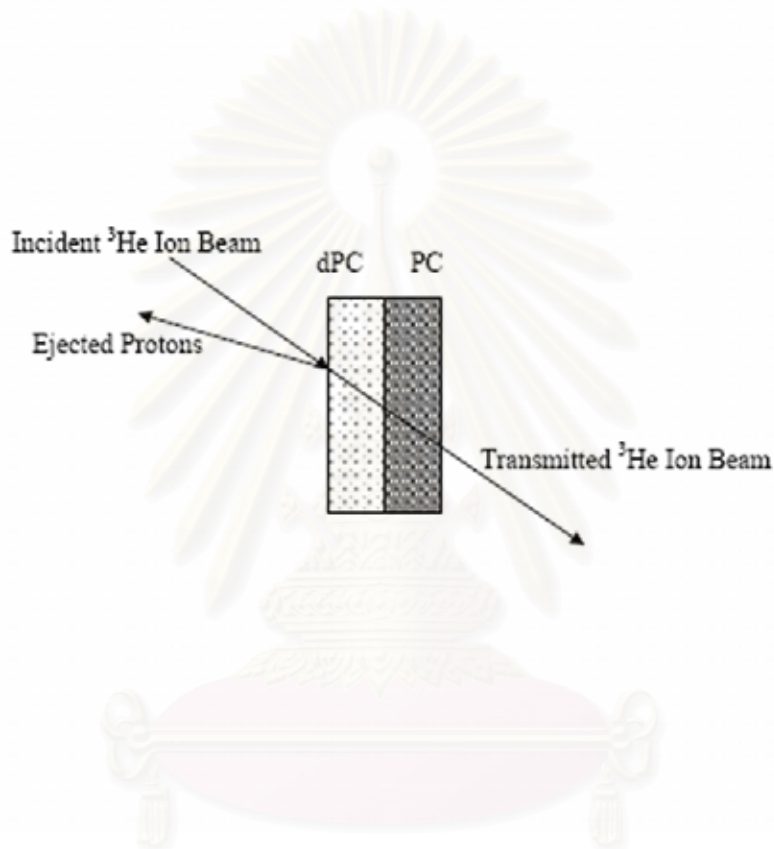
Figure 4-3 Incident ^{3}He ion beam and ejected proton detection geometry.

As the incident ion ^{3}He, with energy E_0, collides with the sample, the single electron is stripped, leaving a doubly charged nucleus. Subsequent to reaction with deuterium, the outgoing ^{4}He and ^{1}H have energies much higher than the incident ion energy E_0. In a typical experimental set up with E_0=700 KeV the outgoing ^{4}He and ^{1}H have different energies[105]. The energy of the ejected particles will be dependent on the energy of the incident ^{3}He ion at the depth of collision and reaction[106]. The high energy protons produced exit the sample with negligible energy loss due to electronic interactions. The ejected ^{4}He ions will be influenced by the electronic interactions and their energy at the detector will be dependent upon the depth of the reaction and ^{4}He

stopping powers within the sample. Hence the energy and yield of particles interacting with the detector can be measured and the counts for a given energy of particle can be recorded. And as the energy change with depth, the detected energy range can be converted into a depth profile. The depth resolution can be varied by varying the angle of incidence of the ^{3}He beam. A calibration experiment can be carried out to determine the energy per channel. The silicon wafer with thin layer of gold is analysed using an analysis software program. The program allows a simulation to be built and fitted to experimental ion beam data. It is most suited to elemental analysis but not polymer system. For a target sample that is not a pure element, it is assumed that the target atoms contribute independently to the total energy loss. This allows the stopping powers to be calculated by a software program called SRIM® (Stopping range of ions in matter). The program can be used to calculate the stopping powers of various polymers. Alternatively, the stopping powers can also be determined experimentally from a film of known thickness to establish the energy lost by the nuclei whilst traveling out of the sample.

4.4.2 Equipment Details

NRA experiments were carried out at the ion beam facility of the Durham University. NEC 5SDH Pelletron accelerator (Figure 4-4) was used to convert ^{3}He or ^{4}He gas to plasma of positive helium ions. The beam of positive ions produced needs to be focused by using eletromagnets that can be fine-tuned to achieve the correct beam shape. Within the accelerator, the ion beam is under high vacuum from the ion source to the end chamber. The beam of ions is steered and focused towards the end station, which holds the samples to be analysed. In an NRA experiment, the products of nuclear reactions between the incident ion and the target nucleus are measured.

4.4.3 Sample preparation

Samples for NRA were prepared by spin casting technique from a co-solvent solution (1:1 choroform and toluene). Films spun from a chloroform-only solution were found to be too rough for NRA measurements.[56] The dilution of PC and dPC into a chloroform/toluene solution resulted in flat films. The thickness of the blend layers was measured by a D-5000 reflectometer and the thickness analysed using the Win-Refsim version 1.2 software program to fit the fringes. Films of dPC/LLC blends were spin coated onto a microscope slide and then peeled off by floating onto deionized water, after which the films were picked up and laid onto a PC/LLC blend which had been spin coated directly onto a silicon wafer. The bilayer film of dPC/PC was dried for a few hours at room temperature and then further dried overnight under vacuum at 80°C.

4.4.4 NRA Experiment

Bilayer samples were broken up into small pieces (approximately 2.25 cm^2) and annealed under vacuum at temperature 170°C (above the Tg of PC) for 1,2,4,8 and 24 hrs. Annealed samples were held in moveable vertical rack, controlled by a sample manipulator. The initial energy 0.7 MeV was used to determine the depth distribution of dPC at an incident beam angle 70°. The products of nuclear reactions between the incident ion and the target nucleus are measured.

Rubidium oven, Produces Rubidium vapour used to convert positive helium ions to neutral or negative charge

Pelletron accelerator

Einzel lens. Focuses negative ions.

High Voltage power supply for pelletron

Bending magnet used for ion selection

Endstation; containing detectors, sample rack, Mylar Film, triple alpha source and sample manipulator

Beam profile monitor

Quadropole magnets

Beam profile monitor

Gap lens. Used to extract negative He ions towards pelletron

Turbo Pump

X and Y direction steering magnets

Source; 100kHz radio frequency pulse converts He has to a plasma of helium ions. Held under a constant potential of 6kV.

N_2 stripper gas inlet. N_2 is then held inside pelletron.

Quadropole magnets

Beam Line Valve; ensures that air does not leak into system

Beam Current integrator
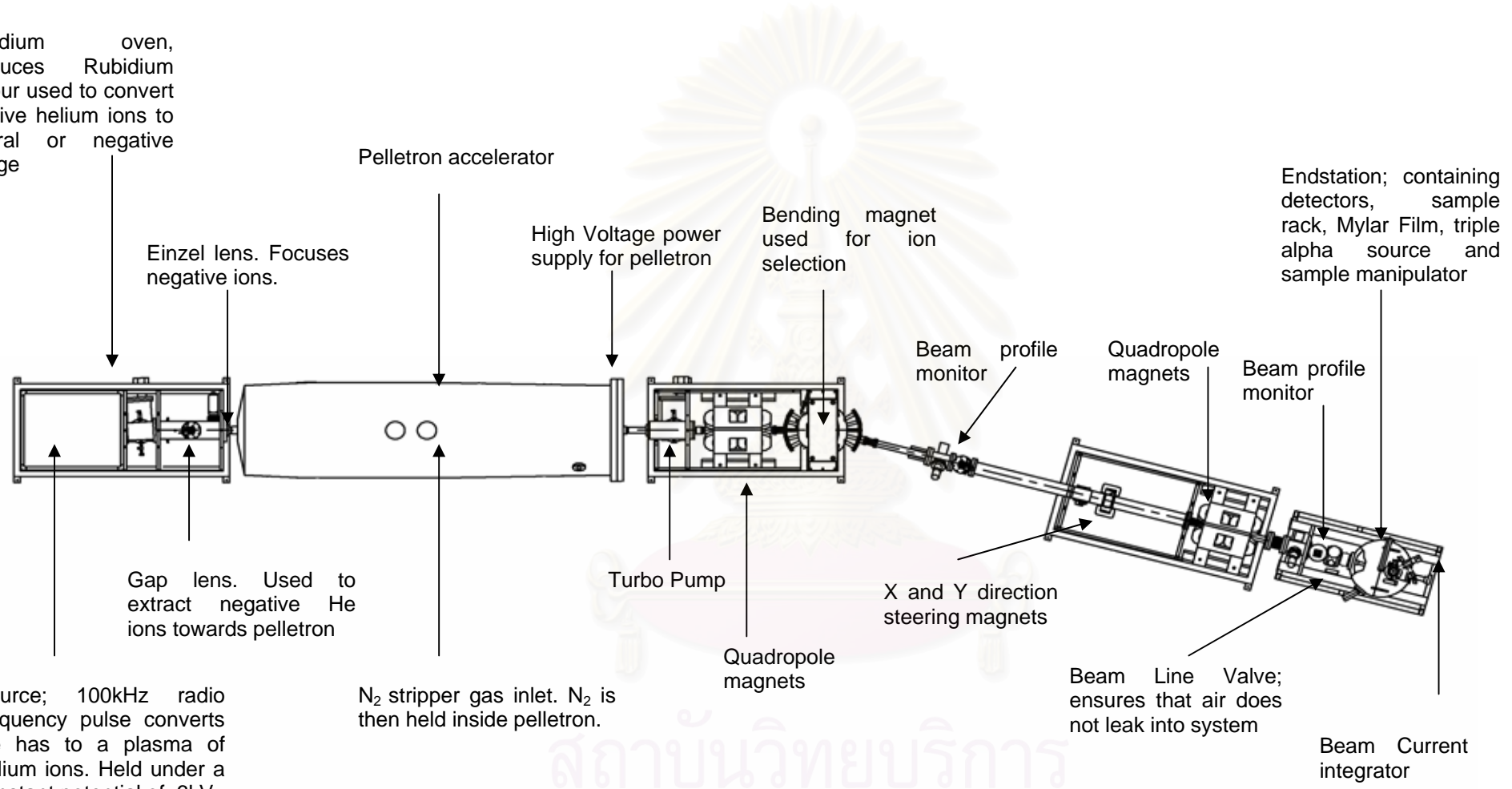
Figure 4-4 Schematic of 5SDH accelerator in Materials Chemistry Building, Durham[107].

4.5 Dynamic Mechanical Analysis (DMA)

The most commonly used method to measure viscoelastic properties as a function of temperature and time (frequency) is dynamic mechanical analysis, which records the response to an application of a sinusoidal strain. Commercial dynamic testing instruments are available for operation in several mode of deformation (e.g. tensile, torsion, shear, compression and flexure) over several decades of frequencies. The principles of dynamic-mechanical analysis are described in section 3.10.

4.5.1 Equipment Details

In order to study the T_g of the blends, dynamic mechanical analysis measurements were taken, using a dual cantilever on a TA instruments DMA Q800.

4.5.2 Sample preparation

The blends for DMA measurement were prepared via the same method as rheological measurement. The sample dimension was approximately 40mm x 9mm x 0.8 mm.

4.5.3 DMA Experiment

The frequency was fixed at 1 Hz and a heating rate of 2^oC/minute utilized. The samples were heated from 100 -175^oC. The storage modulus, loss modulus and tanδ were determined.

CHAPTER V

RESULTS AND DISCUSSIONS

In this research, low molar mass liquid crystal was selected as a polycarbonate additive for reducing viscosity of the blends. The cyclohexylbiphenylcyclohexane backbone liquid crystals, CBC33 and CBC53, were chosen because it was assumed that their anisotropic nature would reduce melt viscosity of the blends. The miscibility and rheological properties of polycarbonate and their blends with low molar mass liquid crystal were investigated. The effect of concentration on the interdiffusion and the glass transition temperature were also studied.

5.1 The role of low molar mass liquid crystal to the miscibility of the blends.

In order to check the phase boundary, we attempted to obtain transparent blends for light scattering experiments. By using the preparation method mentioned earlier, the transparent blends could only be made at the LLC composition below 10%. It is assumed from this simple observation that the cloudy samples are phase separated blends and the clear samples are probably miscible blends.

In order to investigate in further detail of the miscibility, light scattering experiments were performed on the clear samples which are the blends at LLC weight fraction lower than 10%. The phase diagrams were obtained by observing the scattered light intensities while heating samples from the one phase region into the two phase region. From Figure 5-1 and 5-2 the intensity of the scattered light as a function of temperature indicates that the PC39K/LLC blends are miscible for weight fraction of LLC less than 6% over the entire observed temperature range. In contrast, LLC weight fraction of 6,8 and 10% show partial miscibility with PC.

When phase separation occurs, because the two different phases have different refractive indices, there is an increase in the scattered intensity. The partially miscible blends, which are initially clear, become cloudy after heating, indicating lower critical solution temperature (LCST) behaviour.
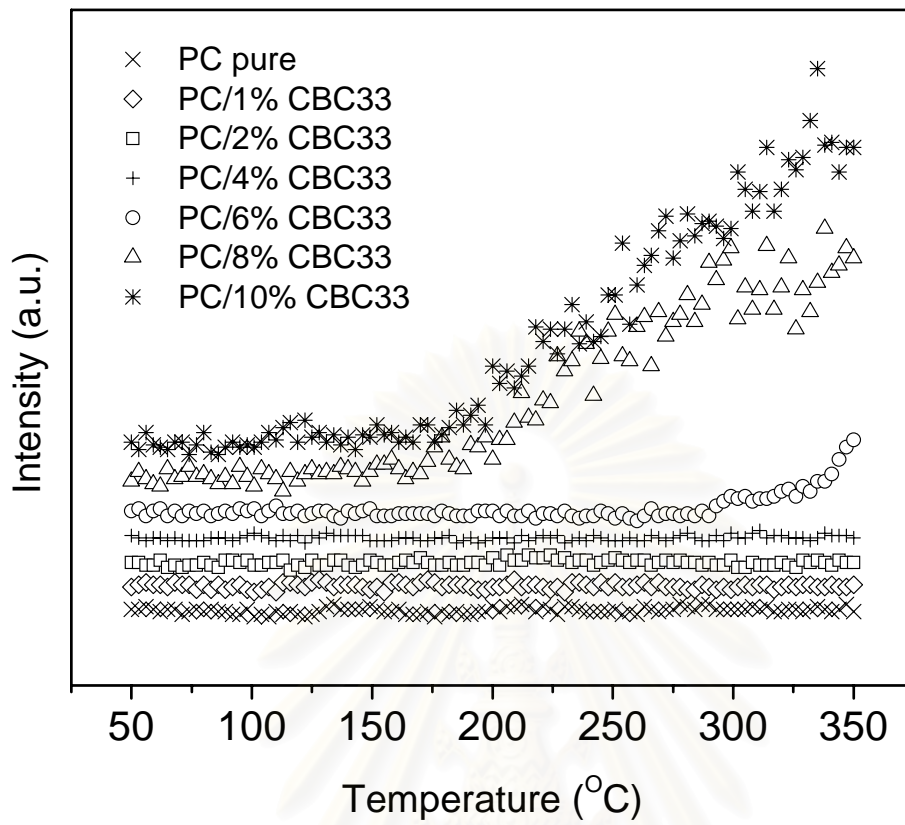
Figure 5-1 Plots of scattered light intensity against temperature for PC39K/CBC33

blends at the heating rate 3.0 °C/min from the specific q = 0.000950 $\overset{o}{A}^{-1}$
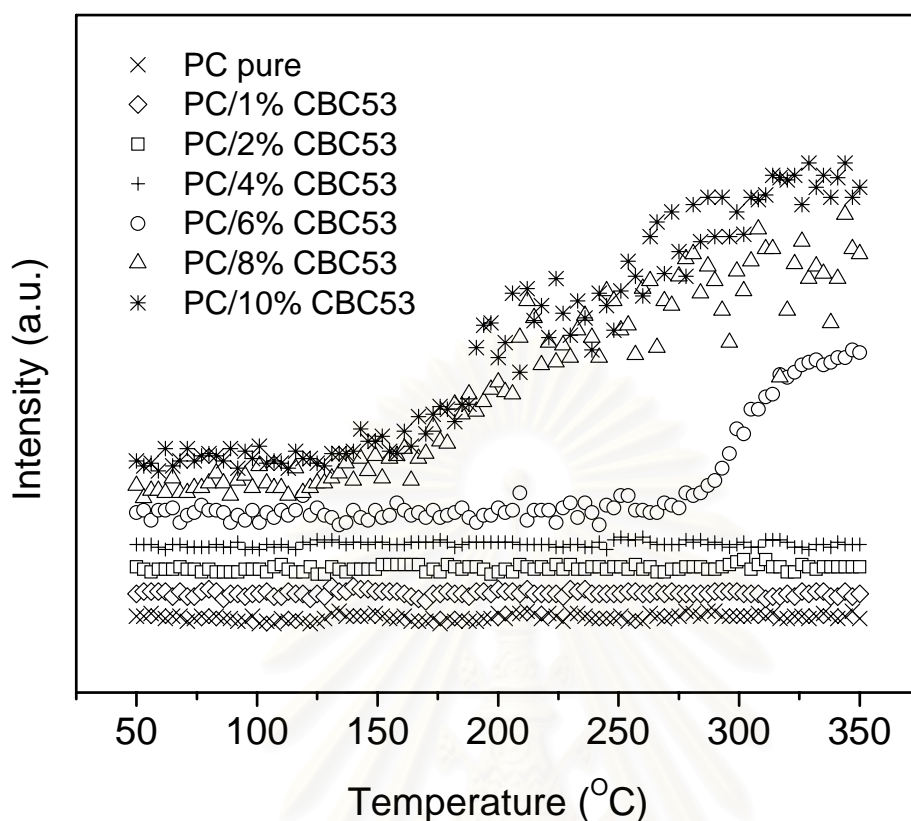
Figure 5-2   Plots of scattered light intensity against temperature for PC39K/CBC53

blends at the heating rate 3.0 ^{o}C/min from the specific q = 0.000950 $\overset{o}{A}^{-1}$

The temperature at which the scattered intensities start to increase, as that shown in Figure 5-1 and 5-2 is defined as the cloud point (T_c). Cloud point curves for PC/LLC blends as observed at the specific scattering vector, q = 0.000950 $\overset{o}{A}^{-1}$, which clearly exhibits an increase in scattered intensity, are shown in Figure 5-3. It can be seen that CBC53 has a higher effect on the phase separation temperature than CBC33. At temperatures below the cloud point curve, the samples are transparent and homogeneous. In other words, at the temperatures above this curve, phase separation occurs. From the result of the phase behaviour, all the further study was performed inside the miscible regime where the LLC concentration was less than 6% to prevent the effect from phase separation.
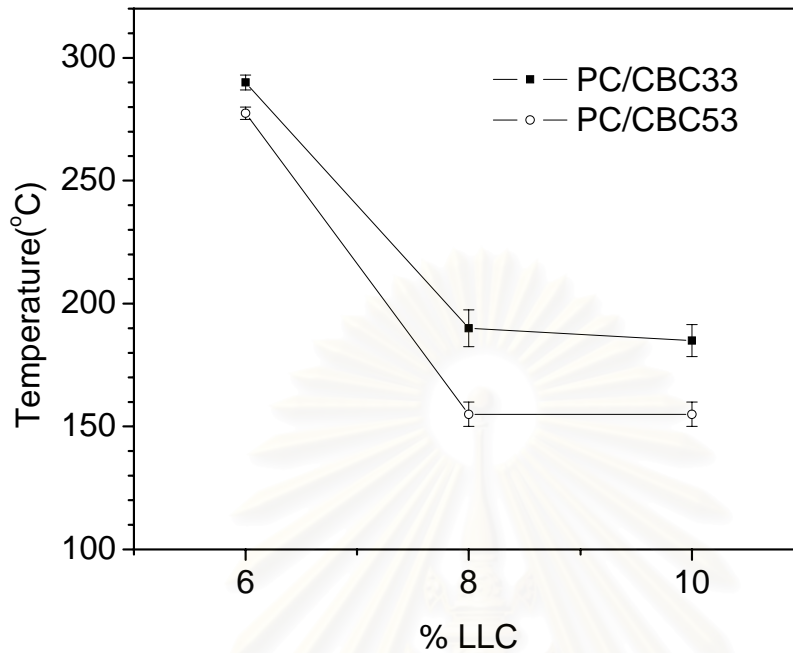
Figure 5-3   Cloud point curves of PC39K/LCC determined by small angle light
                   scattering technique.

5.2 The Rheological Properties according to low molar mass liquid crystal.

Rheological properties characterise the flow behavior of polymers. For Newtonian
liquids, the viscosities are constant and only dependent on temperature and pressure. For
polymeric materials, the rate of deformation is also a key factor, resulting in the
phenomenon of viscoelasticity, in which the response of a material to a deformation
depends on the timescale over which the deformation is applied. Since the macroscopic
viscoelasticity and the microscopic molecular dynamics of polymers are related to each
other, an understanding of the viscoelastic response of a material can be used to elucidate
the molecular motion of polymers. Moreover, the melt viscosity data is of considerable
practical importance in polymer processing because it relates the flow properties to the
operating conditions.

5.2.1 Simple shear viscosity

The shear viscosity, η, as a function of shear rate, $\dot{\gamma}$, for the three miscible blends and for the pure PC at a fixed temperature of 255 $^{\circ}$C and the range of shear rates employed, from 1×10^{-2} to 1×10^{2} s^{-1}, are shown in Figure 5-4 and Figure 5-5.

From the results of the shear viscosity, it can be seen that all the blends exhibit 4 regions of viscosity behaviour. At low shear rates, from 1×10^{-2} s^{-1} to ~ 5×10^{-2} s^{-1}, the melt viscosity of pure PC and the blends are very similar. At higher shear rates, all blends undergo clear shear-thinning, presumably as a consequence of the alignment and resultant anisotropic properties as Onogi and Asada described for liquid crystals and liquid crystal polymers.[20,23] The pure PC only exhibits two rheological regimes, as expected for entangled polymer melts. An abrupt reduction in shear viscosity of the blends was observed with only 1% by weight LLC, whilst the 2% and 5% LLC blends show a smaller decrease compared with the impact of 1% LLC, relative to the LLC content increase. It can be seen from comparison of figures 4a & 4c and 4b & 4d, the LLCs have a greater impact on the viscosity of the lower molecular weight PC. The shear viscosity of PC39K/1%CBC33 was reduced about 57%, while the viscosity of PC39K/1%CBC53 was reduced about 66% in comparison with that of pure PC39K. In the case of PC27K, the viscosity of 1%CBC33 blends and 1%CBC53 blends decrease about 78% and 83% respectively. Similar characteristics were found for both types of LLC. However, CBC53 decreases the melt viscosity of the blends slightly more than the CBC33. This may be due to a tendency of the CBC53 to undergo greater alignment in a shear flow, due to its slightly greater length.

(a)

(b)
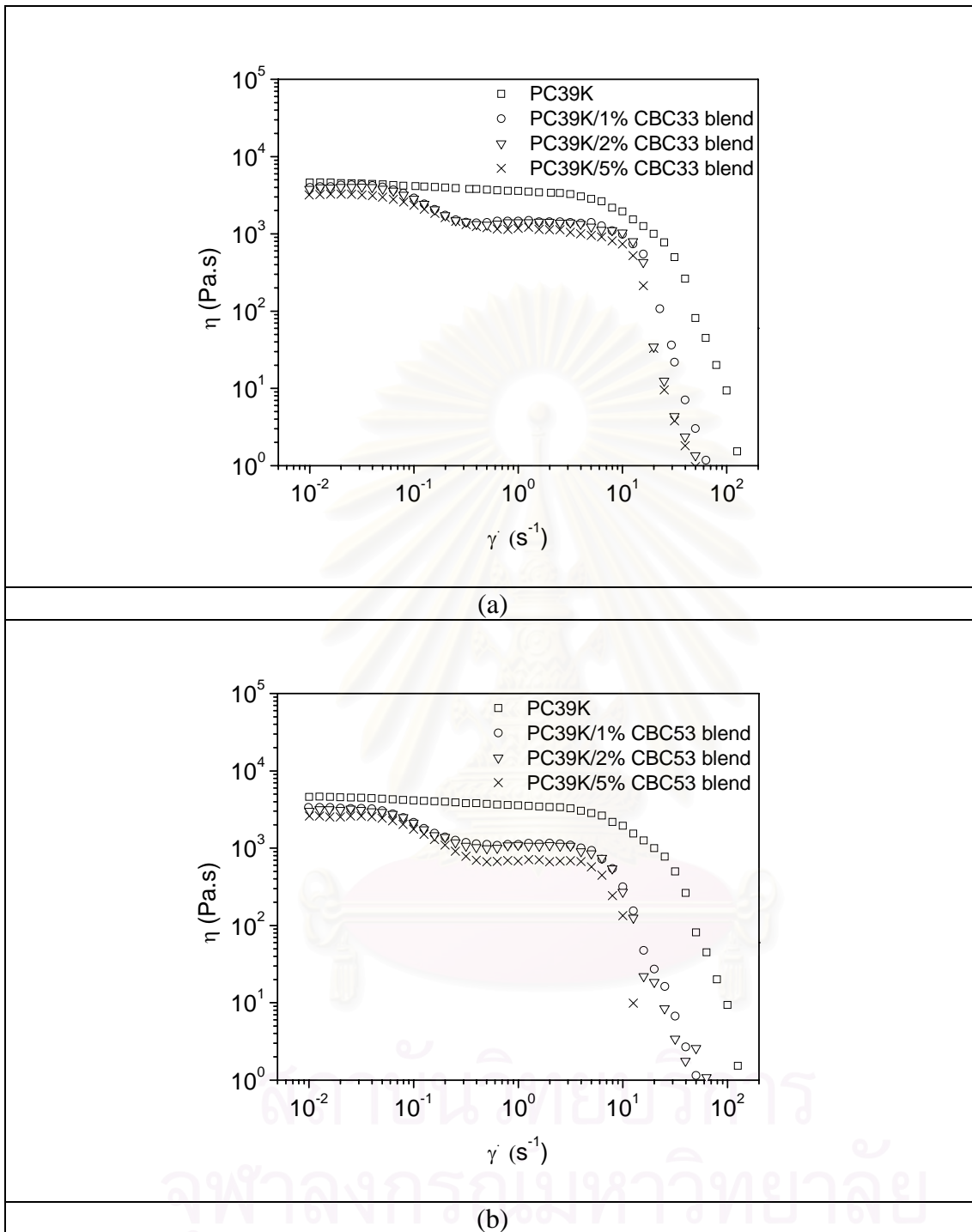
Figure 5-4   Steady shear viscosity of (a) PC38K/CBC33 blends, (b) PC38K/CBC53 blends at 255 °C
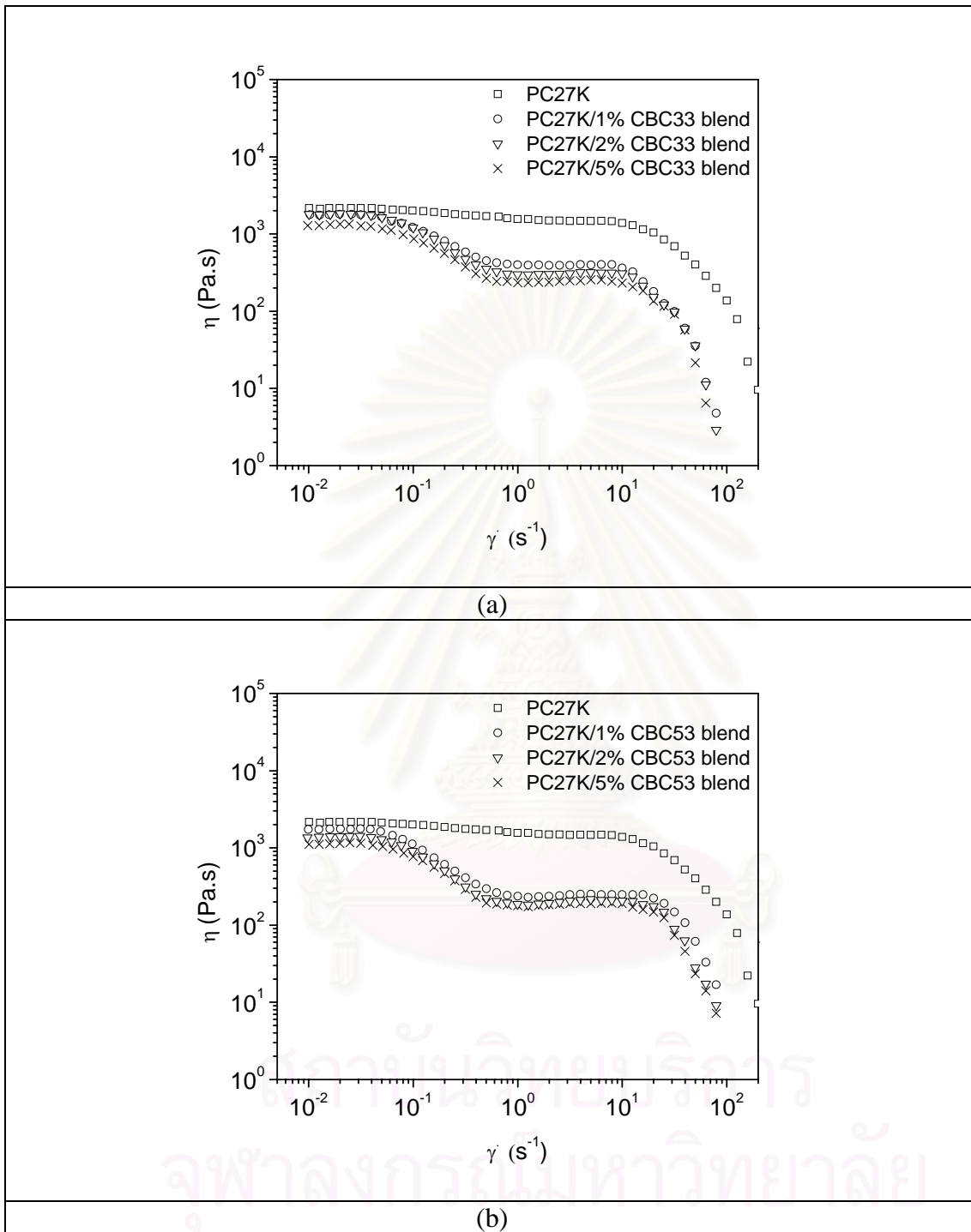
Figure 5-5   Steady shear viscosity of (a) PC27K/CBC33 blends, (b) PC27K/CBC53 blends at 255 ^{o}C

5.2.2 Complex viscosity

The storage modulus, G', loss modulus, G", and dynamic complex viscosity, η^*, were measured as a function of angular frequency, ω, from 0.1 to 100 rad/s at three different temperatures, 255 °C, 260 °C and 265 °C. Complex viscosity versus angular frequency for pure PC and the blends are shown in Figure 5.6 to Figure 5.11.

The influence of LLC on the complex viscosities of the blends was similar to the influence on the steady shear viscosity, with the frequency dependent viscosity decreasing as LLC concentration increased. However CBC53 decreased the complex viscosity of the blends more than the CBC33, and the most pronounced decrease in viscosity was observed upon addition of only 1% by weight LLC. Further increases in LLC content further reduced the viscosity but again by a lesser relative extent.

By studing the viscosity, it was found that both complex and steady shear viscosities of the blends were significantly decreased upon the addition of LLC. The question raised was would other relate parameters have changed to account for this phenomenon. The shear moduli and the diffusion coefficient of the blends were then investigated and discussed in detail in section 5.2.3 and 5.3.
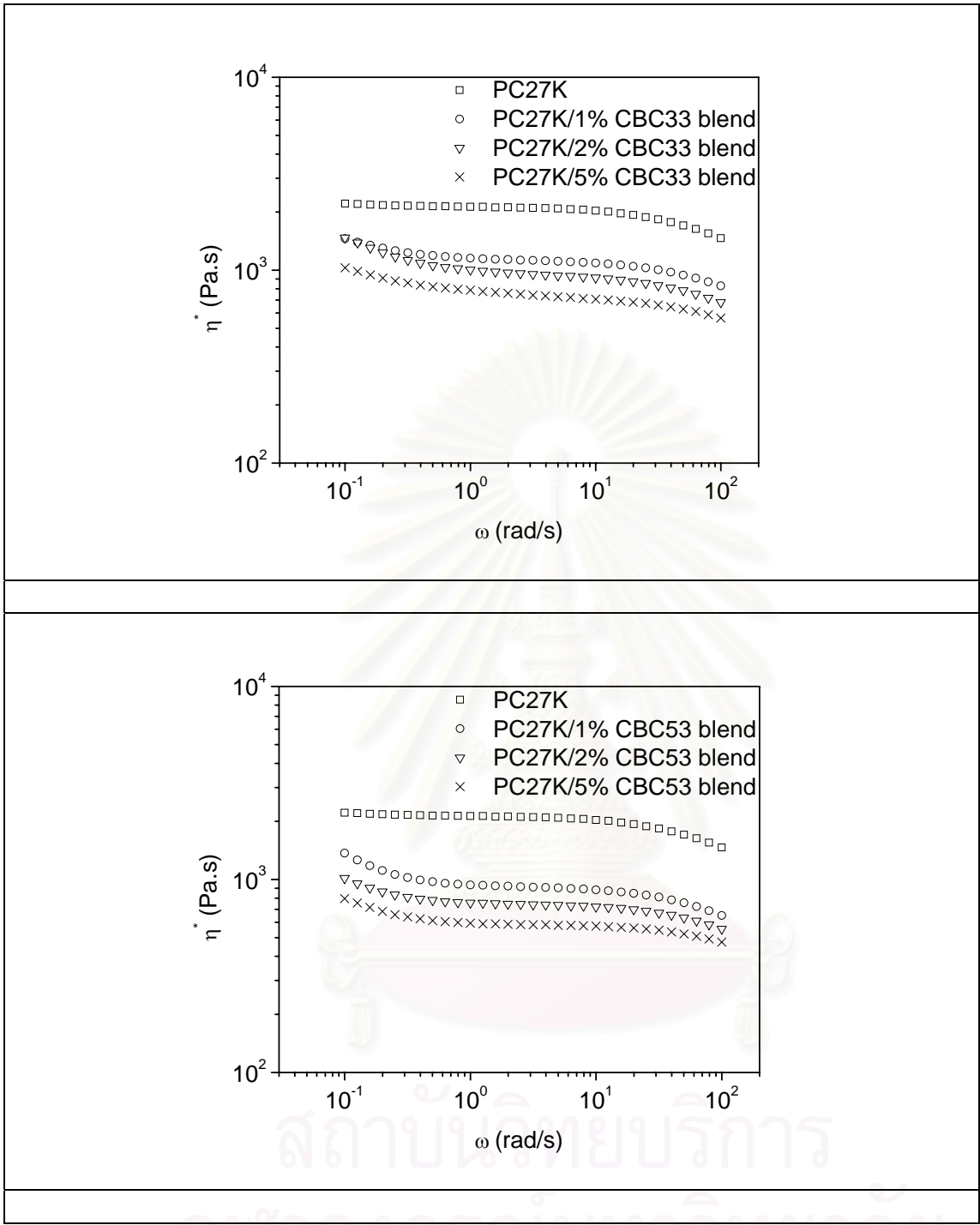
Figure 5-6   Complex viscosity of (a) PC27K/CBC33 blends, (b) PC27K/CBC53 blends at 255 °C.
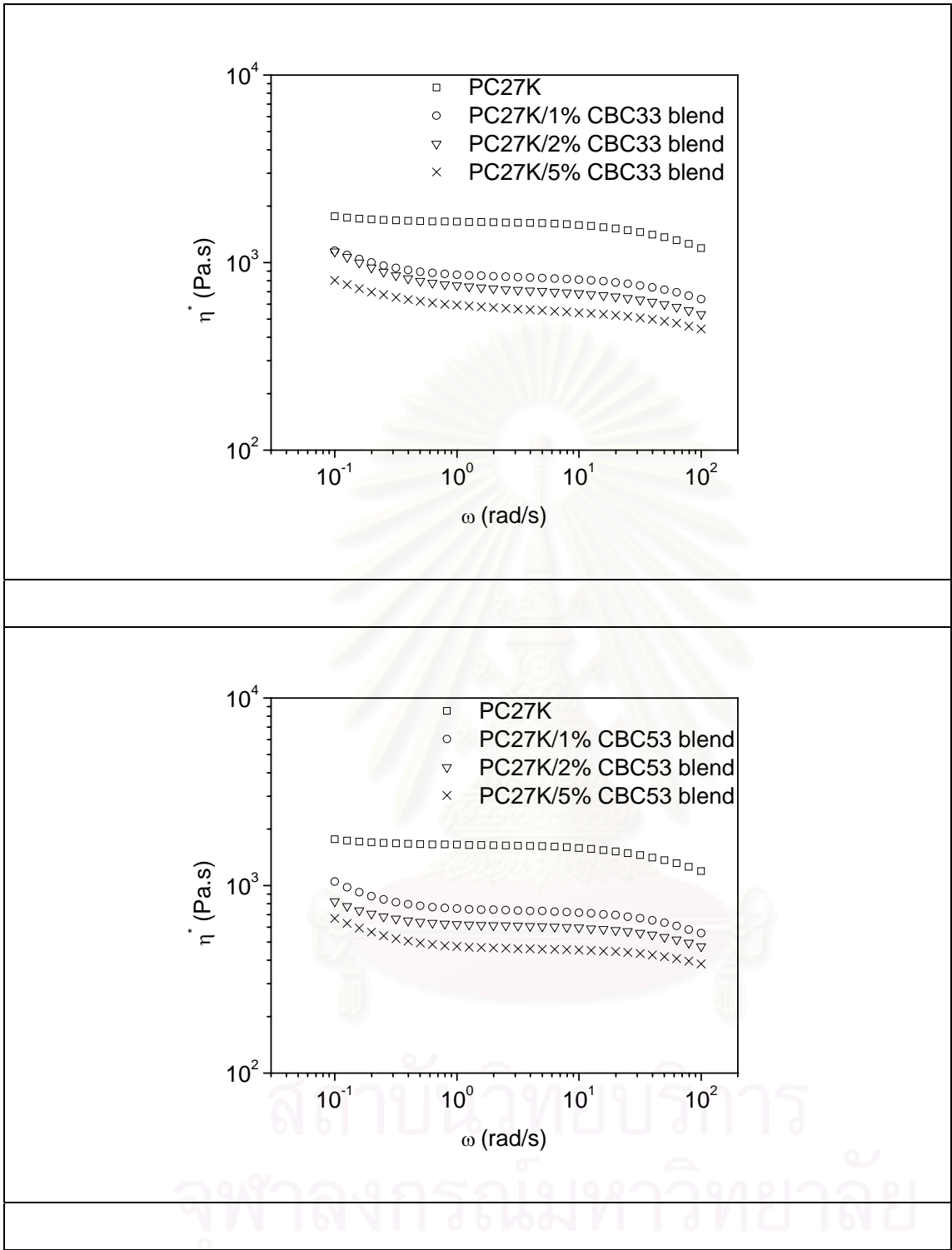
Figure 5-7   Complex viscosity of (a) PC27K/CBC33 blends, (b) PC27K/CBC53 blends at 260 $^{\circ}$C.
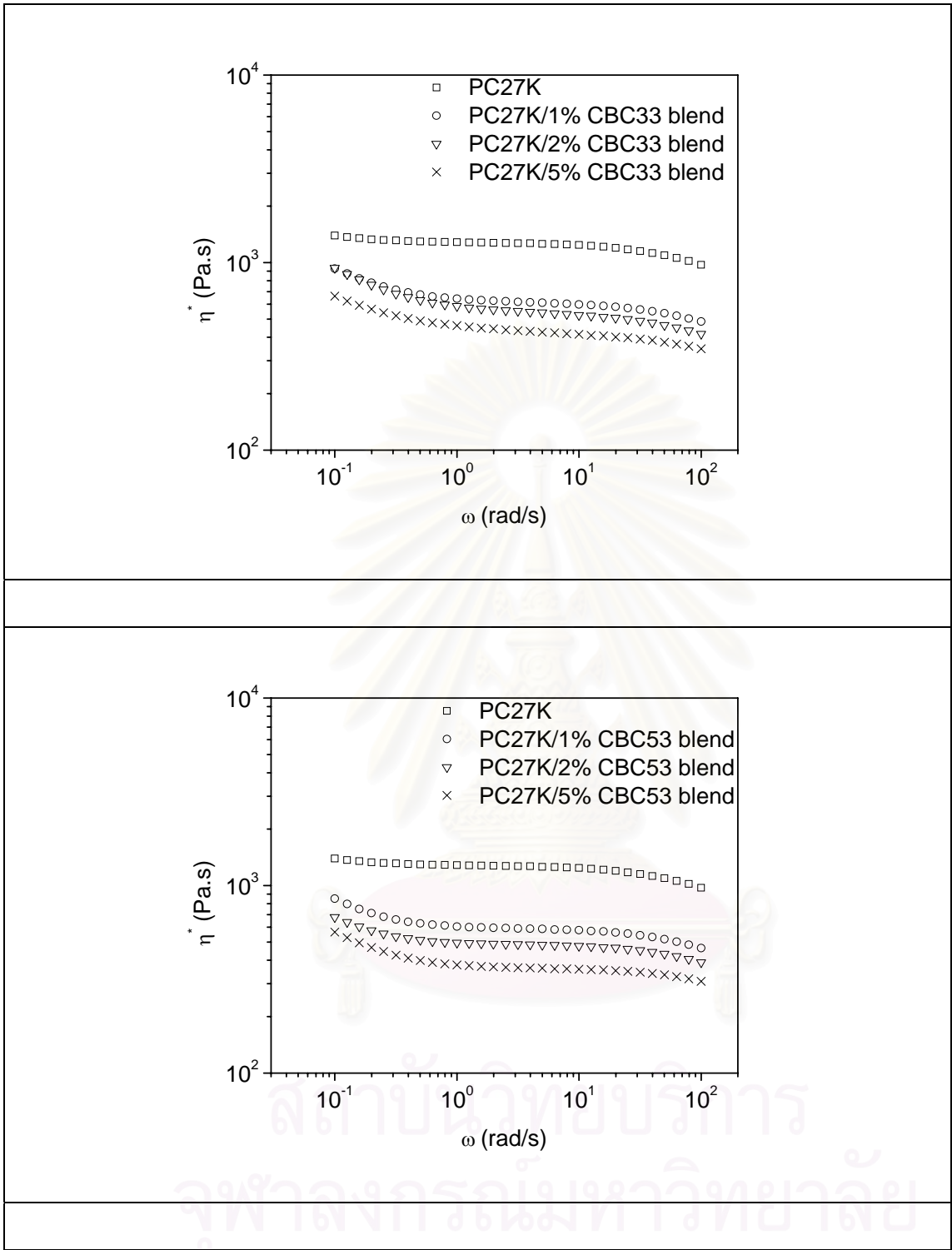
Figure 5-8   Complex viscosity of (a) PC27K/CBC33 blends, (b) PC27K/CBC53
blends at 265 °C.
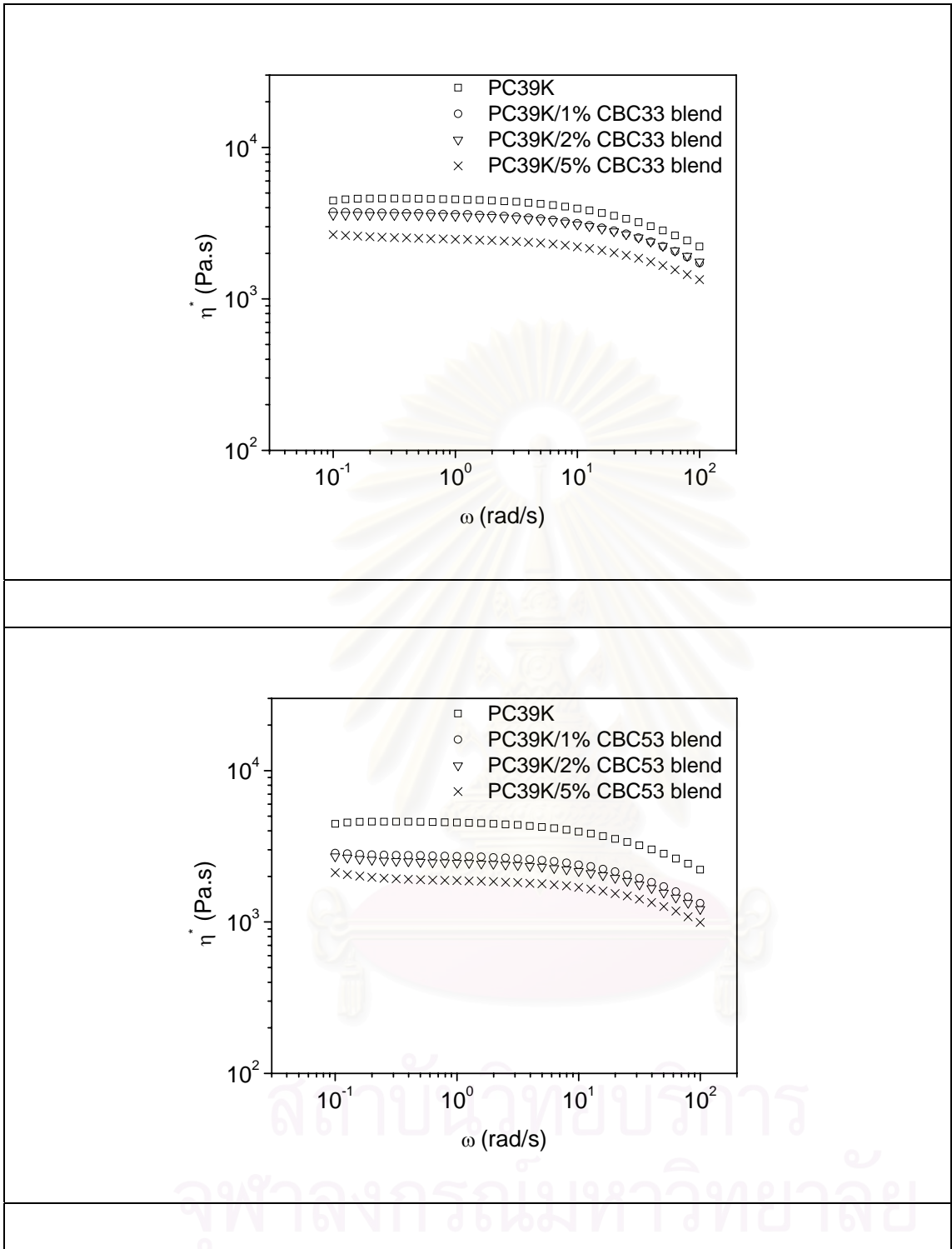
Figure 5-9 Complex viscosity of (a) PC39K/CBC33 blends, (b) PC39K/CBC53 blends at 255 °C.
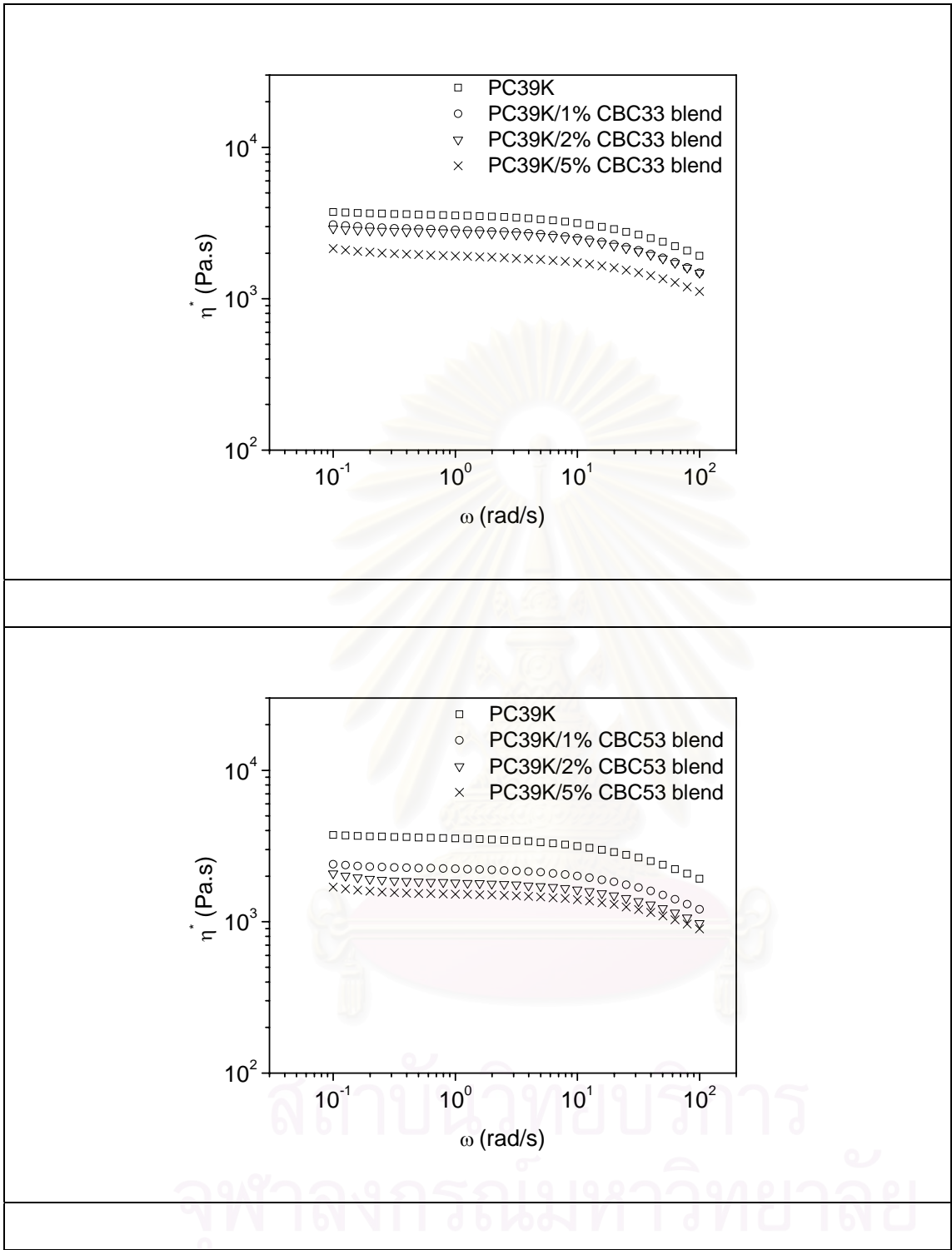
Figure 5-10 Complex viscosity of (a) PC39K/CBC33 blends, (b) PC39K/CBC53 blends at 260 °C.
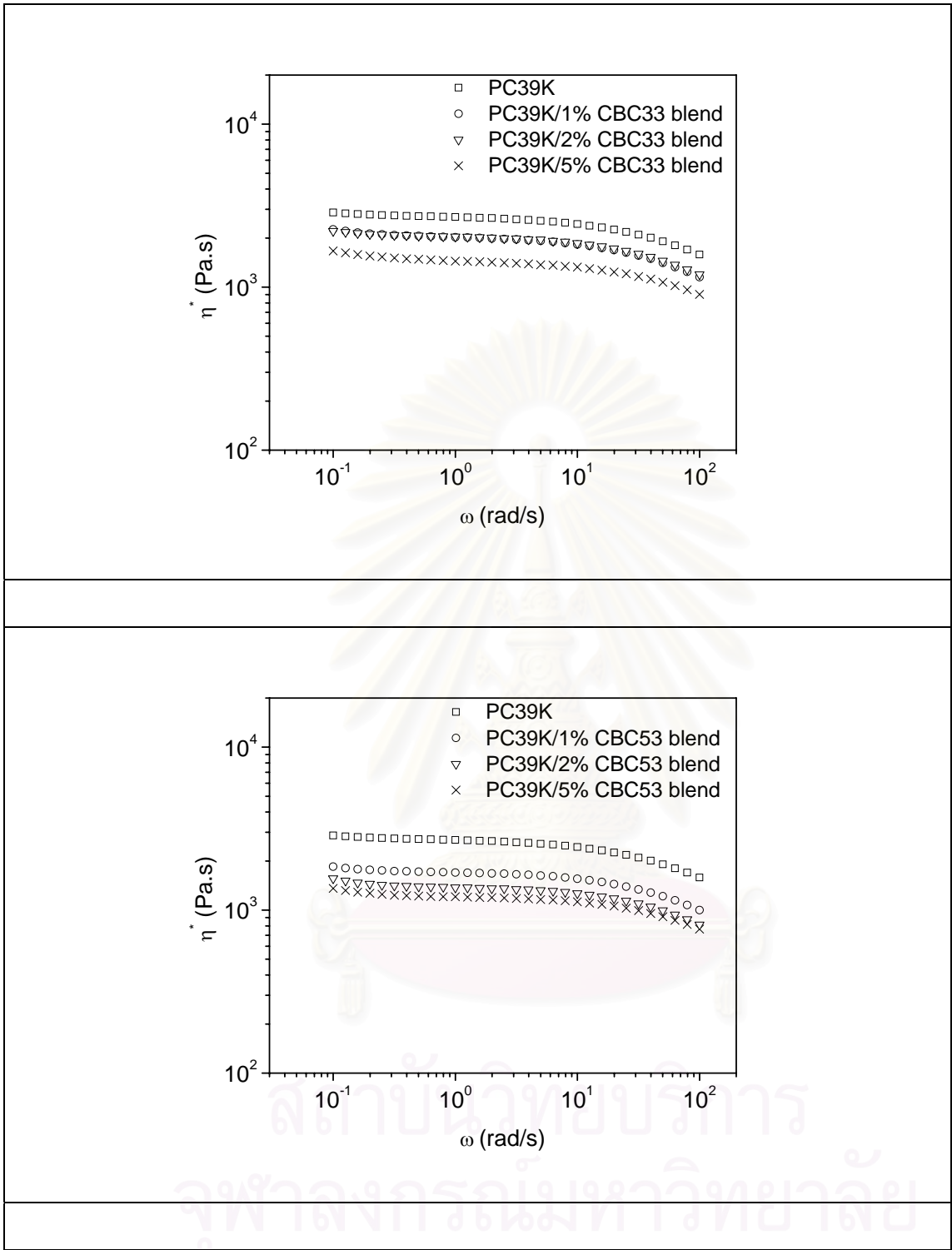
Figure 5-11 Complex viscosity of (a) PC39K/CBC33 blends, (b) PC39K/CBC53 blends at 265 °C.

In order to confirm that the orientation of the LLC causes a viscosity reduction, rather than the migration of LLC to lubricate the metal interface causing the viscosity reduction, an angular frequency loop (increased and then decreased angular frequency experiments) on the oscillatory shear mode of the same samples were performed. At a fixed temperature of 255 $^{\circ}$C, an angular frequency sweep from 1×10^{-2} to 10 rad/s was applied, the samples were then held in the rheometer for 3 minutes without oscillatory shear, followed by an angular frequency sweep in which the frequency was decreased from 10 to 1×10^{-2} rad/s. Figure 5-12 shows the complex viscosity of the blends during both increased and decreased angular frequency. Pure PC, 1% and 2% LLC blends show behaviour that is completely reproducible over the entire angular frequency range. In the case of 5% LLC blends the complex viscosity below 1×10^{-1} rad/s does not return to the original viscosity although, over the frequency 1×10^{-1} rad/s, the viscosity shows perfect recovery. This viscosity observed confirm our claim that it is the orientation of the LLC causing the viscosity reduction. If the LLC is lubricating the metal plates and slip page occurs, the curves should not be reproducible, and the viscosity would remain low as the frequency decreases, rather than showing an increase.
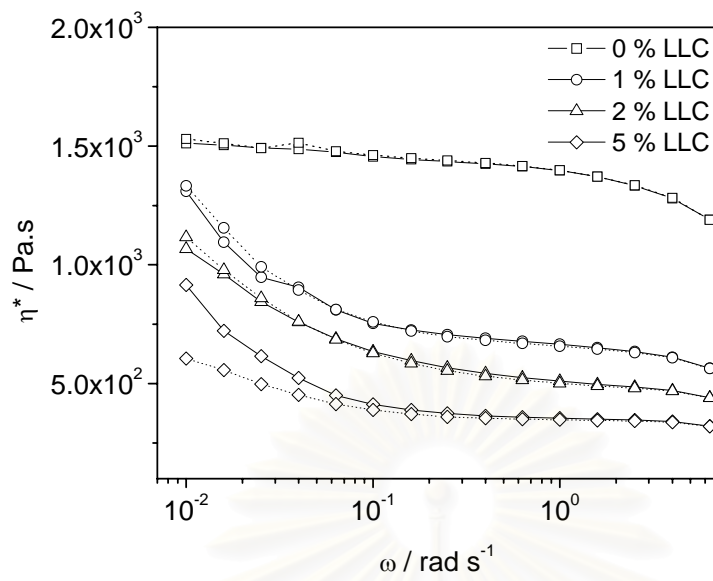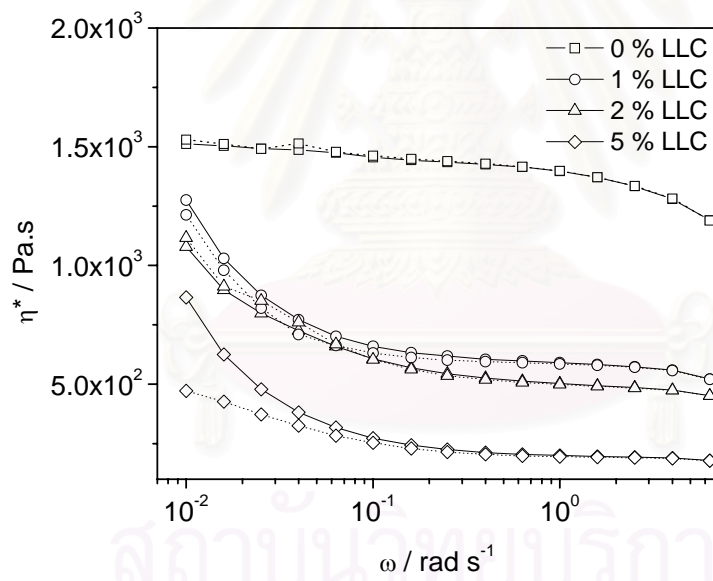
Figure 5-12 Complex viscosity of (a) PC24K/CBC33 blends, (b) PC24K/CBC53 blends at 255°C. Straight lines represent increased angular frequency, and dash lines represent decreased angular frequency.

5.2.3 Estimation of the shear modulus and relaxation time from Maxwell Model

The shear modulus and relaxation time of the PC and the blends were estimated by fitting the loss modulus and storage modulus to a single relaxation time Maxwell model[71,108],

$$G' = \frac{G_0 \omega^2 \tau^2}{1 + \omega^2 \tau^2}$$ Equation 5.1

and,

$$G'' = \frac{G_0 \omega \tau}{1 + \omega^2 \tau^2}$$ Equation 5.2

Examples of the loss modulus along with the fits to the Maxwell model for PC39K, PC27K and their blends with CBC33 and CBC53 are shown in Figure 5-13 and 5-14. The lower molecular weight PC has a lower loss modulus than the high molecular weight, as would be expected. The Maxwell model fits the results reasonably well, enabling a simple qualitative comparison between blends with different LLC concentrations. It is not too surprising that the Maxwell model provides a reasonable description of the low frequency data, since PC has a very low entanglement molecular weight [109] of ~ 2000 g/mol, and hence the polymers studied in this work are highly entangled. The deviation between the theory and the data are probably due to polydispersity. The reptation model [20] predicts that the relaxation of stress is well described by a single relaxation time process, which is the basis of the phenomenological Maxwell model.

(a)

(b)

(c)

(d)
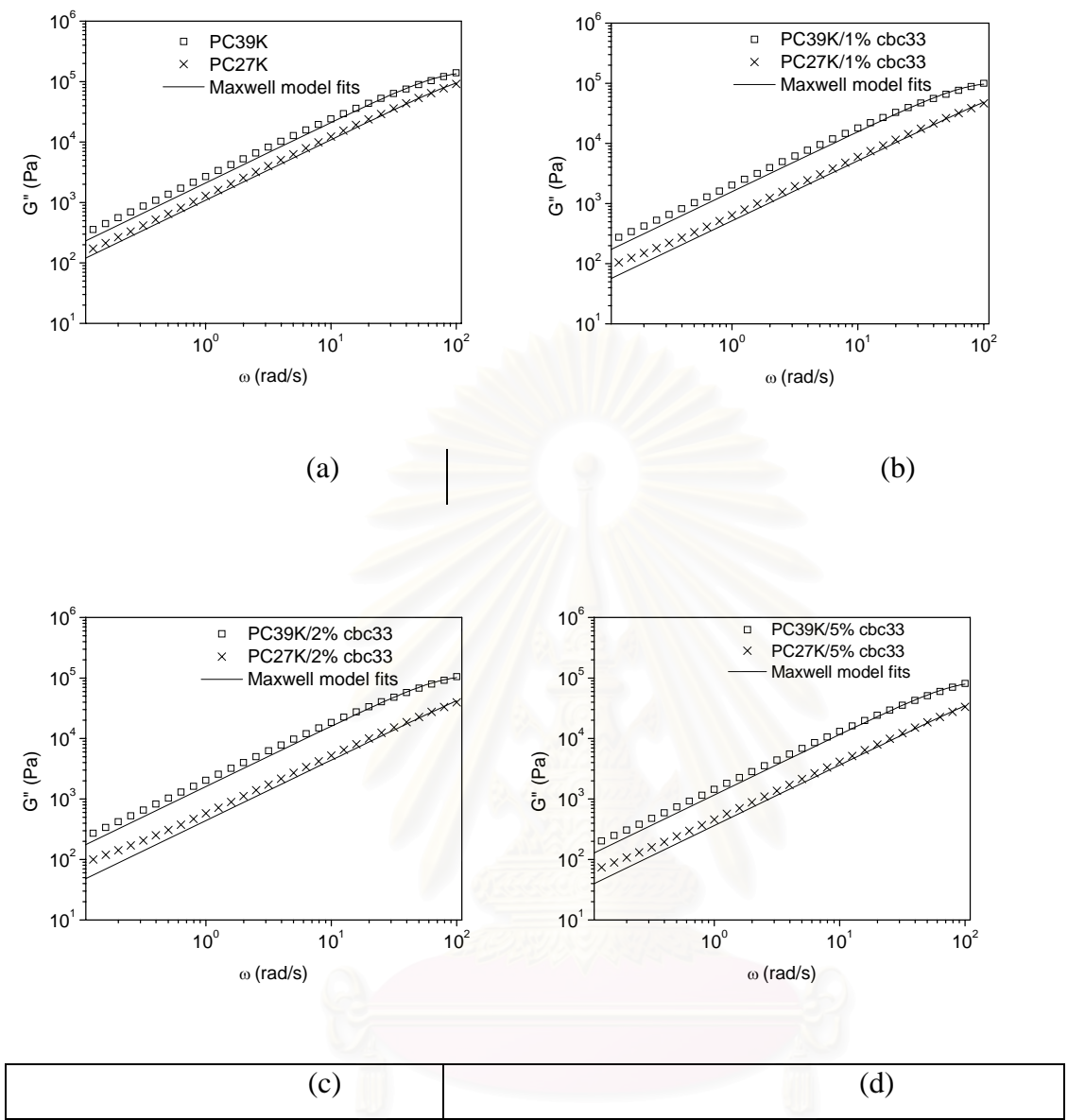
Figure 5-13   Loss modulus and Maxwell model fits of (a) PC39K, PC27K (b)

PC39K/1%CBC33, PC27K/1%CBC33 (c)PC39K/2%CBC33,

PC27K/2%CBC33 (d) PC39K/ 5%CBC33, PC27K/5%CBC33 at 265°C.

	(a)		(b)

	(c)		(d)
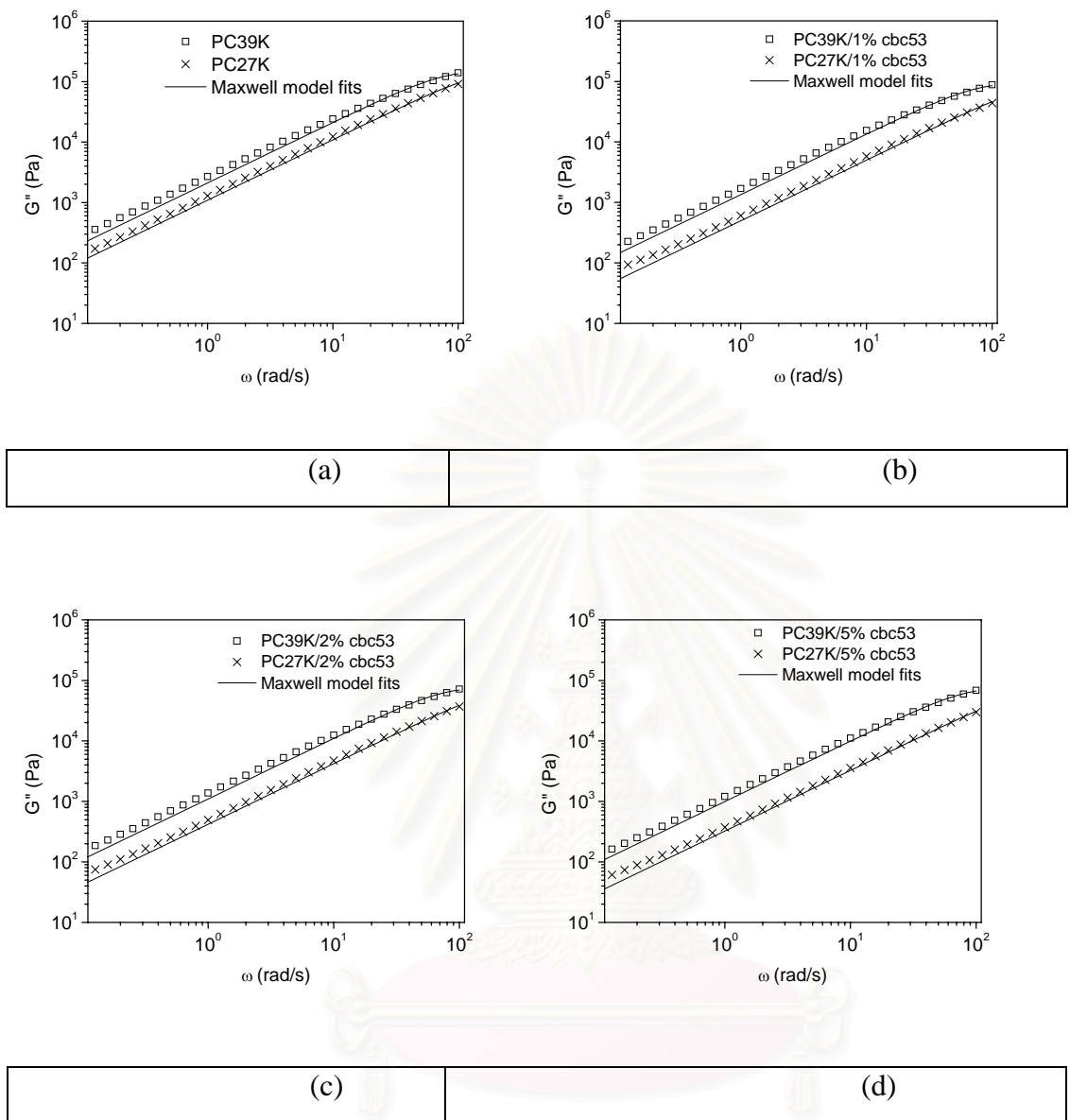
Figure 5-14   Loss modulus and Maxwell model fits of (a) PC39K, PC27K (b)
PC39K/1%CBC53, PC27K/1%CBC53 (c)PC39K/2%CBC53,
PC27K/2%CBC53 (d) PC39K/ 5%CBC53, PC27K/5%CBC53 at 265°C.

The shear modulus estimated from Maxwell model for PC and PC/LLC blends at 1%, 2%
and 5% LLC concentration at various temperatures is shown in Figure 5-15. It can be

seen that the shear modulus of the blends decreases with increasing LLC concentration and temperature. The most sensitive change in the shear modulus was upon addition of 1% LLC. The properties at various temperatures of both LLC types showed the same trend. The CBC53 blends have a lower shear modulus than the CBC33 blend, which corresponds to the shear viscosity results as shown in Figure 5-4 and 5-5. It is clear that CBC53 has a higher potential to reduce the viscosity in the plateau region at the intermediate shear rates than CBC33.
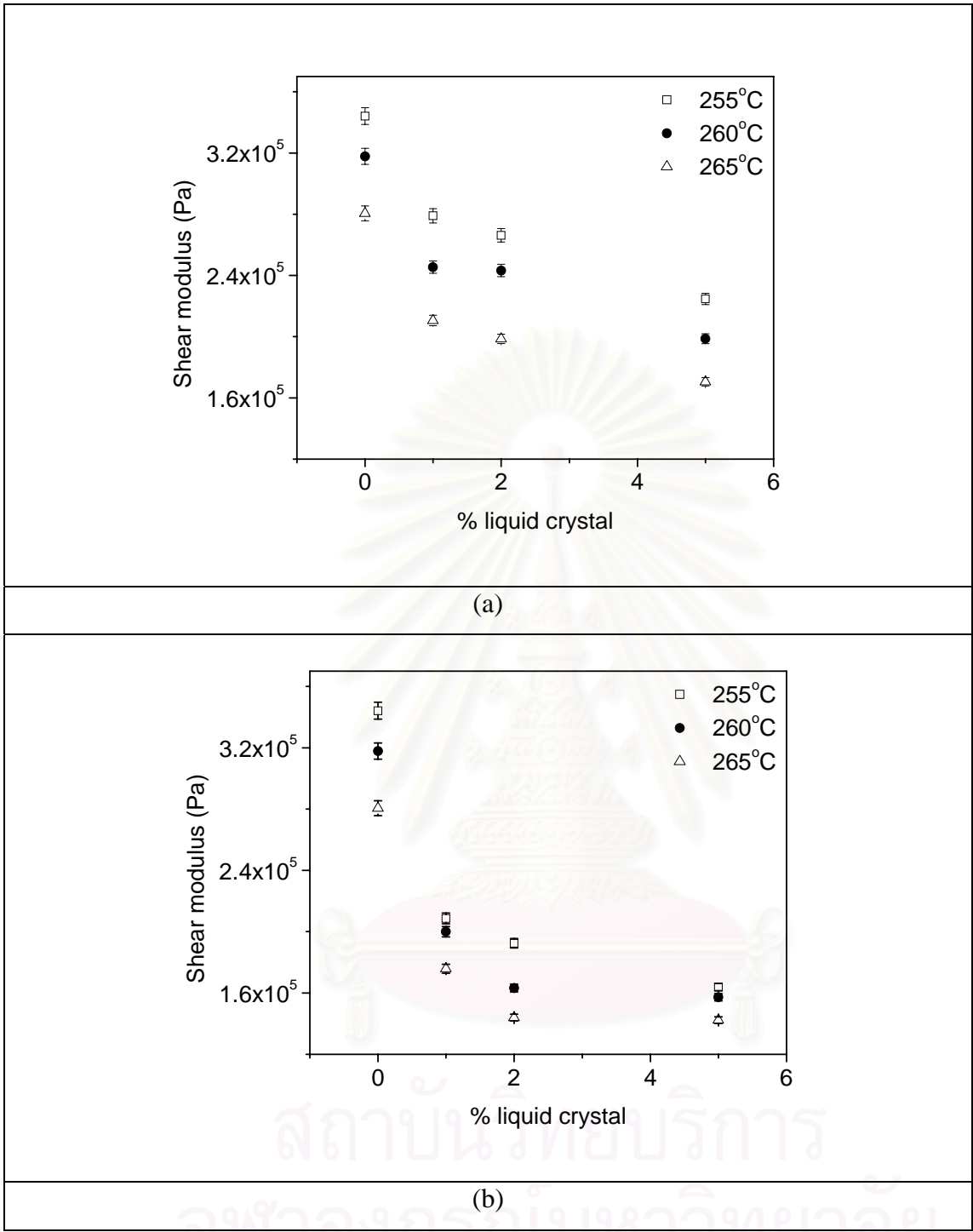
Figure 5-15   The shear modulus of (a) PC and PC/CBC33 blends, (b) PC and PC/CBC53 blends at 1%, 2% and 5% liquid crystal concentration.
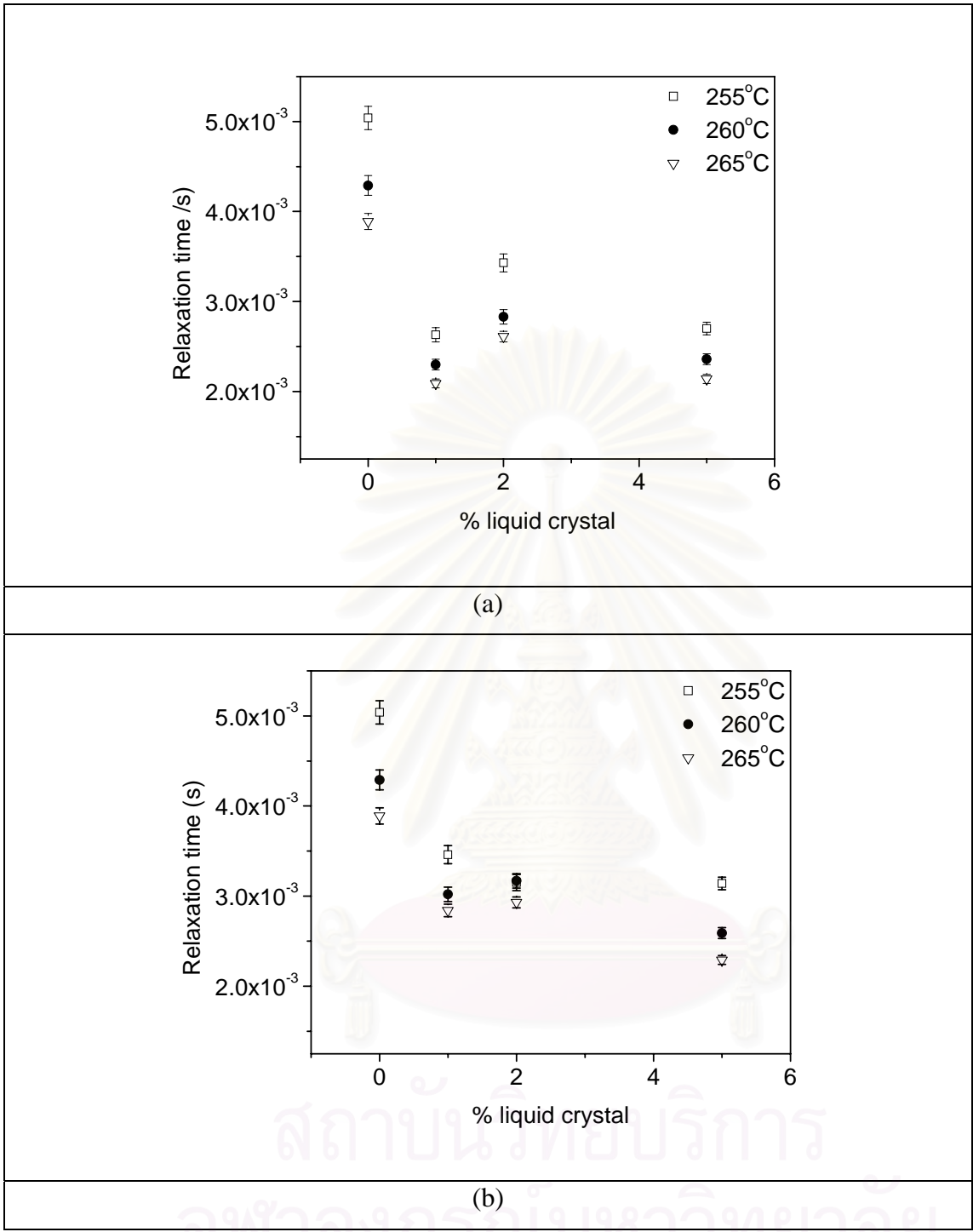
Figure 5-16 The relaxation time of (a) PC27K/CBC33 blends, (b) PC27K/CBC53 blends, at 1%, 2% and 5% liquid crystal concentration.
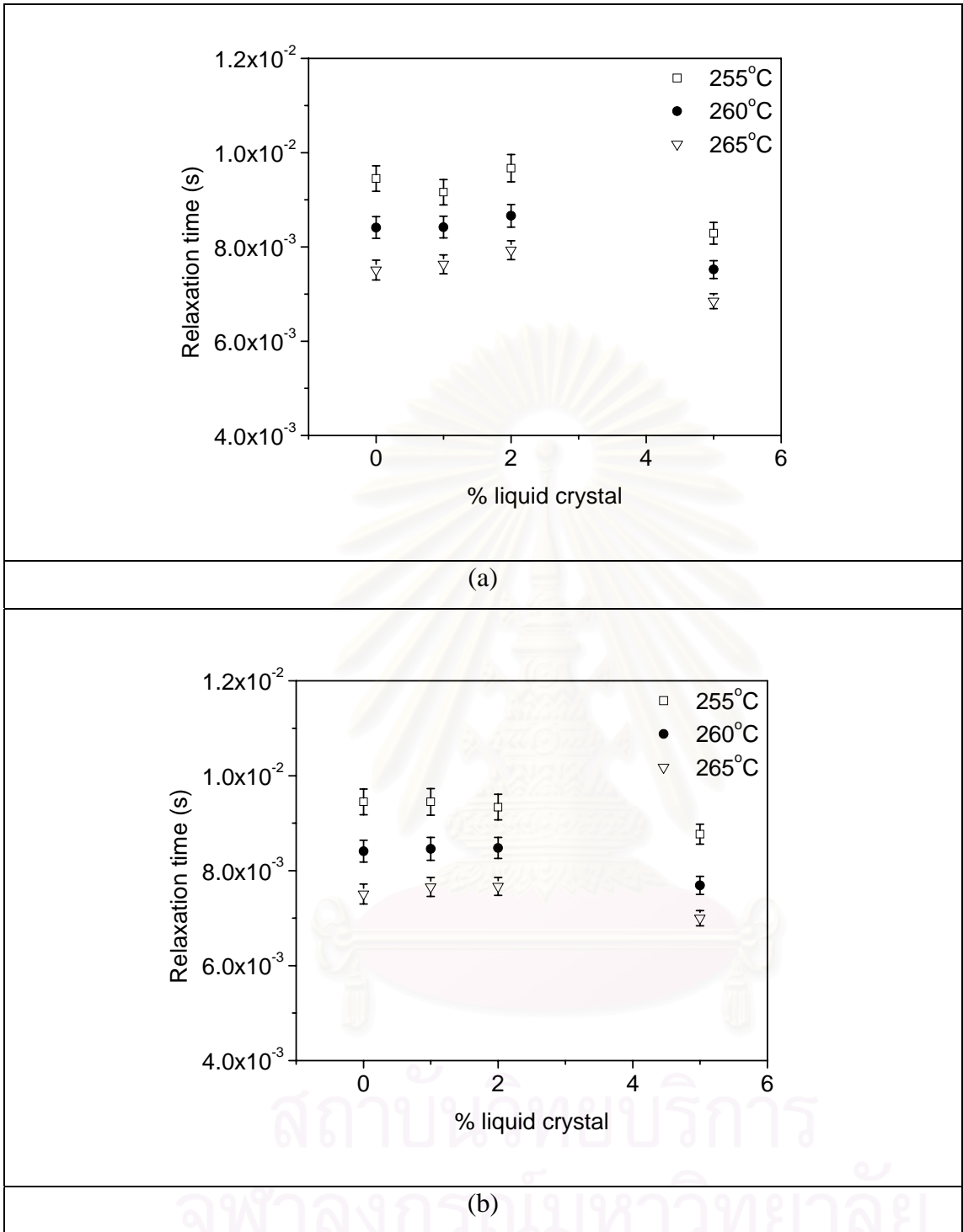
Figure 5-17 The relaxation time of (a) PC39K/CBC33 blends, (b) PC39K/CBC53 blends, at 1%, 2% and 5% liquid crystal concentration.

Figure 5.16, 5-17 show the relaxation time of PC and PC/LLC blends. It can be seen that LLC has a more significant effect on the relaxation time of the low molecular weight PC than the high molecular weight PC. For the lower molecular weight PC, the relaxation time decreases with LLC concentration, whilst, apart from a slight decrease at the highest LLC concentration, there is no clear dependence of the relaxation time on LLC concentration for the higher molecular weigh PC. This can be explained on the basis of the modified form of the reptation model for mixtures[110], the greater the difference between the relaxation times of the individual components (polymer and LLC), the smaller the impact of the diluent on the apparent longest relaxation time, so for the higher molecular weight polycarbonate, the only observable impact of the diluent on the frequency spectrum, at the frequencies we are able to access, is upon the modulus, as observed.

As both complex and steady shear viscosities of the blends were found significantly decrease upon the addition of LLC. Moreover, the estimated shear moduli of the blends were also found decreases with increasing LLC concentration. The increase of diffusion coefficient with the increase of LLC content was expected.

5.3 Diffusion of low molar mass liquid crystal and bisphenol A-polycarbonate blends.

5.3.1 Data Analysis

5.3.1.1 Depth scale conversion

To calculate a depth profile, the volume fraction of a given species at a given depth is required. For forward scattering NRA this means plotting the movement of the peak for the proton particles ejected. It is therefore necessary to convert channel number into depth. A calibration experiment can be carried out to determine the energy per channel.

For NRA, kinematics are used for finding the amount of energy a nuclear reaction at the surface would provide an ejected alpha particle. Once zero depth and energy per channel are known the energy for all channels can be found. The data reduction technique

employed also accounts for the detector angle, beam energy, resolution and geometry and energy to depth.

5.3.1.2 Normalised yield and volume fraction

Counts need to be converted into volume fraction of component. The volume fraction of a given species at a giving depth is required. The NRA proton peak can be divided by data from a thick sample of deuterated polymer collected at the same energy and geometry. Experimental data can be fitted using the simulation programme SIMNRA*. This allows a theoretical target to be built up and the spectrum is simulated after the energy, geometry, charge and other detector parameters are specified. This simulation can then be converted to an axis with a depth scale.

5.3.2 Graphs for volume fraction against depth

Volume fraction with depth profiles were constructed using spreadsheets and experimental parameters as described in data analysis sections 5.3.1. Figure 5-18 and Figure 5-19 show typical profiles for two bilayers. The peak due to ^{2}H from DPC and DPC blend decrease in volume fraction and diffuse to greater depths with time. The change in profile with time show that interdiffusion of the polymers has occurred.
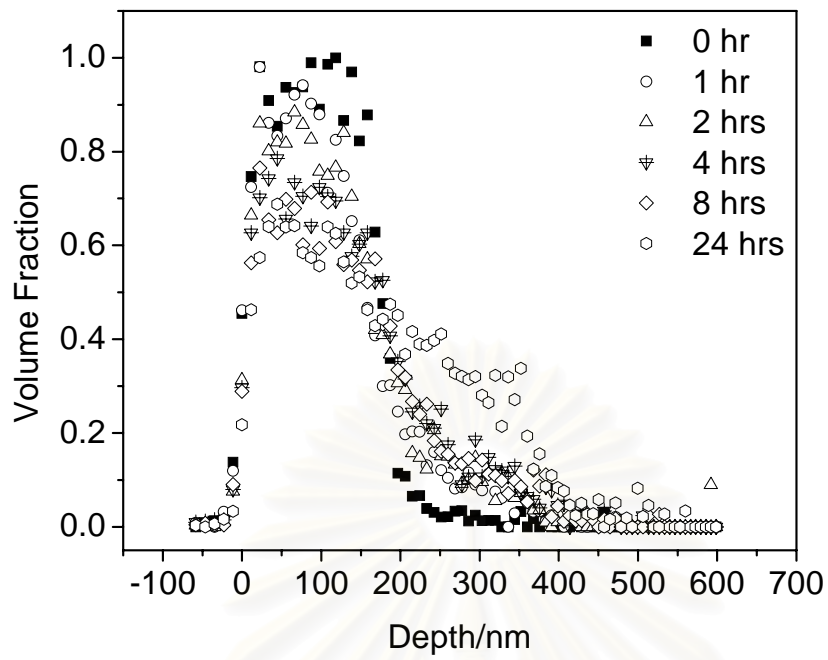
Figure 5.18 Depth profiles of dPC diffusing into PC annealed at 170°C for various time.
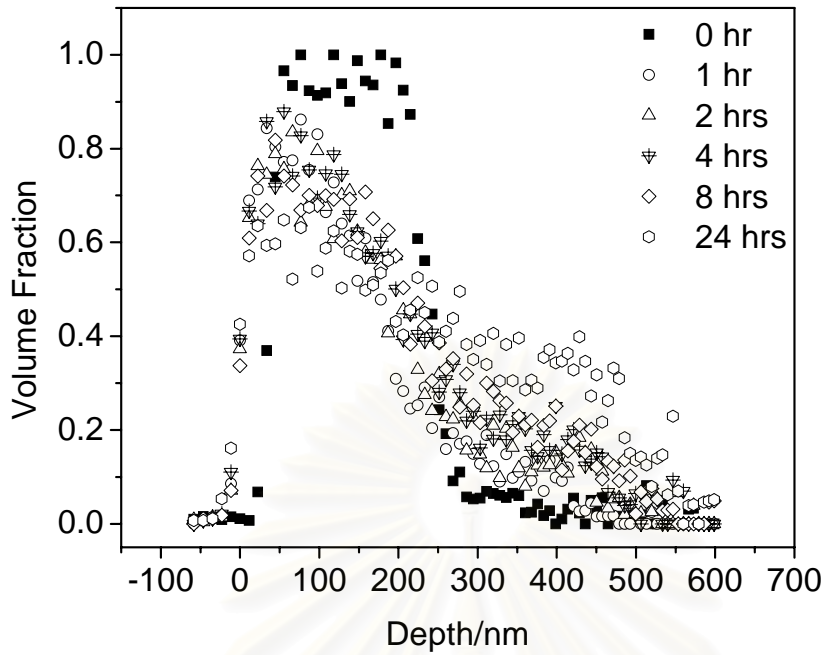
Figure 5.19 Depth profiles of dPC/1%CBC53 diffusing into PC/1%CBC53 annealed at 170°C for various time.

5.3.3 Calcutating diffused depth

A theoretical fit to the depth profiles found experimentally was constructed by using a version of (Equation 3.20)

$$\varphi_A = \frac{1}{2}\left\{ erf\,\frac{h_0 - x}{w_{width}} + erf\,\frac{h_0 + x}{w_{width}} \right\} \qquad \text{Equation 5.3}$$

where x is the depth and the interfacial width w_{width}, is related to the tracer diffusion coefficient by, $w_{width} = 2\sqrt{(D*t)}$. A FORTRAN program ('Errfit' by R. Thompson, University of Durham) was used to convolute Equation 5.3 with the instrumental resolution function, the total width of the sample and the resolution. All samples of the same bilayer construction were assumed to have the same resolution and the same

original thickness. Error fitting of non-annealed sample data was first used to find h_0 and the resolution, which were then fixed for the rest of the samples. Examples of fits using the FORTRAN program are shown in Figure 5-20 to Figure 5-22. The peak volume fraction should ideally be or close to 1 for the unannealed sample. Note that due to small variations in the total integrated charge striking each sample and in the thickness of the films, the integrated amount of dPC does not appear constant. However since interfacial width values are independent of the absolute value of the volume fractions the results for w_{width} and the diffusion coefficient are unaffected.
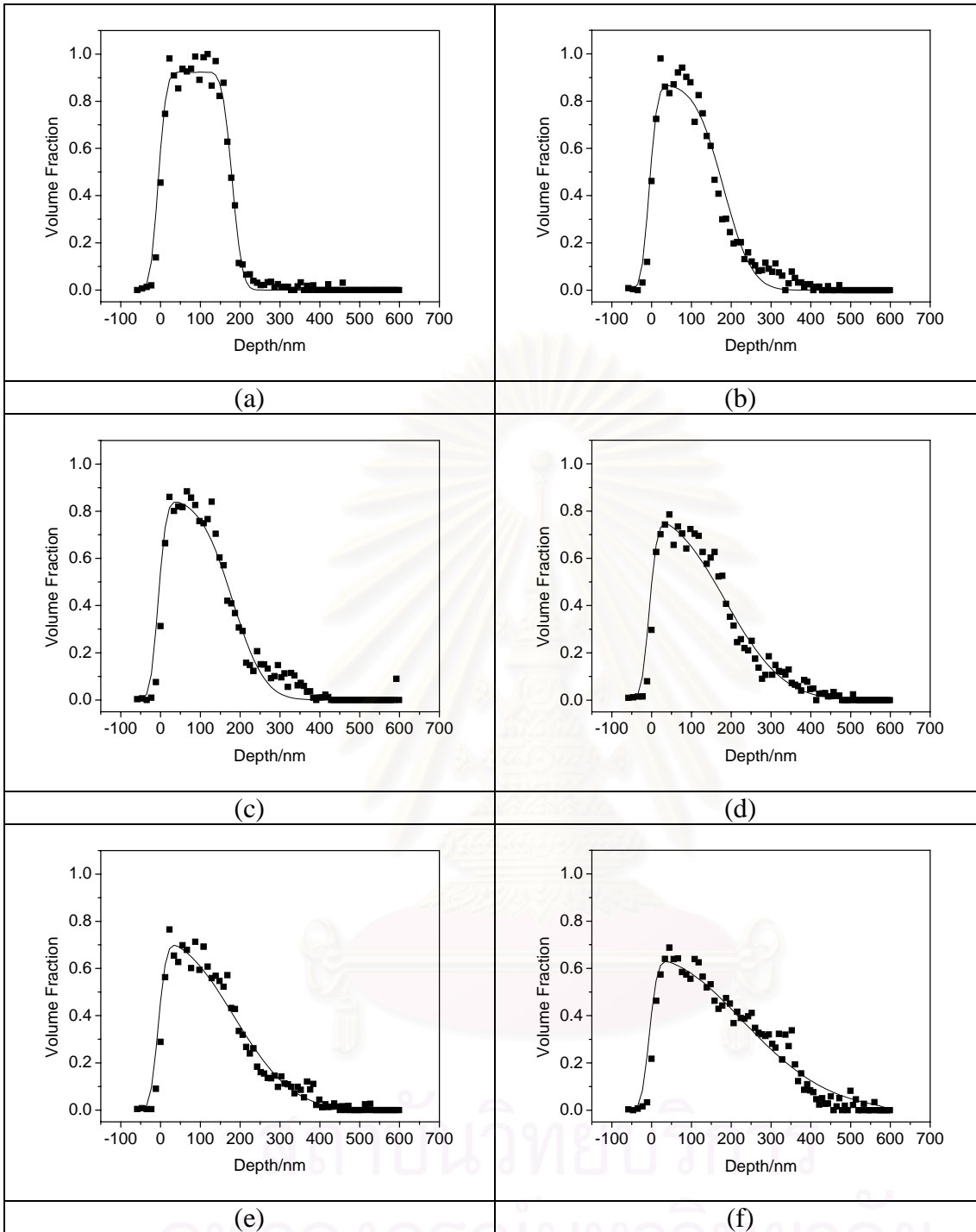
Figure 5-20   Depth profiles and fits of dPC diffusing into PC annealed at 170°C for various time: (a) 0 hour, (b) 1 hour, (c) 2 hours,   (d) 4 hours, (e) 8 hours, (f) 24 hours.
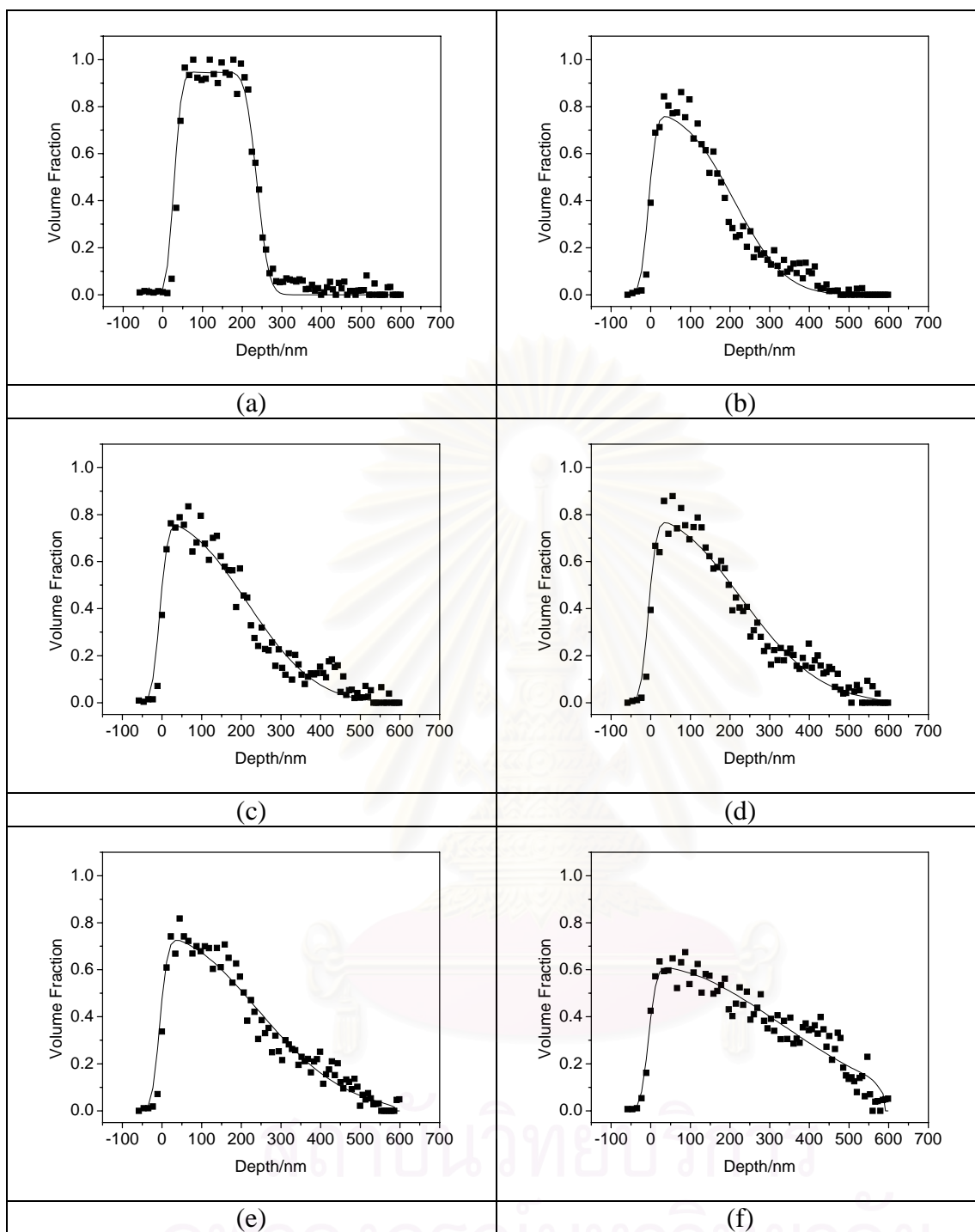
Figure 5-21   Depth profiles and fits of dPC/1%CBC53 diffusing into PC/1%CBC53
annealed at 170°C for various time: (a) 0 hour, (b) 1 hour, (c) 2 hours,
(d) 4 hours, (e) 8 hours, (f) 24 hours.
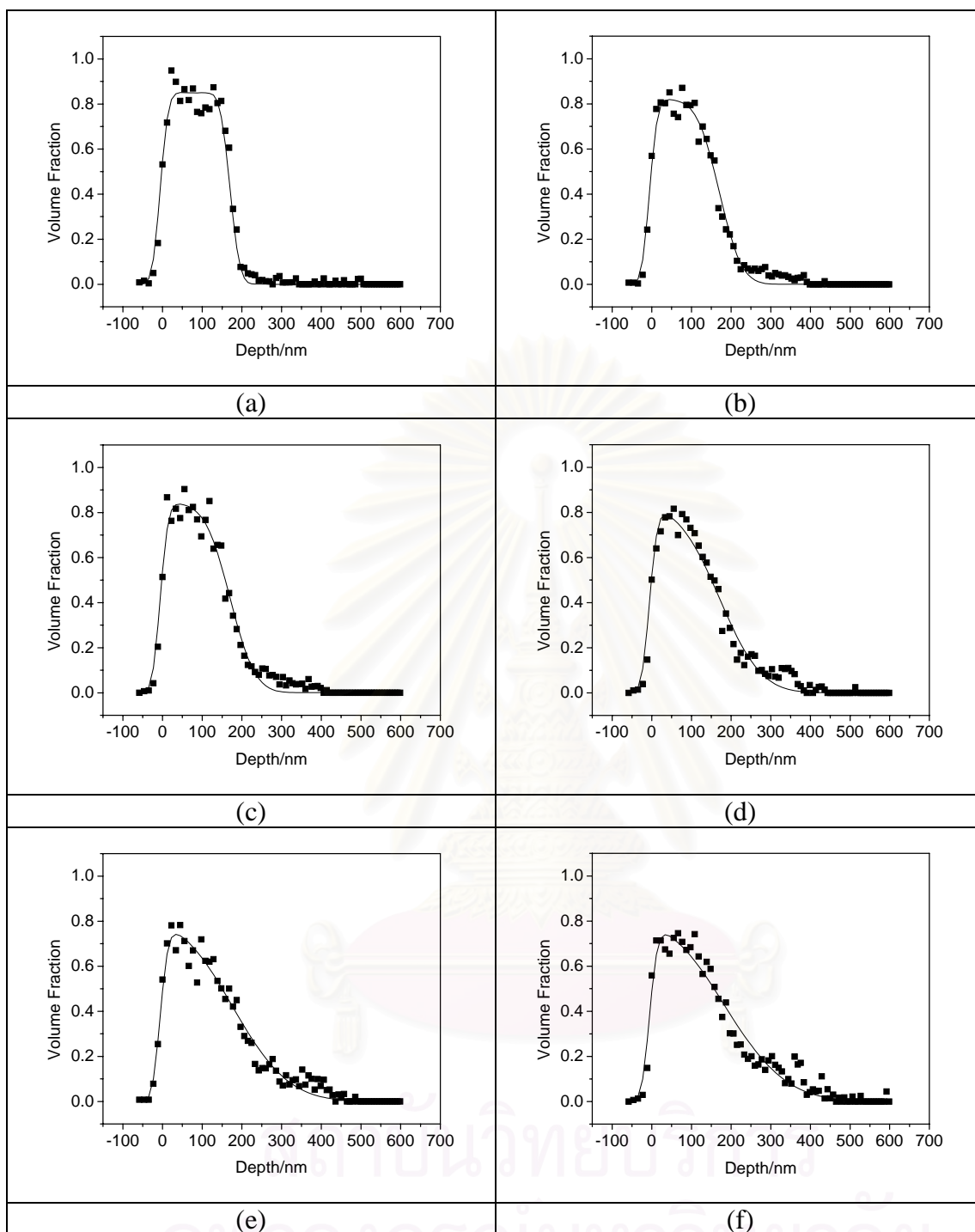
Figure 5-22 Depth profiles and fits of dPC/5%CBC53 diffusing into PC/5%CBC53
annealed at 170°C for various time: (a) 0 hour, (b) 1 hour, (c) 2 hours,
(d) 4 hours, (e) 8 hours, (f) 24 hours.

The w_{width} was assumed to be zero for no anneal time. Once the data was fitted and the values of w_{width} obtained, a plot of $w_{width}^2/4$ against time results in a line with gradient equal to D^*.
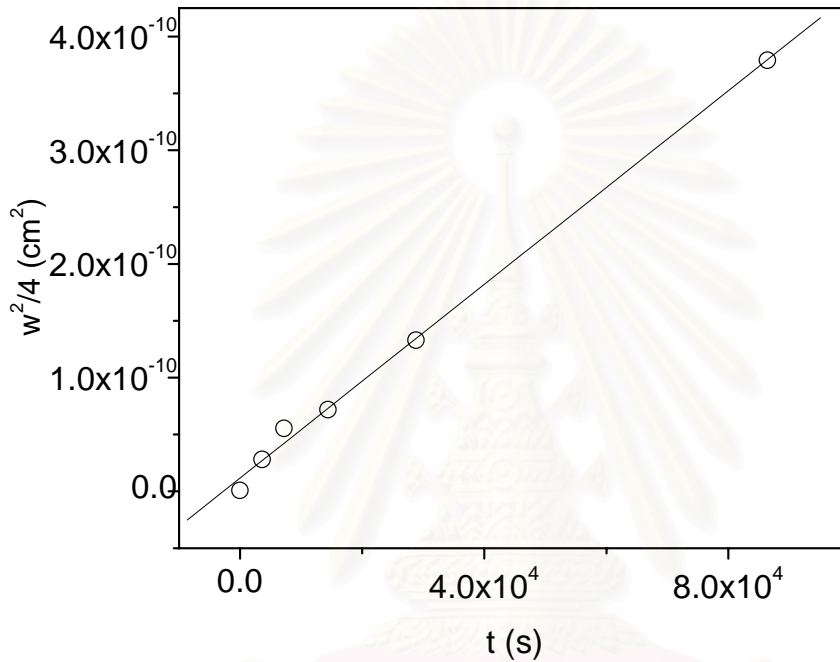
Figure 5-23 Plot of $w^2/4$ as a function of annealing time for dPC/1%CBC33 diffusion into PC/1%CBC33 at 170°C.

The D^* for different concentrations of LLC are shown in Figure 5-24. The addition of 1wt% LLC increases the D^*, which implies that PC diffuses faster upon addition of LLC regardless of the type of the LLC. However, at the higher concentration of the LLC, D^* decreases. At 5wt% LLC, the diffusion coefficient is even lower than the pure PC. These results appear to contradict the rheological studies, which show a decrease in both linear and non-linear viscosity as a function of LLC concentration.

(a)

(b)
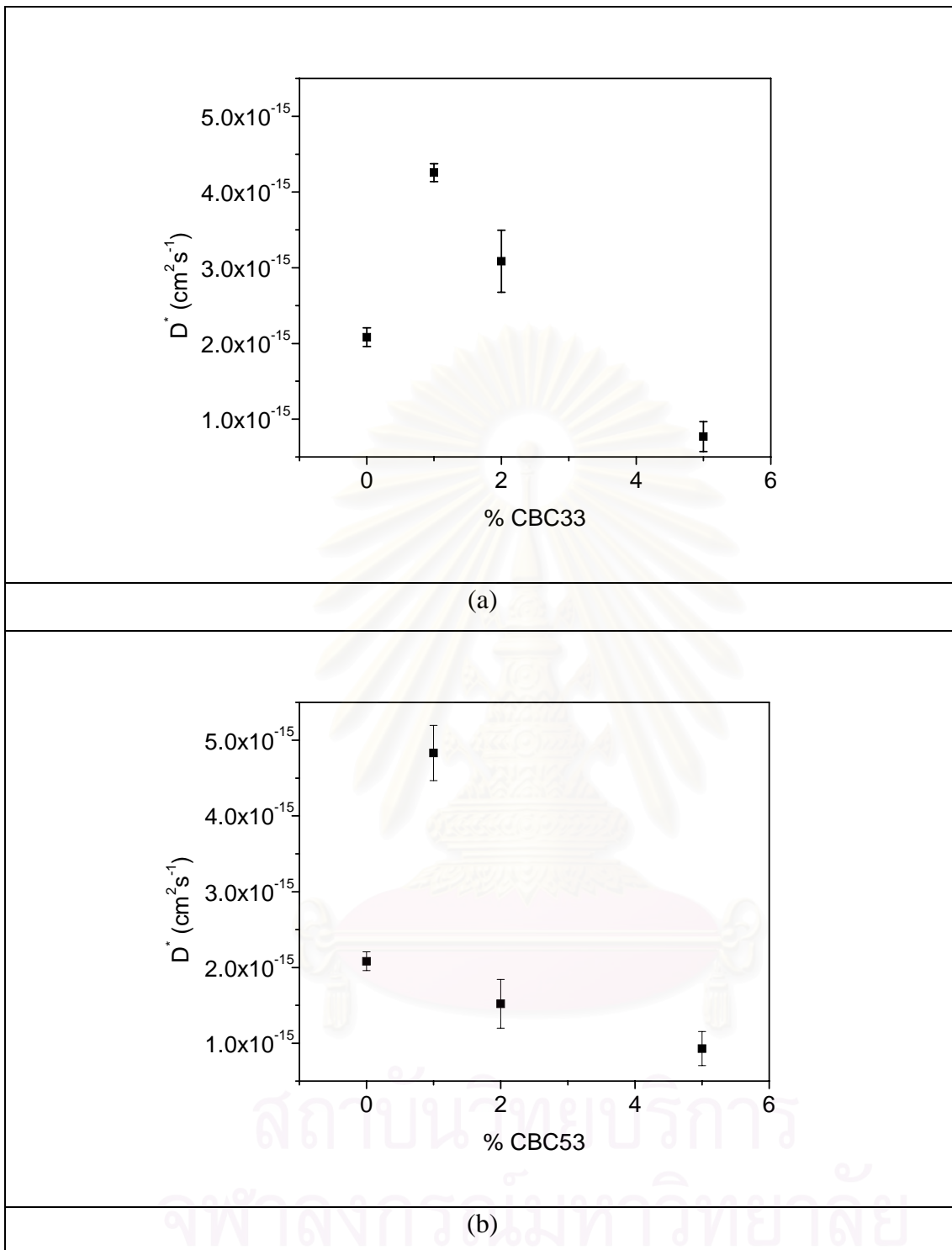
Figure 5-24 Diffusion coefficients at various concentration for (a) dPC/CBC33 ,
PC/CBC33 and (b) dPC/CBC53 , PC/CBC53.

In consideration of depth profiles and fits, the fits using Equation 5.3 were imperfect for some of the data. Figure 5-25 shows the depth profile of the dPC/5%CBC33, PC/5%CBC33 bilayers samples after 4 hours annealing. As shown in Figure 5-25 (a) the fit of Equation 5.3 to the data is not perfect over the entire data range, indicating that diffusion does not completely follow the Fickian diffusion model. The data appear to follow a step-like profile with a fairly sharp interface at ~180 nm, consistent with slow dPC/PC diffusion across the interface. However, it is not entirely clear how the step-like profile at high LLC concentration relate to the slow down of the rate of inter-diffusion between the two polymer layers, note that the results are self-consistent in that for higher concentrations of LLC, the retardation of inter-diffusion is greater.

To further probe the enriched layer, the data were also fitted to a modified functional form,

$$\varphi_A = \frac{1}{2}\left(a + (1-a)\left\{ erf\,\frac{h_0 - x}{w_{width}} + erf\,\frac{h_0 + x}{w_{width}} \right\} \right) \qquad \text{Equation 5.4}$$

which is able to model the step observed in the profile as shown in Figure 5-25 (b).

(a)

(b)
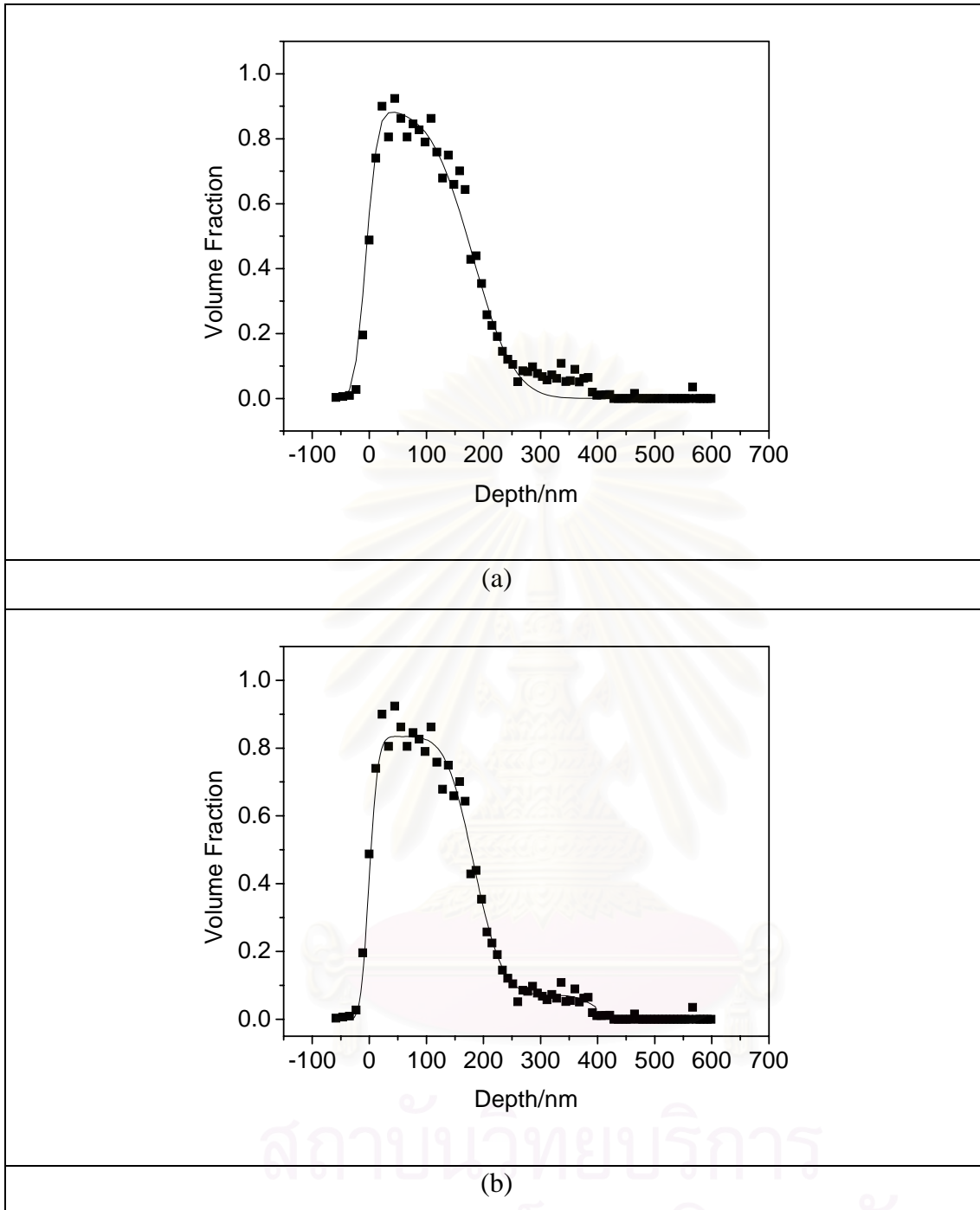
Figure 5-25   Comparison of the depth profile of dPC/5%CBC33 and fits (a) fit to
equation 5.3 (b) fit to equation 5.4, annealing time 4 hours at 170°C.

Figure 5-26 and Figure 5-27 show the comparison of the fits to equation 5.3 and equation
5.4 for a blend with 5% by weight CBC33, CBC53 unannealed and annealed for 24
hours.

(a)

(b)
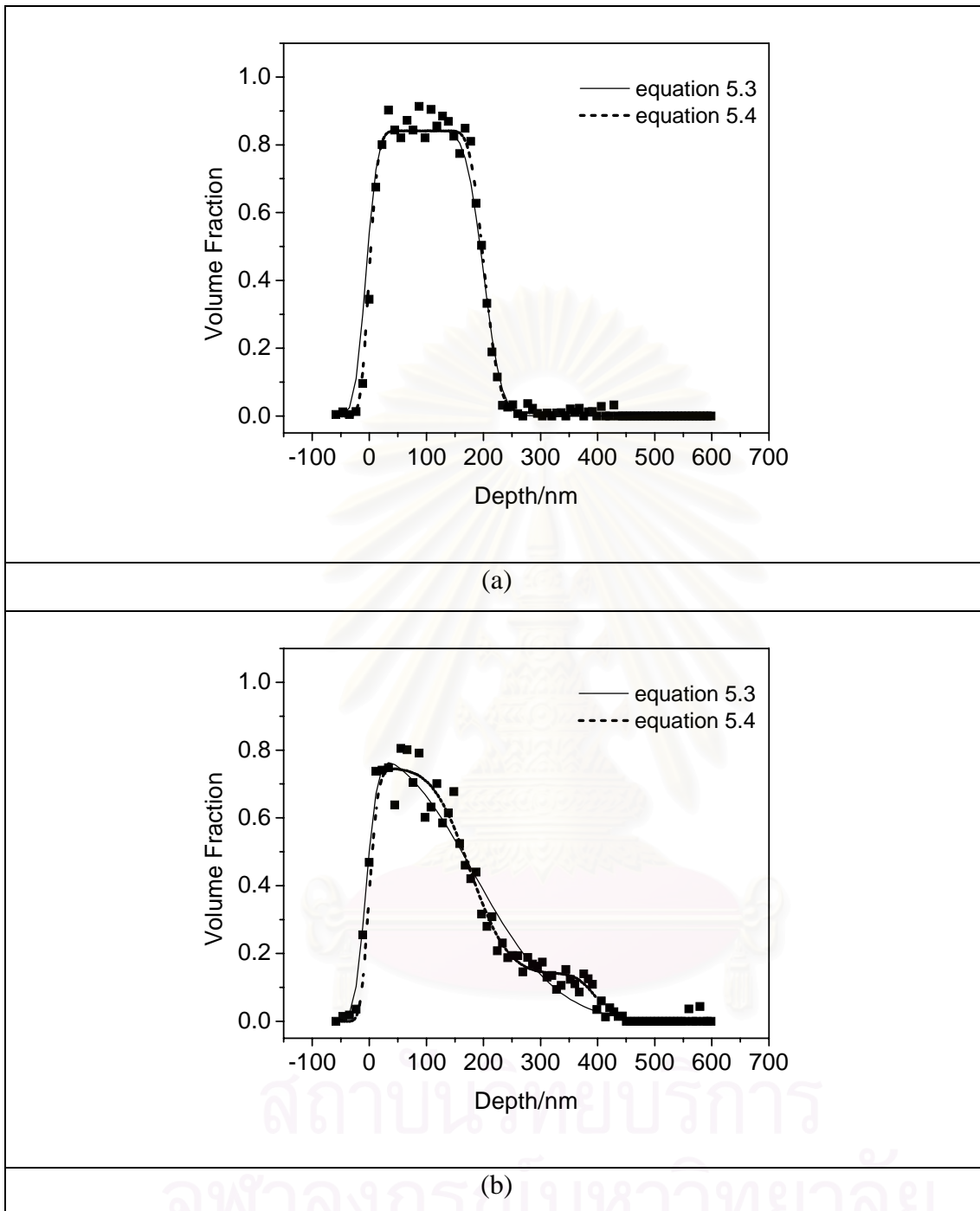
Figure 5-26 The depth profiles of dPC/5%CBC33 annealed at 170°C fit to equation 5.3 and equation 5.4 (a) unannealed (b) after 24 hours annealing.
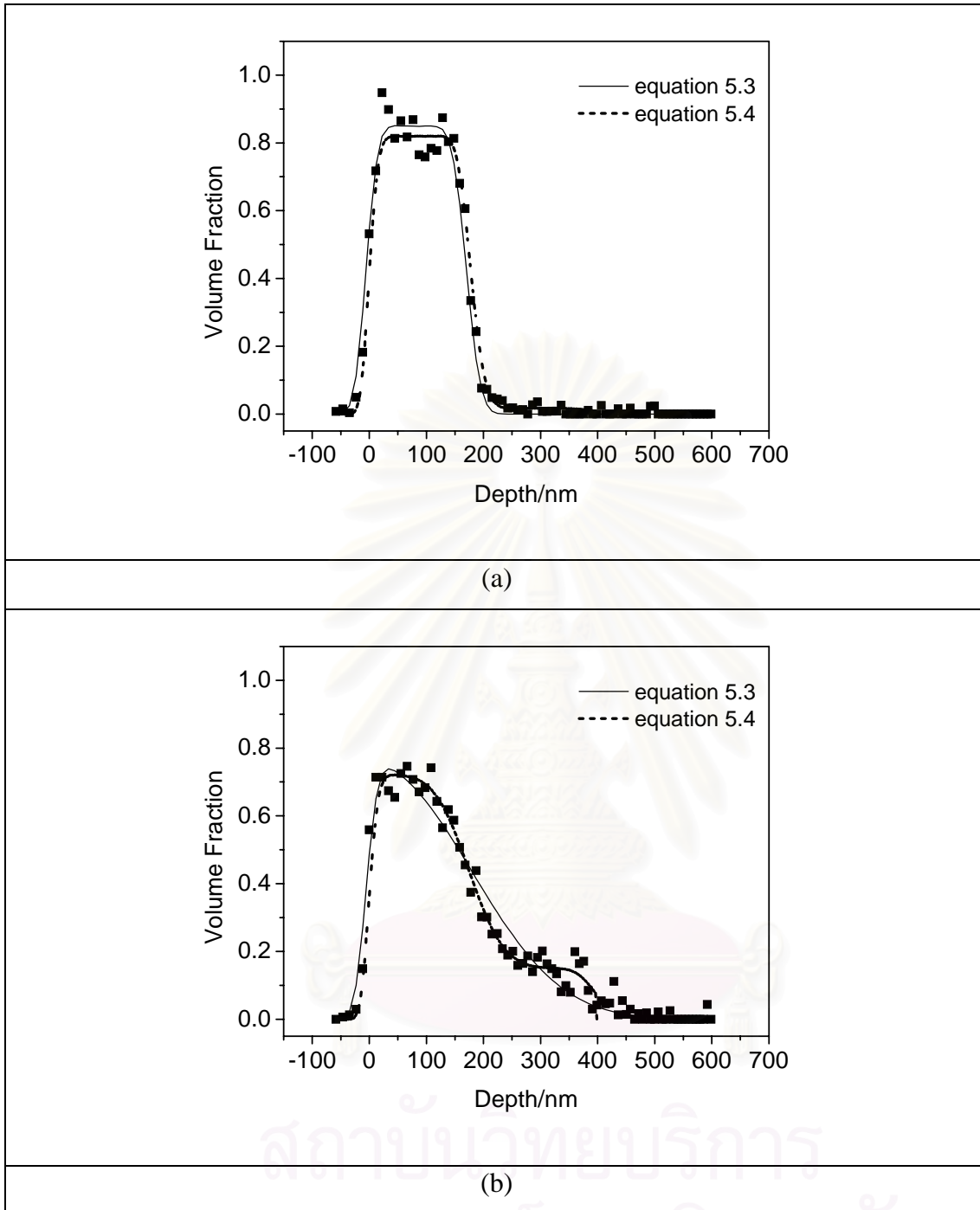
Figure 5-27 The depth profiles of dPC/5%CBC53 annealed at 170°C fit to equation 5.3 and equation 5.4 (a) unannealed (b) after 24 hours annealing.

The improved fit is consistent with reduced PC/dPC interdiffusion in the interfacial region relative to the rest of the film. In Figure 5-28, we show the resultant time dependence of the width according to the modified profile. This shows that in almost all cases (relative to 0% additive) the long-term growth of interfacial width is increased by the presence of liquid crystal.

As shown in Figure 5-28 the plots of $w_{width}^{2}/4$ against time did not produce straight lines, but rather curves. So the straight line drawn through only the early section of the data gives the slope at early stages of diffusion, the resulting diffusion coefficients are shown in Figure 5-29.
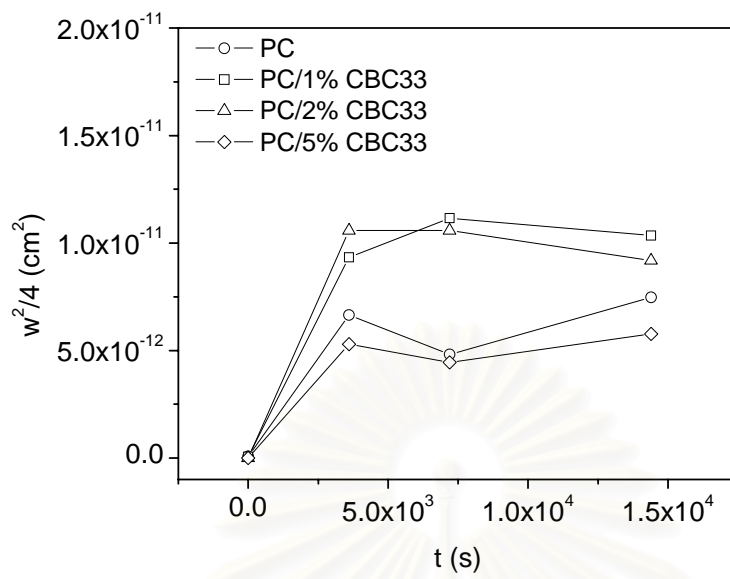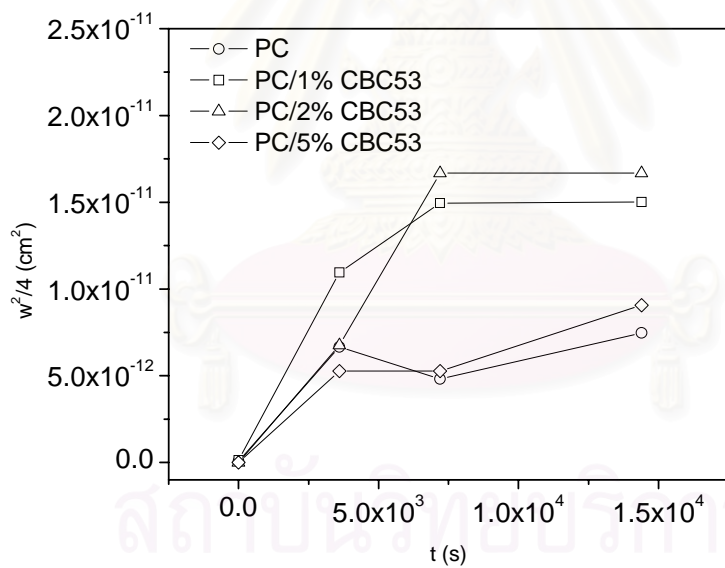
Figure 5-28 Variation of width with time for each of the blends, according to the fit of equation 5.4

(a)

(b)
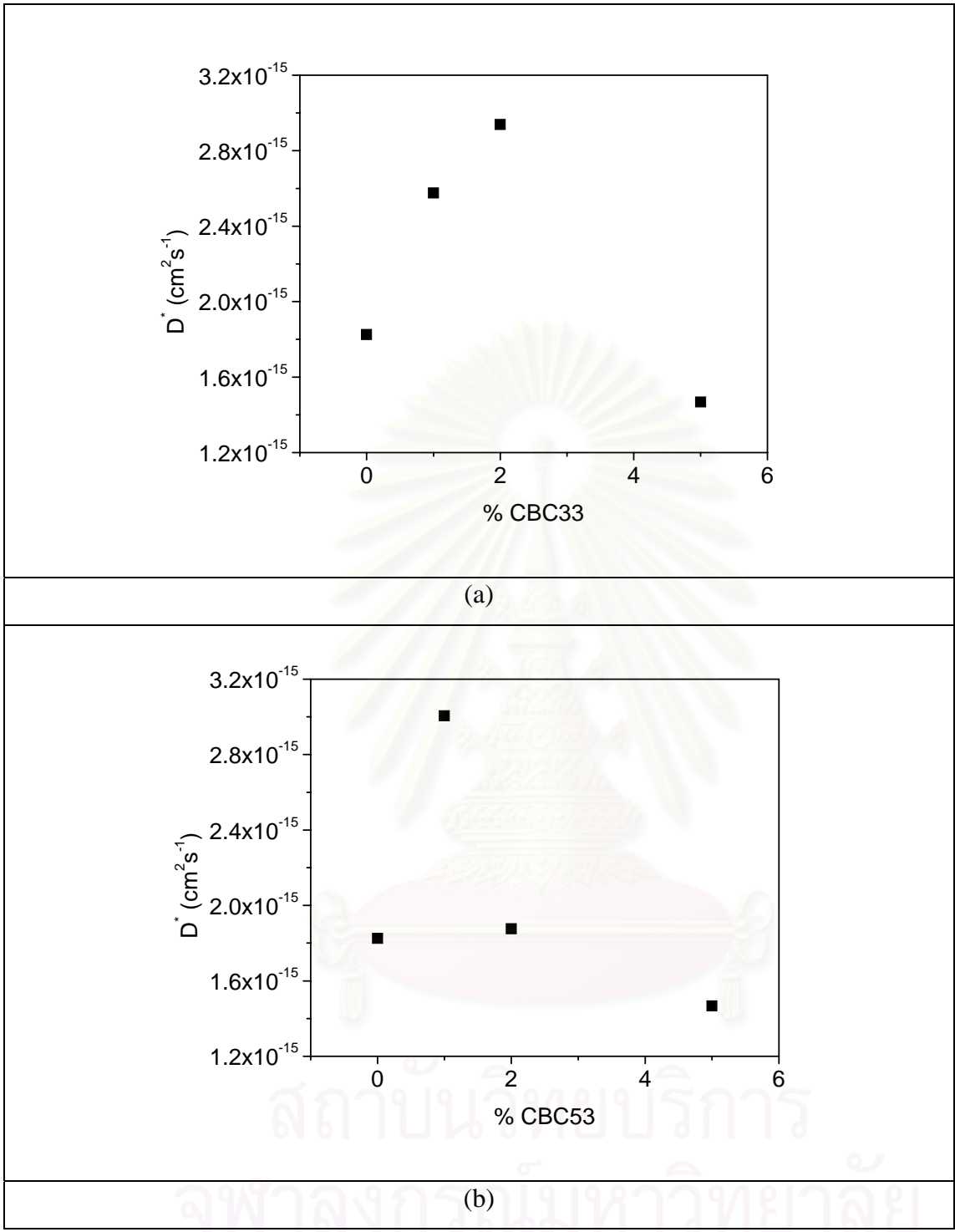
Figure 5-29 Early stage diffusion coefficients used w_{width} from equation 5.4 for (a) dPC/CBC33 , PC/CBC33 and (b) dPC/CBC53 , PC/CBC53.

From Figure 5-29, we can see qualitatively the same effect for the LLC blends as observed in Figure 5-24, when the data is analysed with a simpler form, with regards to the effect of liquid crystal content on the diffusion of polycarbonate. The diffusion is seen to initially increase upon addition of a small amount of liquid crystal, but then decreases with a further increase in the LLC content.

The concentration of dPC present in the lower layer of the film (depth 200 – 400 nm) indicates that polymer diffusion within this layer is relatively rapid. So it is reasonable to assume that at high LLC concentration, there exists a slight excess of LLC at the interface, perhaps due to surface segregation occurring during annealing of the films, probably behaves like an additional layer which may slow down the interdiffusion process between the two polymer layers as shown in Figure 5-30. Surface enrichment effects would also explain why there is not a corresponding increase in viscosity with LC concentration.
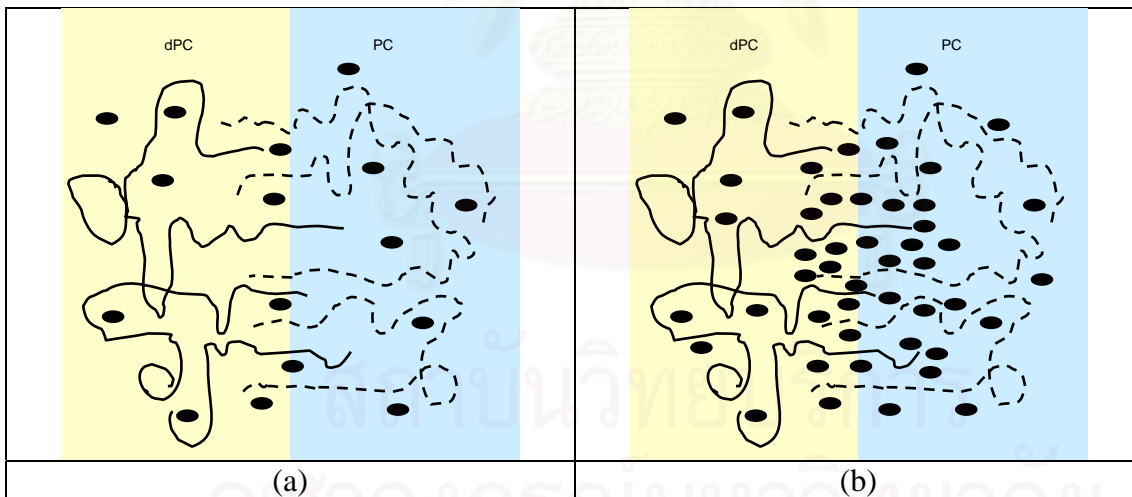
Figure 5-30   Interface regions of (a) low concentration of liquid crystal and (b) high concentration of liquid crystal.

5.4 Glass transition temperature of the blends.

Typical scans for values of the T_g found using TA instruments fitting program (TA Universal Analysis v. 4.1D) are shown in Figure 5-30 to Figure 5-33. Some investigators use the loss tangent peak $(\tan \delta)$ and others use the loss modulus peak (E'') to define T_g. T_gs were consequently found from both the loss modulus and $\tan \delta$. Figure 5-30 shows the comparison scans for pure PC39K and PC27K. For PC39K, the peak in $\tan \delta$ indicates the T_g at 159 ^{o}C whilst the loss modulus demonstrates a T_g at 154 ^{o}C. In the case of PC27K, the $\tan \delta$ peak and the loss modulus indicate T_gs at 160 and 151 ^{o}C consequently.
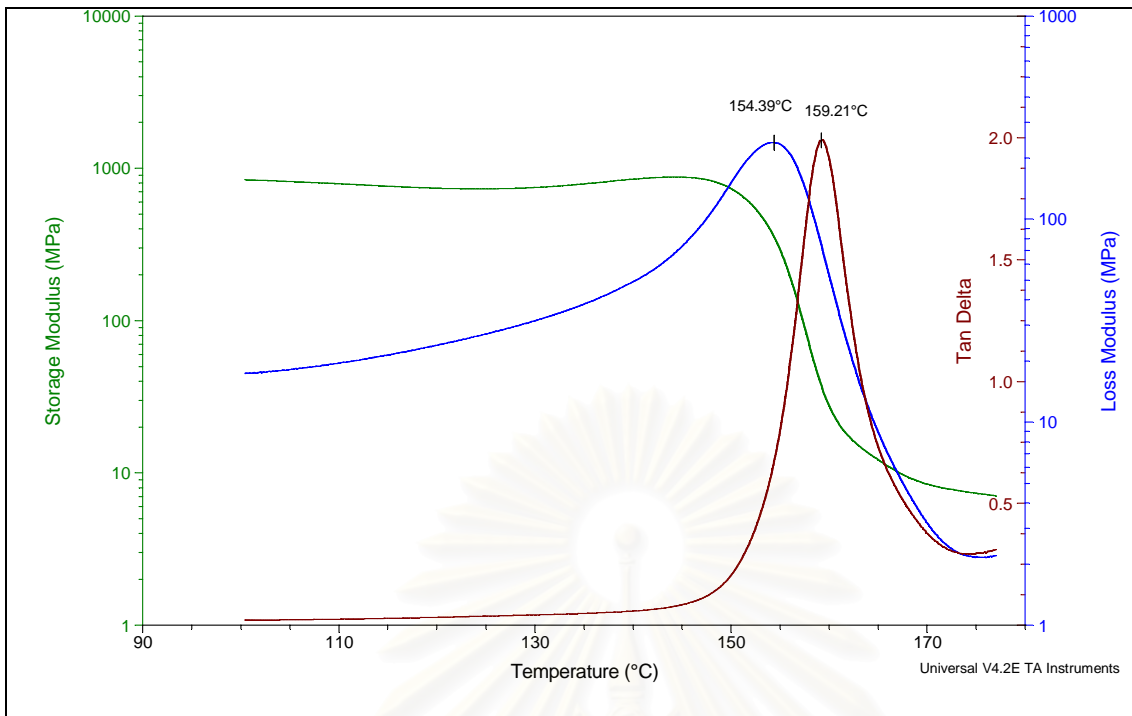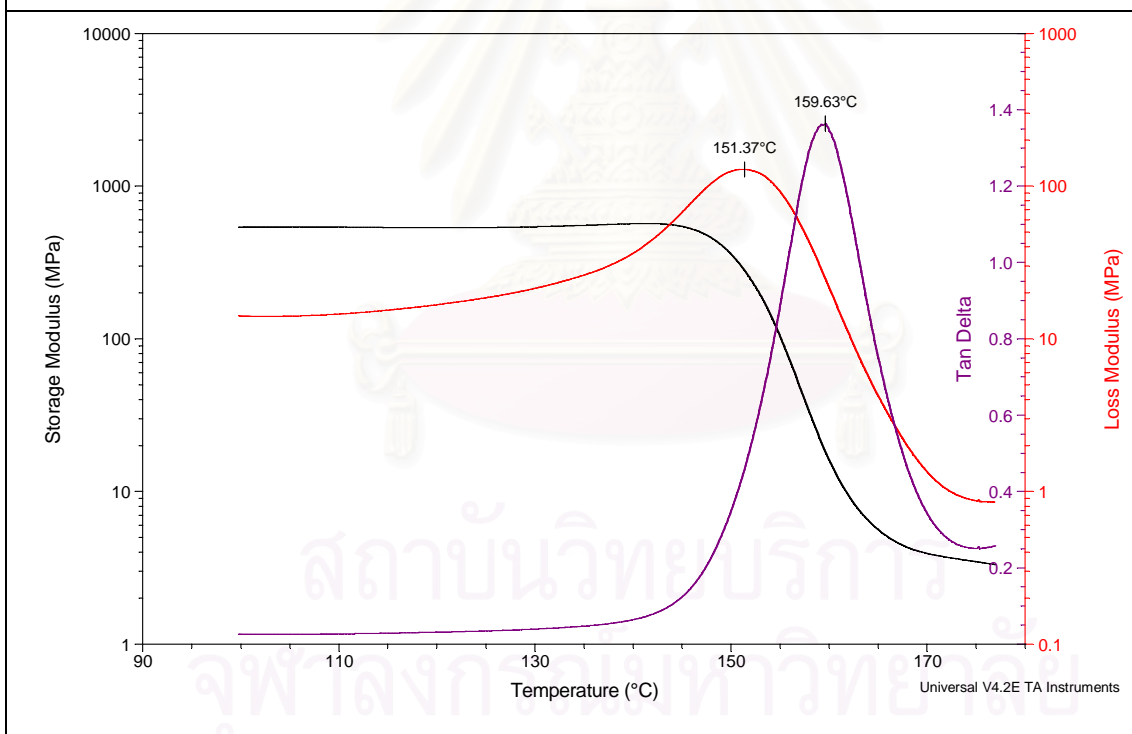
Figure 5-31   DMA scan and fitted values for Tg for (a) PC39K (b) PC27K.
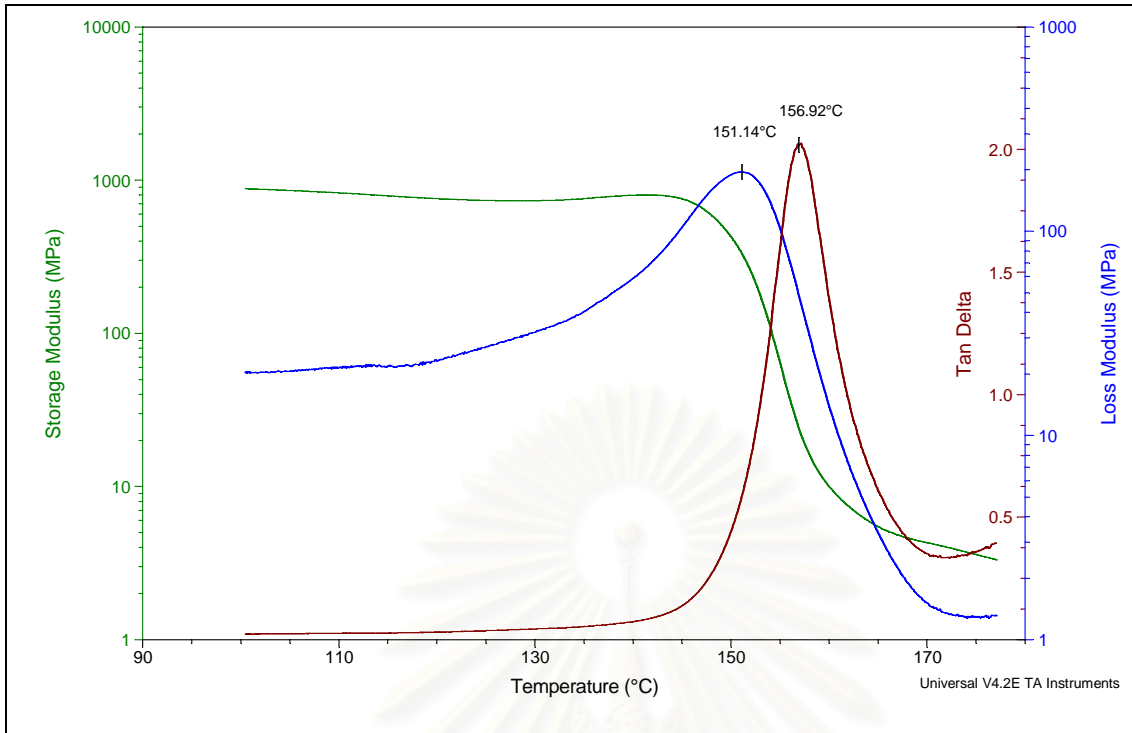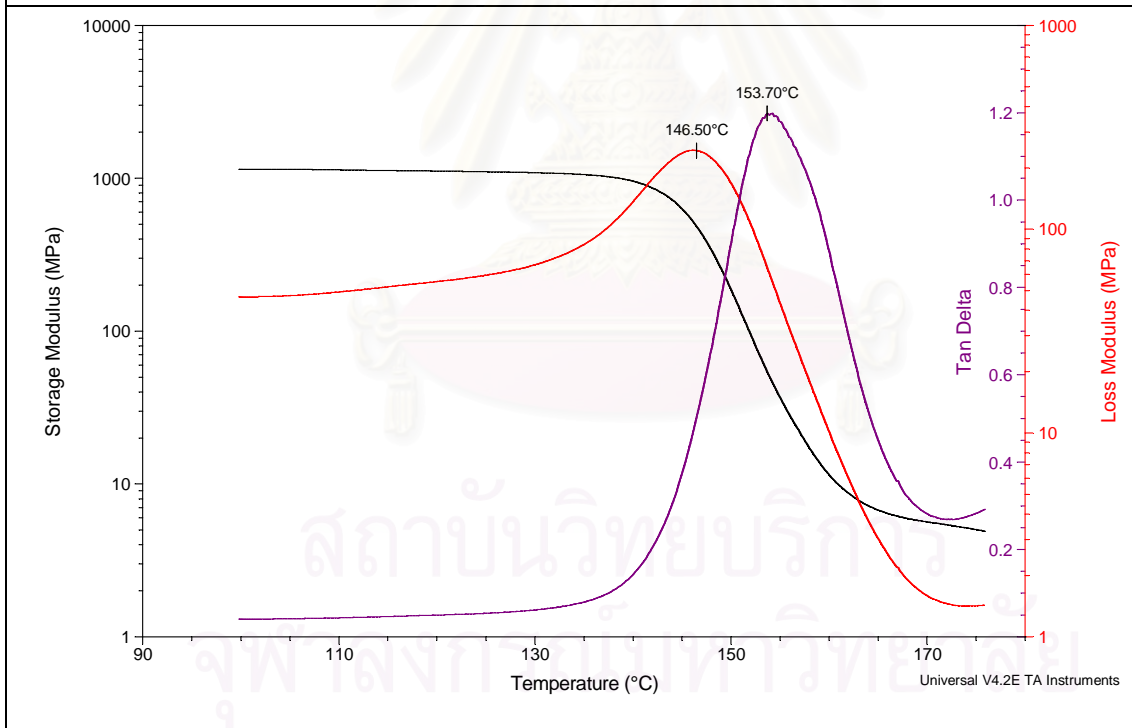
Figure 5-32   DMA scan and fitted values for Tg for (a) PC39K/1%CBC33 (b) PC27K/1%CBC33.
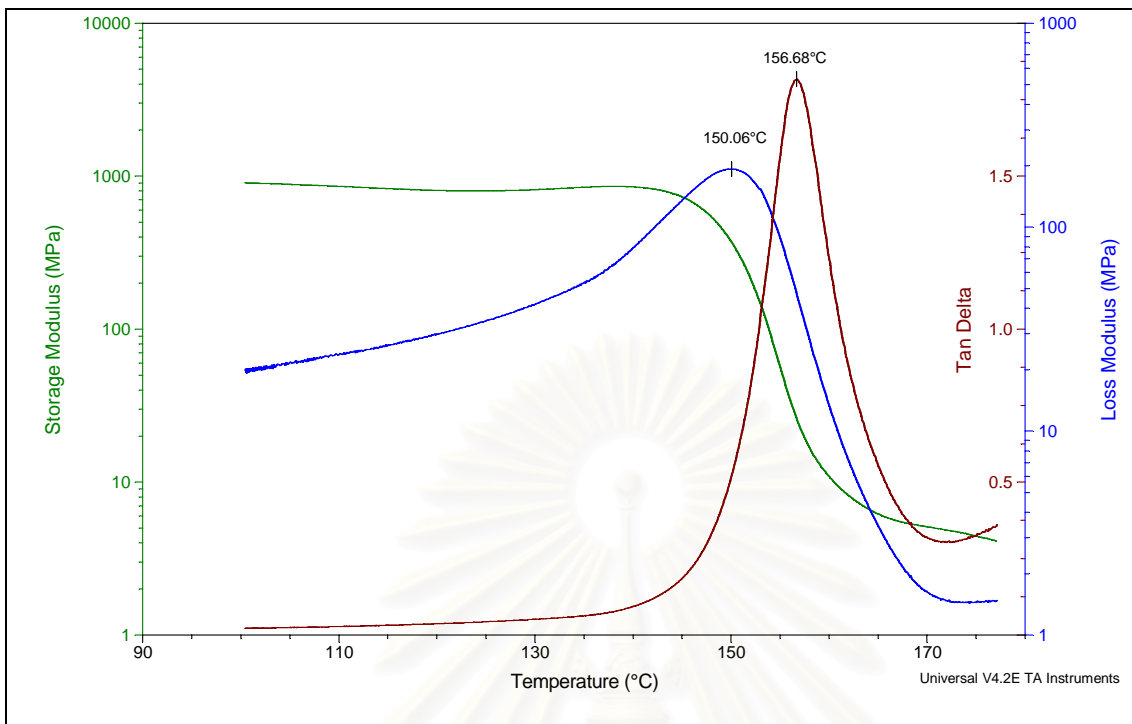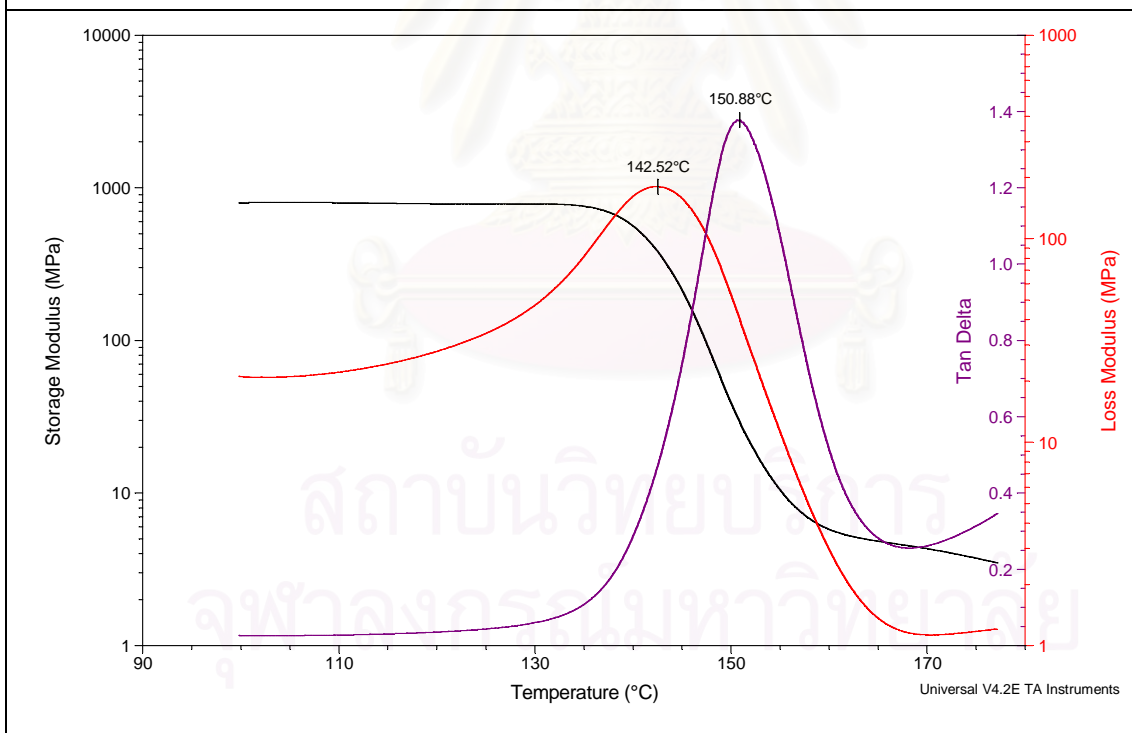
Figure 5-33 DMA scan and fitted values for Tg for (a) PC39K/2%CBC33 (b) PC27K/2%CBC33.
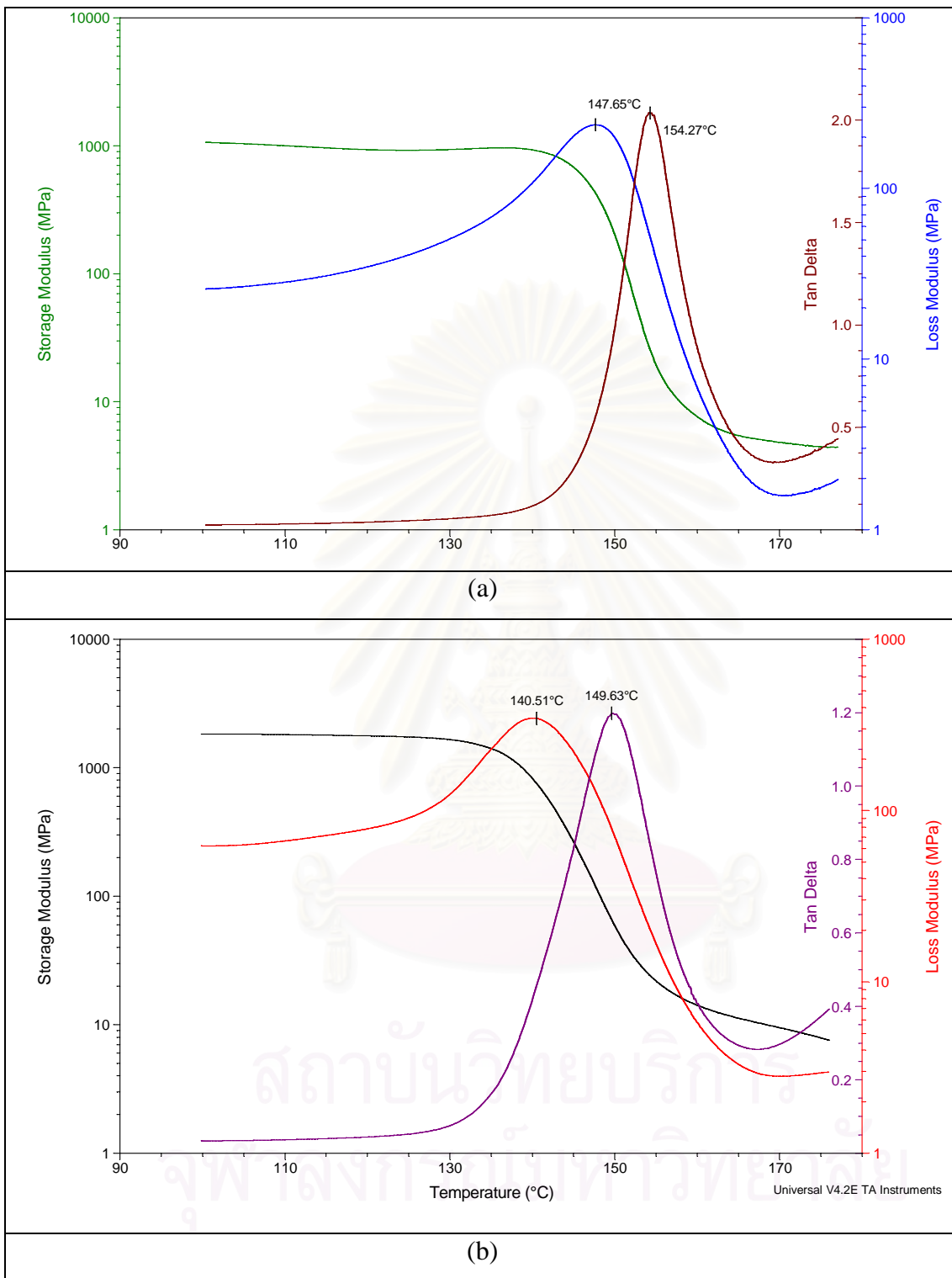
Figure 5-34   DMA scan and fitted values for Tg for (a) PC39K/5%CBC33 (b)
PC27K/5%CBC33.

Table 5-1 lists the glass transition temperatures of pure polycarbonate, PC39K PC27K, and the blends from the DMA measurements. All T_g of the blends decrease slightly with liquid crystal content.

Table 5-1 T_g of polycarbonate and the blends from DMA measurements at a frequency of 1 Hz and a heating rate of 2^oC/minute.

Sample	T_g (^oC)		Sample	T_g (^oC)	
	From E''	From $\tan\delta$		From E''	From $\tan\delta$
PC39K	154.4	159.2	PC27K	151.37	159.6
PC39K+1%CBC33	151.1	156.9	PC27K+1%CBC33	146.50	153.7
PC39K+1%CBC53	151.0	156.8	PC27K+1%CBC53	144.57	150.3
PC39K+2%CBC33	150.0	156.7	PC27K+2%CBC33	142.52	150.9
PC39K+2%CBC53	148.9	155.2	PC27K+2%CBC53	142.20	149.6
PC39K+5%CBC33	147.6	154.3	PC27K+5%CBC33	140.51	149.6
PC39K+5%CBC53	146.9	153.4	PC27K+5%CBC53	137.39	147.8

The T_g decreases with liquid crystal content and in addition to the rheological properties, dynamic mechanical property and diffusion studies, similar trends for the different types of LLC were found. However, CBC53 affects all rheological, dynamic mechanical and diffusion properties slightly more strongly than CBC33. This may be due to the greater anisotropic nature of CBC53 leads to a greater impact on the molecular orientation of the LLC in the blends.

5.5 Summary

The studied of the miscibility of polycarbonate and low molar mass liquid crystal described in this chapter have been shown that the low molar mass liquid crystals are miscible in the mixture for weight fractions of LLC less than 6%. With this criterion of the miscibility, all the further study was perform inside the miscible regime to avoid the effect from phase separation.

For the effects of low molar mass liquid crystal on the viscosity, two methods of viscosity study were performed due to different purposes. The shear viscosity studied was taken for understanding and being able to predict the trend of viscosity in the real process, while the study of oscillatory shear was performed because of the attempt to explain the behaviour in terms of parameters. It is found that both complex and steady shear viscosities of the blends were significantly decreased upon addition of LLC. The estimated shear moduli of the blends were also found decreases with increasing LLC concentration.

Further study was made considering the effects of the LLC concentration on the diffusion behaviour. In general, the chain diffusion is related to the viscosity characteristic. The increase of diffusion coefficient was expected while the decrease of viscosity was observed. Unfortunately, the diffusion coefficients were found increase and then decrease with a further increase in the LLC content.

The glass transition temperature was also determined to study the bulk property of the blends. The T_g of the blend shows the decrease upon the increase of LLC content.

CHAPTER VI

CONCLUSIONS AND RECOMMENDATIONS

6.1 Conclusions

The objective of the work reported in this thesis was to study the reduction in melt viscosity of polycarbonate by low molar mass liquid crystal and also, the extent to which a simple viscoelastic model could be used to investigate the rheological parameters of the system. The following studies have been carried out:

The effect of liquid crystal concentration on the blend miscibility: Small angle light scattering has been used to observe the phase boundaries of blends of polycarbonate and low molar mass liquid crystal. The lack of a change in light intensity with temperature indicates that the low molar mass liquid crystals are miscible in the mixture for weight fractions of LLC less than 6% over the entire temperature range. The blends become partially miscible and exhibited lower critical solution temperature behaviour for liquid crystal weight fraction 6, 8 and 10%. Such LCST behaviour is unusual for polymer solutions and suggests specific interactions between the polycarbonate and the liquid crystal.

The effect of liquid crystal concentration on the blend viscosity: The melt rheology of blends of a low molar mass liquid crystal and polycarbonate are reported. The rheological properties of the blended sample within the miscible regime of the blends vary with liquid crystal content. Both the complex and steady shear viscosities of the blends were found to be significantly decreased upon addition of small amounts of liquid crystal. For low shear rates the viscosity of the blends are similar to that of pure PC, at higher shear rates the viscosity of the blends follows the trend of anisotropic liquid crystalline polymers. The influence of LLC on the complex viscosities of the blends was similar to the influence on the steady shear viscosity, with the frequency dependent viscosity decreasing as LLC concentration increased. The frequency dependency of the complex viscosity of each of the blends is clearly different from that of pure PC, due to the

induced alignment of the LLC. The decrease in melt viscosity of polycarbonate that was observed upon addition of LLC is not due to lubrication effects at the interfaces, as shown by reproducible oscillatory shear flow sweeps.

The estimated rheological property parameters of the blends: The shear modulus of the PC and the blends was estimated by fitting the loss modulus and storage modulus to a single relaxation time Maxwell model. The model fits the results reasonably well, enabling a simple qualitative comparison between blends with different LLC concentrations. It is shown that the shear modulus of the blends estimated from Maxwell model decreases with increasing LLC concentration and temperature. The LLC has a more significant effect on the relaxation time of the low molecular weight PC than the high molecular weight PC.

The diffusion properties of the blends: The diffusion coefficient obtained from nuclear reaction analysis shows an increase upon addition of a small amount of liquid crystal (1wt%), which implies that PC diffuses faster upon addition of LLC regardless of the type of the LLC. In contrast, the diffusion coefficient then decreases with a further increase in the LLC content. The appearance of the step-like profile in the concentration against depth data indicates that, at high LLC concentration, there exists a slight excess of LLC at the interface between the films. The excess LLC probably behaves like an additional layer which may slow down the interdiffusion process between the two polymer layers. We have attempted to explore the reason for this reverse phenomenon, as the diffusion results appear to contradict the rheological studies, which show a decrease in both linear and non-linear viscosity as a function of LLC concentration. Unfortunately, this point has not been experimentally resolved in this present work.

The bulk mechanical property of the blends: A decrease in T_g with liquid crystal content was found in this study and CBC53 clearly affects the dynamic mechanical properties more strongly than CBC33. It is also shown that the LLC has a more significant effect on the T_g of the low molecular weight PC blends than the high molecular weight PC blends.

6.2 Recommendations for further studies

Another pair of engineering polymer and low molar mass liquid crystals chemical should be chosen for study. In addition to finding a more suitable pairs for blending, this will enable an exploration of the extent to which the results we have found are dependent on the specific interactions between PC and the LLC.

It should be interesting to investigate the morphologies of low molar mass liquid crystal chemical and the base polymer, when the blends exhibit phase separation. Such morphologies may themselves lead to enhanced properties, although they may also result in degraded optical properties.

The alignment of the LLC reported in this thesis has been inferred from indirect rheological data. In order to understand and directly observe the alignment of the low molar mass liquid crystal in polymer matrix, after applying the shear force the samples could be rapidly quenched and characterized via other appropriate techniques, such as spectroscopy or microscopy. Alignment could also be directly observed in flow by using small angle neutron scattering if appropriately deuterated polymers were available.

REFERENCES

[1] Beery, D.; Kenig, S.; Siegmann, A.; Narkis, M., Polym. Eng. Sci. 32 (1992): 14-19.

[2] Lin, Y. C.; Lee, H. W.; Winter, H. H., Polymer 34 (1993): 4703-4709.

[3] Brostow, W.; Sterzynski, T.; Triouleyre, S., Polymer 37 (1996): 1561-1574.

[4] Rivera-Gastélum, M. J.; Wagner, N. J., J. Polym. Sci. Part B: Polym. Phys. 34 (1996): 2433-2445.

[5] Campoy, I.; Gómez, M.A.; Marco, C., Polymer 39 (1998): 6279-6288.

[6] Eijndhoven-Rivera, M. J. V.; Wagner, N. J.; Hsiao, B., J. Polym. Sci. Part B: Polym. Phys. 36 (1998): 1769-1780.

[7] Li, S.; Järvelä, P. K.; Järvelä, P. A., J. Appl. Polym. Sci. 71 (1999):1649-1656.

[8] Hsieh, T.-T.; Tiu, C.; Hsieh, K.-H.; Simon, G. P., J. Appl. Polym. Sci. 77 (2000): 2319-2330.

[9] Jiang, L.; Lam, Y. C.; Zhang, J., J. Polym. Sci. Part B: Polym. Phys. 43 (2005): 2683-2693.

[10] Huh, W.; Weiss, R. A.; Nicolais, L., Polym. Eng. Sci. 25 (1983): 779-783.

[11] Buckley, A.; Conciatori, A. B.; Calundann, G. W., U.S. Patent, 4,434,262, (1984).

[12] George, E. R.; Porter, R. S.; Griffin, A. C., Molec. Cryst. Liq. Cryst. 110 (1984): 27-40.

[13] Kajiyama, T.; Washizu, S.; Takayanagi, M., J. Appl. Polym. Sci. 29 (1984): 3955-3964.

[14] Ballauff, M., Molec. Cryst. Liq. Cryst. 4 (1986):15-22.

[15] Dutta, D.; Fruitwala, H.; Kohli, A.; Weiss, R.A., Polym. Eng. Sci. 30 (1990): 1005-1018.

[16] Sakane, Y.; Inomata, K.; Morita, H.; Kawakatsu, T.; Doi, M.; Nose, T., Polymer 42 (2001): 3883-3891.

[17] Filip, D.; Simionescu, C. I.; Macocinschi, D., Thermochim Acta 395 (2003): 217-223.

[18]   Watcharawichanant, S.; Thongyai, S.; Tanodekaew, S.; Higgins, J. S.; Clarke, N., Polymer 45 (2004):2201-2209.

[19]   Demus, D.; Goodby, J.; Gray, G.W.; Spiess, H.-W.; Vill, V. Handbook of liquid crystals 2A:low molecular weight liquid crystal I.; Wiley-VCH Press: Weinheim, 1998.

[20]   Larson, R. G. The Structure and Rheology of complex Fluids; Oxford University Press: New York, 1999.

[21]   Sperling, L. H. Introduction to Physical Polymer Science 3rd ed.; John Wiley & Son: New York, 2001.

[22]   Olabisi, O. Handbook of Thermoplastics; Marcel Dekker: New York, 1997.

[23]   Van Krevelen, D. W. Properties of polymers, 3rd ed.; Elsevier: Amsterdam, 1990.

[24]   Payne, R. S.; Clough, A. S.; Murphy, P.; Mills, P., J Nucl Instrum Methods Phys Res Sect B 42 (1989): 130-134.

[25]   Kimura, M.; Porter, R. S., J. Polym. Sci. Part B: Polym. Phys. 22 (1984):1697-1699.

[26]   Zhuang, P.; Kyu, T.; White, J. L., SPEANTEC Tech Papers 34 (1988):1237.

[27]   Chuah, H. H.; Kyu, T.; Halminiak, T., Polymer 28 (1987): 2130-2133.

[28]   Nakai, A.; Shiwaku, T.; Hasegawa, H.; Hashimoto, T., Macromolecules 19 (1986): 3008.

[29]   Kyu, T.; Zhuang, P., Polym. Commun. 29, 4 (1988): 99.

[30]   Nobile, M. R.; Amendola, E.; Nicolasis, L.; Acierno, D.; Carfagna, C., Polym. Eng. Sci. 29 (1989): 244.

[31]   Joseph, E. G.; Wilkes, G. L.; Baird, D. G. In Polymer Liquid Crystal, Blumstein, A., ed., Plenum Press, New York, 1984.

[32]   Joseph, E. G.; Wilkes, G. L.; Baird, D. G., Am. Chem. Soc, Div. Polym. Chem, Polym. Prepr. 24 (1983): 304.

[33]   Sharma, S. K.; Tendolkar, A.; Misra, A., Molec. Cryst. Liq. Cryst. 157 (1988): 597.

[34]   George, E. R.; Porter, R. S.; Griffin, A. C., Molec. Cryst. Liq. Cryst. 110 (1984): 27.

[35]   Sigaud, G. Achard, M. F.; Hardouin, F.; Gasparous, H., Molec. Cryst. Liq. Cryst. 155 (1988): 443.

[36]   Belfiore, L. A., <u>Am. Chem. Soc., Div. Polym. Chem., Polym. Prepr</u>. 28
         (1987): 158.

[37]   Patwardhan, A. A.; Belfiore, L. A., <u>Polym. Eng. Sci</u>. 28 (1988): 916.

[38]   Lipatov, Y.; Tsukruk, V. V.; Shilov, V. V.; Boyarski, G. Y., <u>Polym. Sci.
         U.S.S.R.</u> 28 (1986): 60.

[39]   Brostow, W.; Hess, M.; Lopez, B. L. and Sterzynski., <u>Polymer</u> 37 (1996):
         1551-1560.

[40]   Lee, S.; Mather, P. T. and Peason, D. S., <u>J. Appl. Polym. Sci.</u> 59 (1996): 243-
         250.

[41]   Rodrigues, J. R. S.; Kaito, A.; Soldi, V.; Pires, A. T. N., <u>Polym. Int.</u> 46
         (1998):138.

[42]   Cogswell, F. N.; Griffin, B. P.; Rose, J. B., <u>U.S. Patent 4,438,236</u>, (1984).

[43]   Siegmann, A.; Dagan, A.; Kening, S., <u>Polymer</u> 26 (1985): 1325-1330.

[44]   Kiss, G., <u>Polym. Eng. Sci.</u> 27 (1987): 410.

[45]   Blizard, K. G.; Baird, D. G., <u>Polym. Eng. Sci.</u> 27(1987): 653-662.

[46]   Acierno, D.; Amendola, E.; Carfagna, C.; Nicolais, L.; Nobile, R., <u>Molec.
         Cryst. Liq. Cryst.</u> 153 (1987): 533.

[47]   West, J. L., <u>Molec. Cryst. Liq. Cryst.</u> 157 (1988): 427.

[48]   Malik, T. M.; Carreau, P. J. and Chapleau, N., <u>Polym. Eng. Sci.</u> 29 (1989):
         600.

[49]   Heino, M. T. and Seppala, J. V., <u>J. Appl. Polym. Sci.</u> 44 (1992): 2185-2195.

[50]   Beery, D.; Kenig, S.; Siegmann, A.; Narkis, M., <u>Polym. Eng. Sci.</u> 32 (1992):
         14-19.

[51]   Brostow, W.; Sterzynski, T.; Triouleyre, S., <u>Polymer</u> 37 (1996): 1561-1574.

[52]   Chik, G.L.; Li, R.K.Y.; Choy, C.L., <u>Mat Proc Tech</u> 63 (1997): 488.

[53]   Pezolet, M. et al, <u>Biochim. Biophys. Acta</u> 533 (1973): 263.

[54]   Xie, X. L.; Tjong, S. C. and Li, R. K. Y., <u>J. Appl. Polym. Sci.</u> 77 (2000):
         1975-1988.

[55]   Thongyai, S.; Powanusorn, S., <u>Master's thesis</u>, Department of Chemical
         Engineering, Graduate School, Chulalongkorn University, 2000.

[56]   Hutchings, L. R.; Richards, R. W.; Thompson, R. L.; Clough, A. S.;
         Langridge, S., <u>J. Polym. Sci. Part B: Polym. Phys.</u> 39 (2001): 2351-
         2362.

[57]   Helmroth, E.; Dekker, M.; Hankemier, Th., <u>Food Additives and Contaminents</u>
        19 (2002): 176-183.

[58]   Colley, F. R.; Collins, S. A.; Richards, R. W., <u>J. Mater. Chem.</u> 13 (2003):
        2765.

[59]   Lopez, R.; Guedeau-Boudeville, M. A.; Gambin, Y.; Rodriguez-Beas, C.;
        Maldonado, A.; Urbach, W., <u>J. Colloid. Interface Sci.</u> 300 (2006): 105.

[60]   Bryson, J. A., <u>Plastic Materials 7<u>th</u> ed.;</u> Butterworth Scientific: London, 1999.

[61]   Crawford, R. J., <u>Plastics Engineering</u>; BPCC Wheatons, 1987.

[62]   Strobl, G. R., <u>The Physics of Polymers: concepts for understanding their
        structures and behaviour</u>; Springer Verlag: Berlin, 1997

[63]   Flory, P. J., <u>J. Chem. Phys.</u> 9 (1941): 660-661.

[64]   Flory, P. J., <u>J. Chem. Phys.</u> 10 (1942): 51-61.

[65]   Flory, P. J.; Orwoll, R. A.; Vrij, A., <u>J. Am. Chem. Soc.</u> 86 (1964): 3507-
        3520.

[66]   Folkes, M. J.; Hope, P., <u>Polymer Blends and Alloys</u>; Chapman & Hall:
        London, 1993.

[67]   Olabisi, O.; Robeson, L. M.; Shaw, M. T., <u>Polymer-polymer miscibility</u>;
        Academic Press, Inc.: London, 1979.

[68]   Utraki, L. A., <u>Polymer alloys and blends: thermodynamics and rheology</u>;
        Hanser Publishers: New York, 1989.

[69]   Crank, J., <u>The Mathematics of diffusion</u>; Oxford University Press: London,
        1975.

[70]   Neogi, P., <u>Diffusion in polymers</u>; Marcel Dekker, Inc.: New York, 1996.

[71]   Macosko, C. W., <u>Rheology: Principles, Measurements and Applications</u>;
        VCH Publishers, Inc.: USA, 1994.

[72]   Rodriguez, F., <u>Principles of Polymer Systems 5<u>th</u> ed</u>; Taylor & Francis Bocks,
        Inc.: New York, 2003.

[73]   Shenoy, A. V.; Saini, D. R., <u>Thermoplastic Melt Rheology and Processing</u>;
        Marcel Dekker, Inc.: New York, 1996.

[74]   Fried, J. R., <u>Polymer Science and Technology 2<u>nd</u> ed</u>; Pearson Education, Inc.:
        USA, 2003.

[75]   Benninghoven, A., <u>Secondary Ion Mass Spectroscopy</u>; Springer Verlag: New
        York, 1985.

[76]   Briggs, D., <u>Handbook of X-ray and Ultraviolet Plotoeletron Spectroscopy</u>; Heyden and Son, Ltd.: London, 1978.

[77]   Chu, W. K.; Mayer, J. W.; Nicolet, M. A., <u>Backscattering Spectrometry</u>, Academic Press, New York, 1978.

[78]   Doyle, B. L.; Peercy, P. S., <u>Appl Phys Lett</u> 34 (1979): 811.

[79]   Turos, A.; Meyer, O., <u>Nucl. Instr. Meth. Phys. Res.</u> B4 (1984): 92.

[80]   Rouse, P. E., <u>J. Chem. Phys.</u> 21 (1953): 1272.

[81]   Doi, M.; Edwards, S. F., <u>J. Chem. Soc, Faraday Trans. II</u> 10 (1978): 1789.

[82]   Doi, M.; Edwards, S. F., <u>The Theory of Polymer Dynamics</u>; Oxford University Press: United Kingdoms, 1986.

[83]   deGennes, P. G., <u>Scaling Concepts in Polymer Physics</u>; Cornell University Press: New York, 1979.

[84]   Graessley, W. W., <u>J. Polym. Sci: Polym. Phys.</u> 18 (1980): 27.

[85]   Ferry, J. D., <u>Viscoelastic Properties of Polymers</u>; Wiley, New York, 1980

[86]   Green, P. F.; Kramer, E. J., <u>J. Mat. Res.</u> 1 (1986): 202.

[87]   Nemoto, N.; Landry, M. R.; Noh, I.; Yu, H., <u>Polym. Comm.</u> 25 (1984): 141.

[88]   Hess, W., <u>Macromolecules</u> 21 (1988): 2587.

[89]   Graessley, W. W., <u>Adv. Polym. Sci.</u> 47 (1982): 67.

[90]   Wantanabe, H.; Tirrell, M., <u>Macromolecules</u> 22 (1989): 927.

[91]   Daoud, M.; deGennes, P. G., <u>J. Polym. Sci: Polym. Phys.</u> 17 (1979): 1971.

[92]   Klein, J., <u>Macromolecules</u> 19 (1986): 105.

[93]   Flory, P. J., <u>Principles of Polymer Chemistry</u>; Cornell University Press: New York, 1953.

[94]   Sillescu, H., <u>Makromol. Chem: Rapid Comm</u> 8 (1987): 393.

[95]   Foley, G.; Cohen, C., <u>J. Polym. Sci: Polym. Phys.</u> 25 (1987): 2027.

[96]   Brochard, F.; Jouffroy, J.; Levinston, P., <u>Macromolecules</u> 17 (1984): 2925.

[97]   Composto, R. J.; Mayer, J. W.; Krammer, E. J.; White, D. M., <u>Phys. Rev. Lett.</u> 57 (1986): 1312.

[98]   Manard, K. P., <u>Dynamic Mechanical Analysis</u>; CRC Press LLC: Florida, 1999.

[99]   Hatakeyama, T.; Quinn, F. X., <u>Thermal Analysis: Fundamentals and Applications to Polymer Science 2<u>nd</u> ed</u>; John Wiley & Sons Ltd: England, 1999.

[100] Mooney, M., <u>J. Appl. Phys</u>. 35 (1934): 23

[101]   Russell, R. J., <u>Ph.D. thesis</u>: London University, 1946.

[102]   Greensmith, H. W.; Rivlin, R. S., <u>Phil. Trans</u>. A245 (1953): 399.

[103]   Kotaka, T.; Kurata, M.; Tamura, M., <u>J. Appl. Phys</u>. 30 (1959): 1705

[104]   Payne, R. S.; Clough, A. S.; Murphy, P.; Mills, P., <u>J. Nucl. Instrum. Methods.
          In Phys. Res</u>. B 42 (1989): 130.

[105]   Composto, R. J.; Walters, R. M.; Genzer, J., <u>Materials Science & Engineering
          R-Reports</u> 38 (2002): 107-180.

[106]   Kramer, E., <u>J. Physica B</u> 1991, 173.

[107]   Houghton, K. A., Ph.D. thesis: University of Durham, 2005.

[108]   Cogswell, F. N., <u>Polymer Melt Rheology</u>; John Wiley & Son: New York,
          1981.

[109]   Leon, S.; van der Vegt, N.; Delle Site, L.; Kremer, K., <u>Macromolecules</u> 38
          (2005): 8078.

[110]   Mead, D.W., <u>Journal of Rheology</u> 40 (1996): 633.

VITAE

Miss Noppawan Motong was born in Uttaradit, Thailand in September 17, 1979. She received the Bachelor Degree of Engineering in Plastics Engineering from the Material and Metallurgical Engineering, Rajamangala Institute of Technology in 1999. She graduated the Master of Engineering in Chemical Engineering from Chulalongkorn University in 2002. She entered the doctoral of Engineering in Chemical Engineering Program at Chulalongkorn University in 2003.

PUBLICATION AND PRESENTATIONS

1. Noppawan Motong, Supakanok Thongyai and Wannee Chinsirikul, The 8th Pacific Polymer Conference (PPC8), Bangkok, November, 2003.

2. Noppawan Motong, Supaknok Thongyai, Tomoo Shiomi, Hiroki Takeshita, The 8th European Symposium on Polymer Blends and Eurofillers, Bruges, Belgium, May 2005.

3. Noppawan Motong, Supakanok Thongyai and Nigel Clarke. "Miscibility of low molar mass liquid crystal and polycarbonate blends" Polymer Physics Group Biennial Meeting; Physical Aspects of Polymer Science, Leeds, UK, September, 2005.

4. Supakanok Thongyai, Nigel Clarke and Noppawan Motong, Phase Transition in Polymeric System, London, UK, November 2005.

5. N. Motong, S. Thongyai, N. Clarke, R. L. Thompson, S. A. Collins, Journal of Polymer Science Part B: Polymer Physics, 2007, Volume 45, Issue 16, Pages: 2187-2195.

6. Noppawan Motong, Supakanok Thongyai, Nigel Clarke, Journal of Applied Polymer Science, In Press.